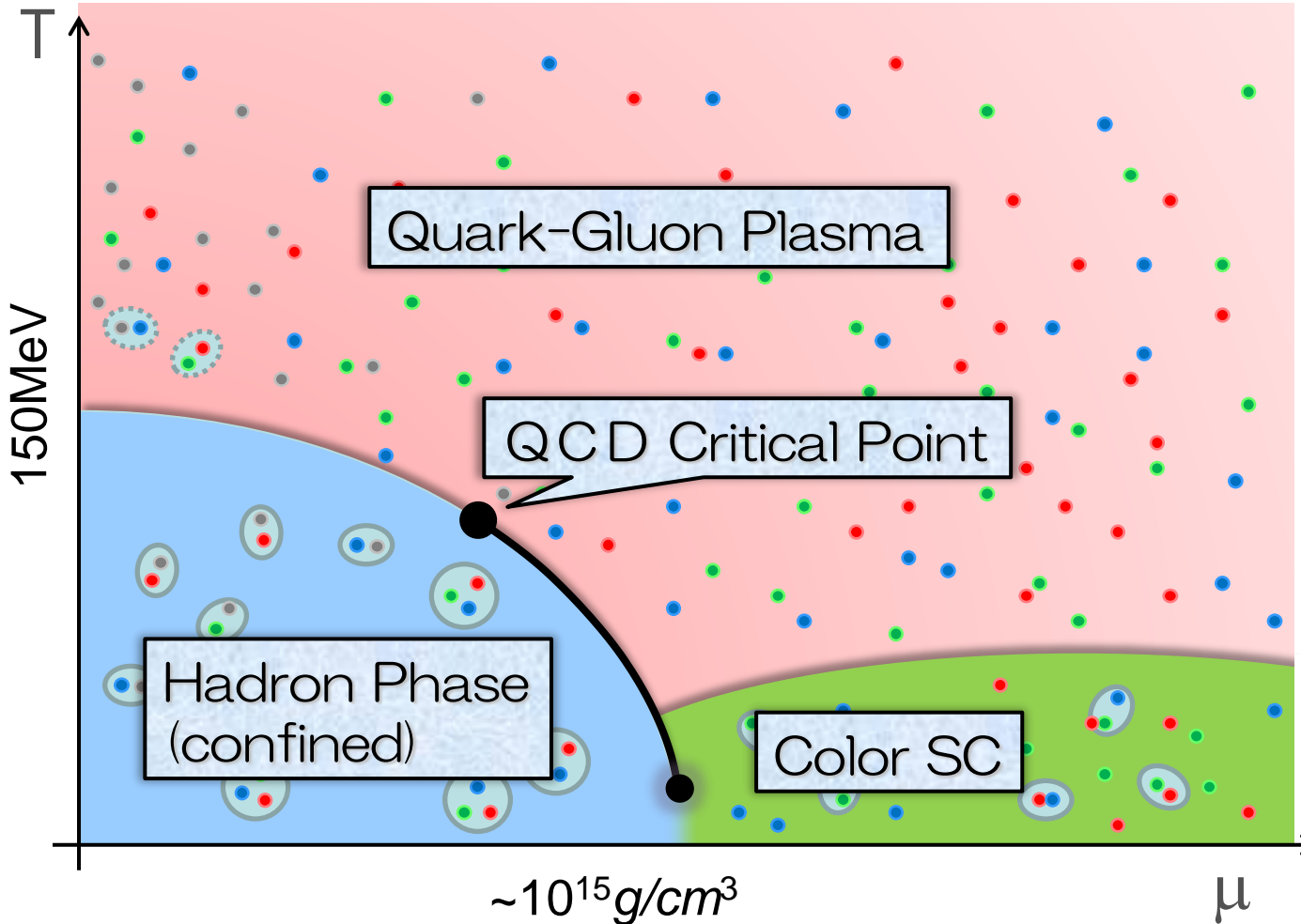


Three topics to explore matter under extreme conditions

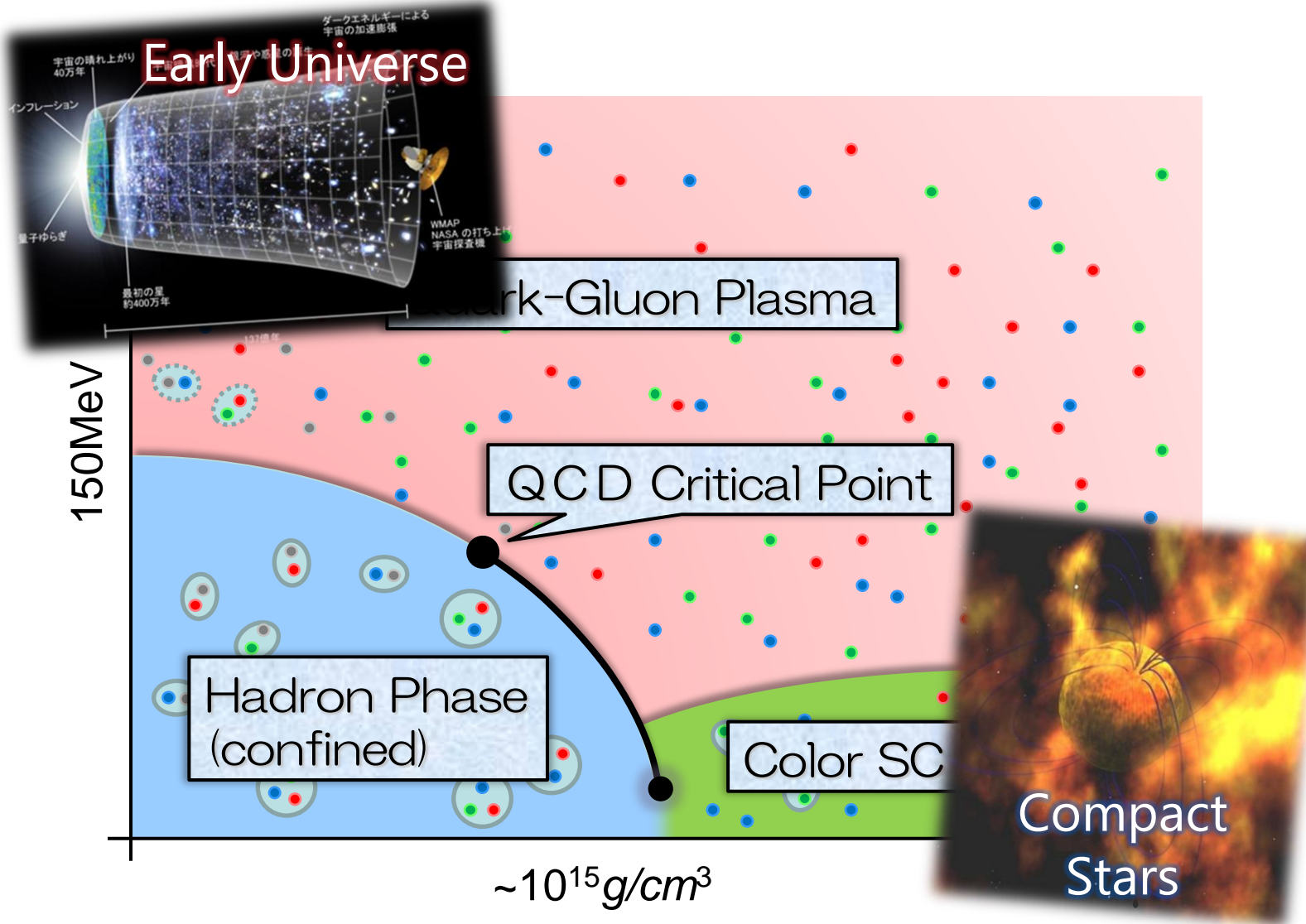
Masakiyo Kitazawa
(YITP, Kyoto)

QCD Phase Diagram



- Possible first-order transition and QCD critical point in dense region
- Multiple QCD-CP? MK+ ('02)
- Color superconducting phases in dense and cold quark matter

QCD Phase Diagram



- Possible first-order transition and QCD critical point in dense region
- Multiple QCD-CP? MK+ ('02)
- Color superconducting phases in dense and cold quark matter

Contents

1. Optimal collision energy for studying dense matter in heavy-ion collisions

Taya, Jinno, MK, Nara, 2409.07685

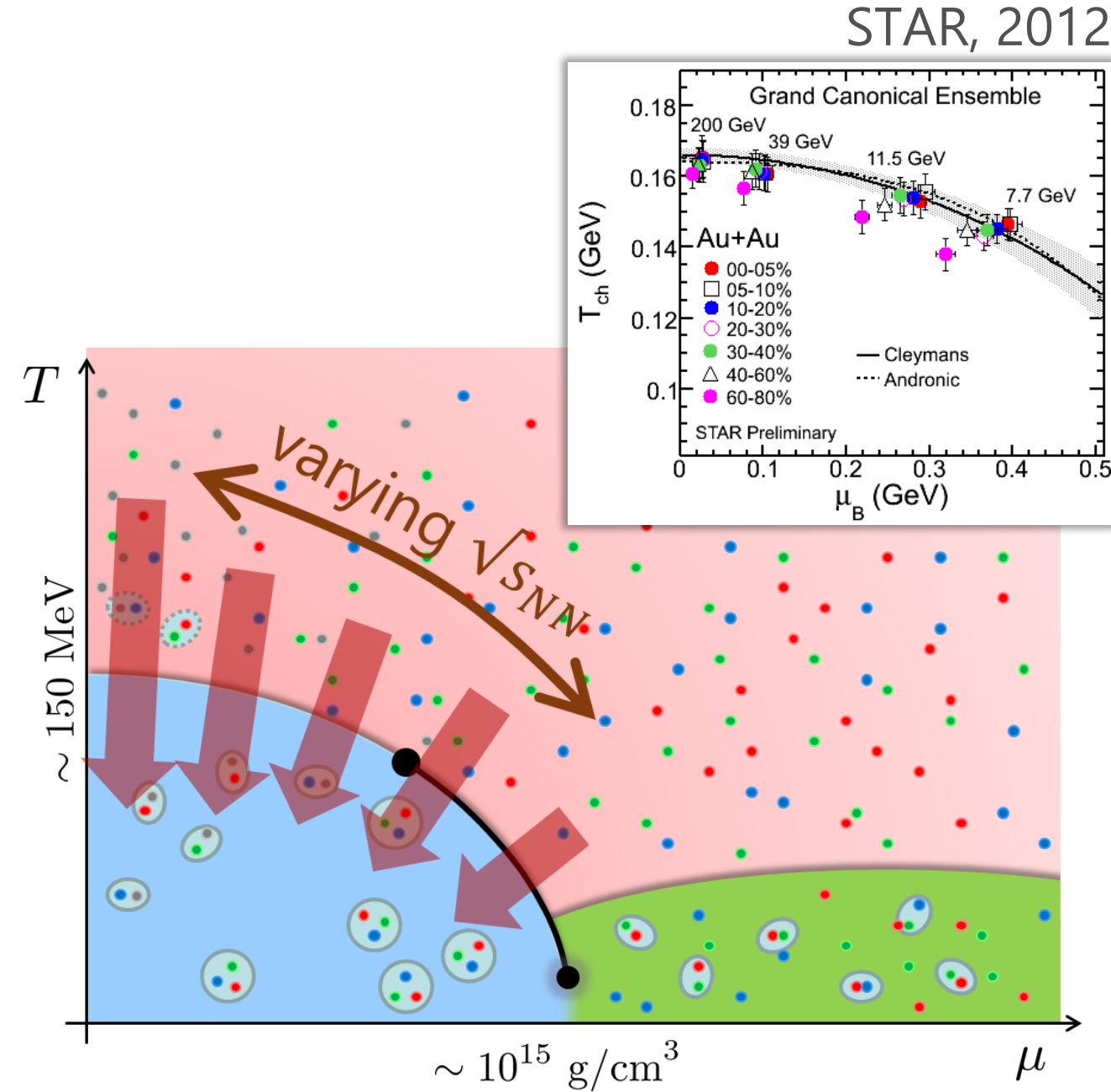
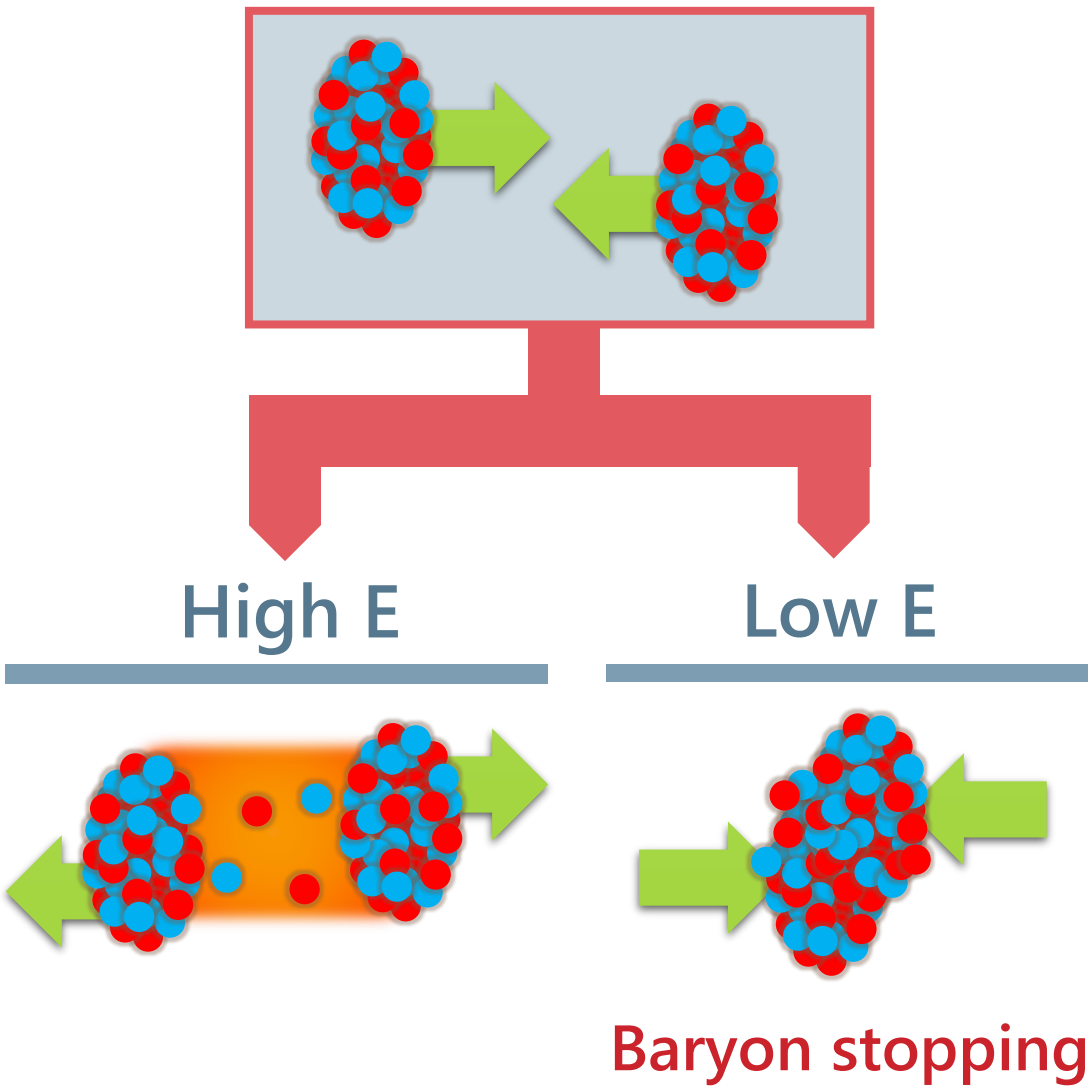
2. Dilepton production for a signal of phase transitions in dense matter

Nishimura, MK, Kunihiro, Ann. Phys. 469 (2024) 169768; PTEP 2023, 053D01; PTEP 2022, 093D02

3. Novel critical points in SU(3) Yang-Mills theory with boundary conditions

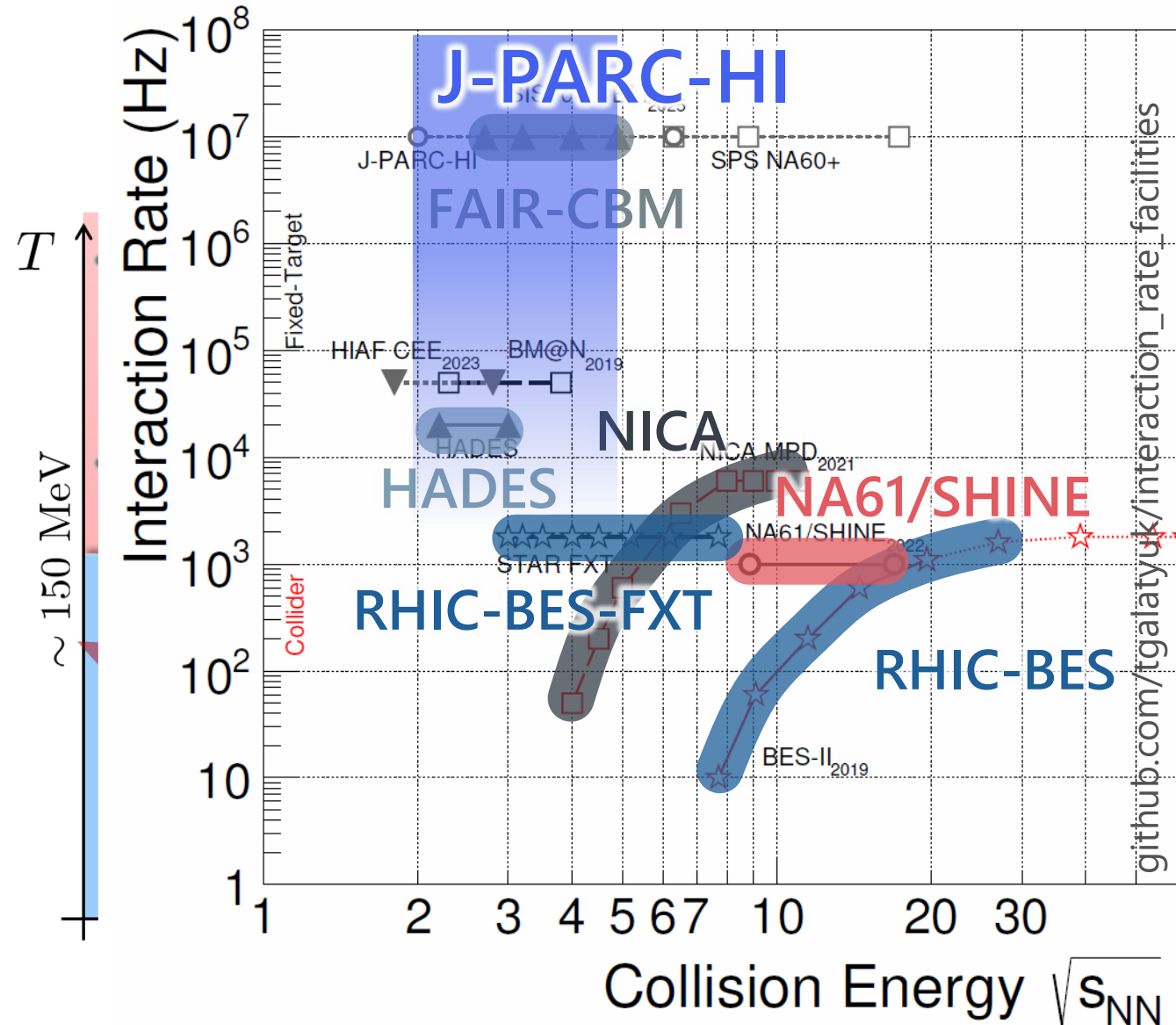
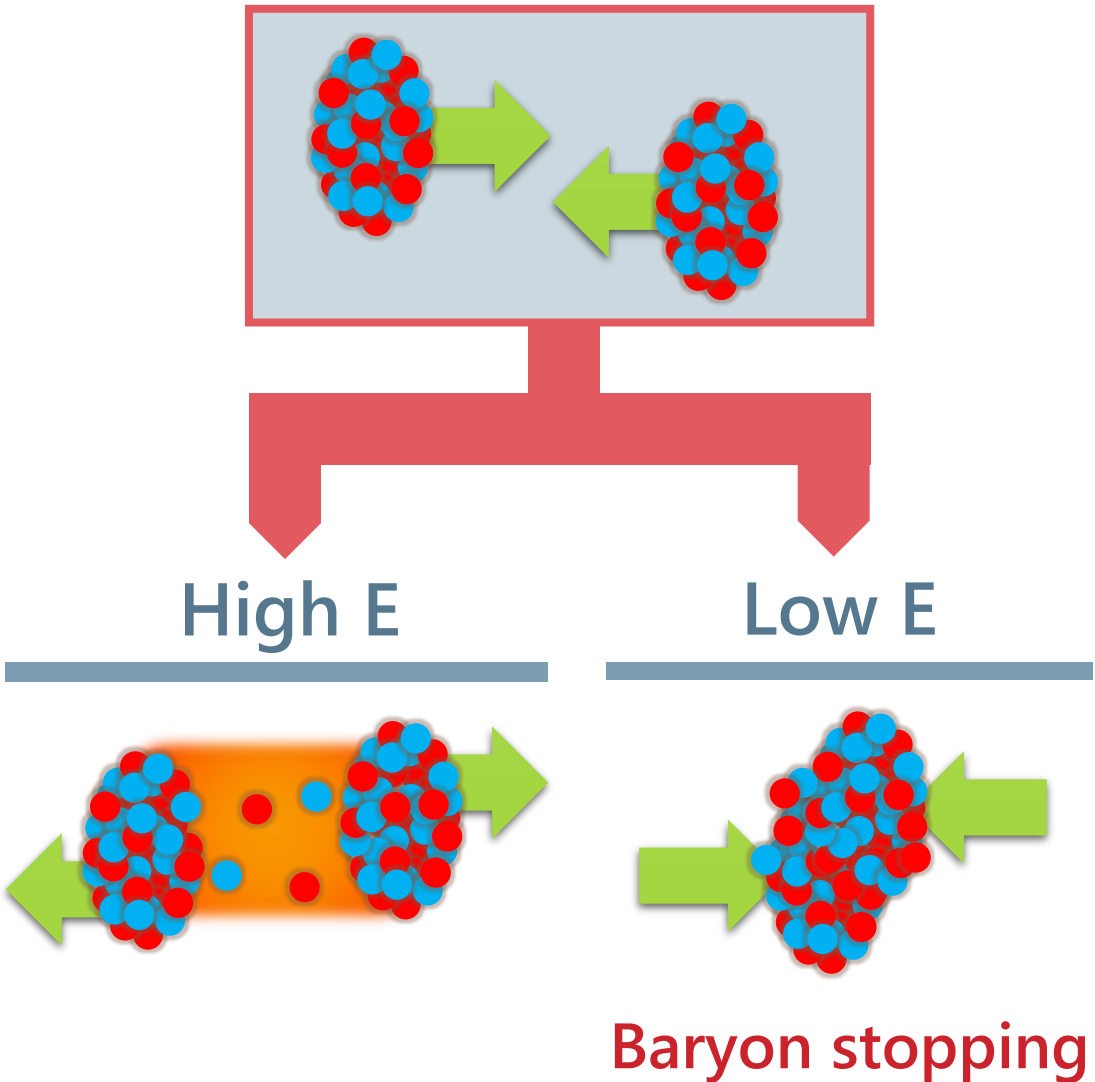
MK+, PRD99 (2019) 094507; Suenaga, MK, PRD107 (2023) 074502; Fujii, Iwanaka, Suenaga, MK, PRD110 (2024) 094016

Beam-Energy Scan



Beam-Energy Scan

STAR, 2012



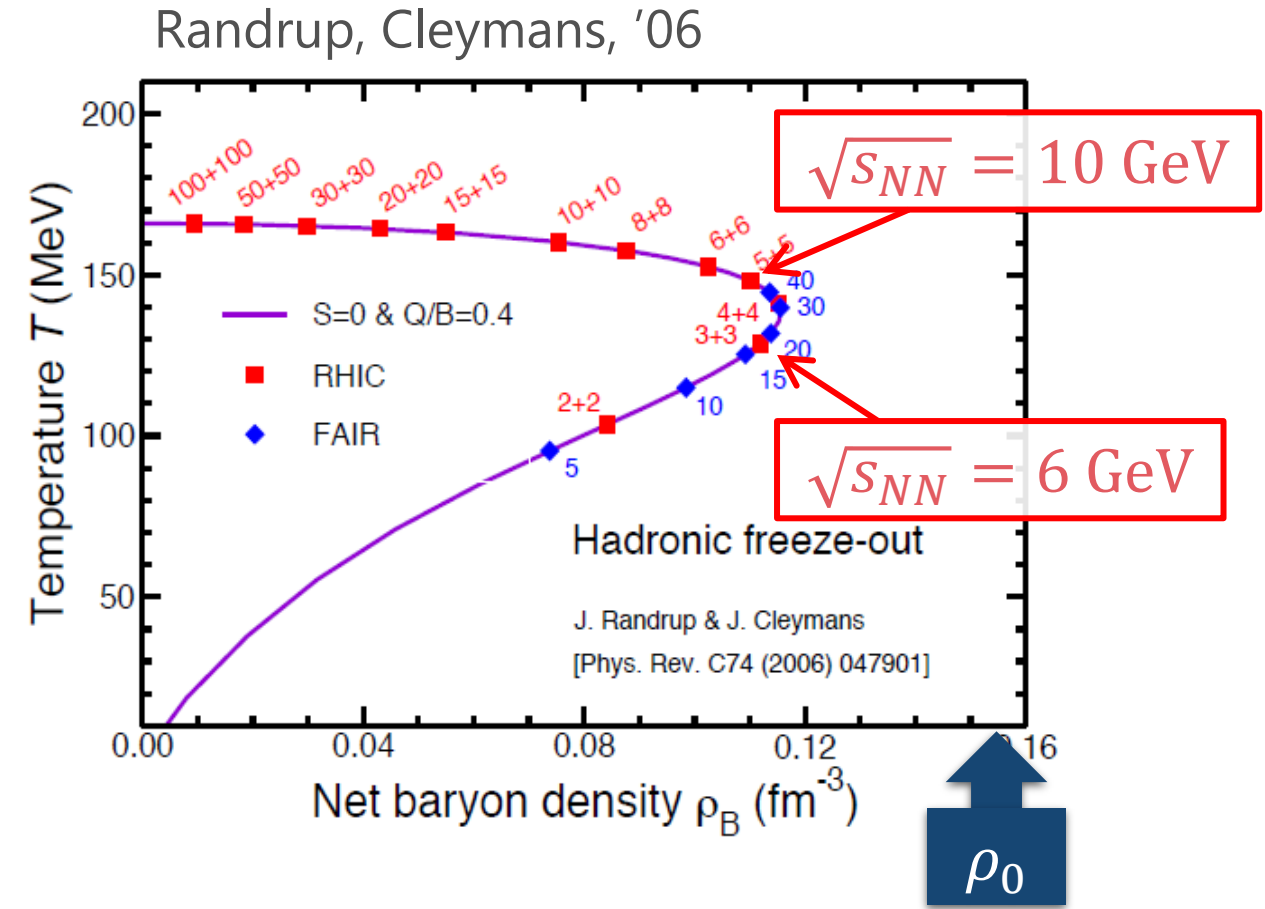
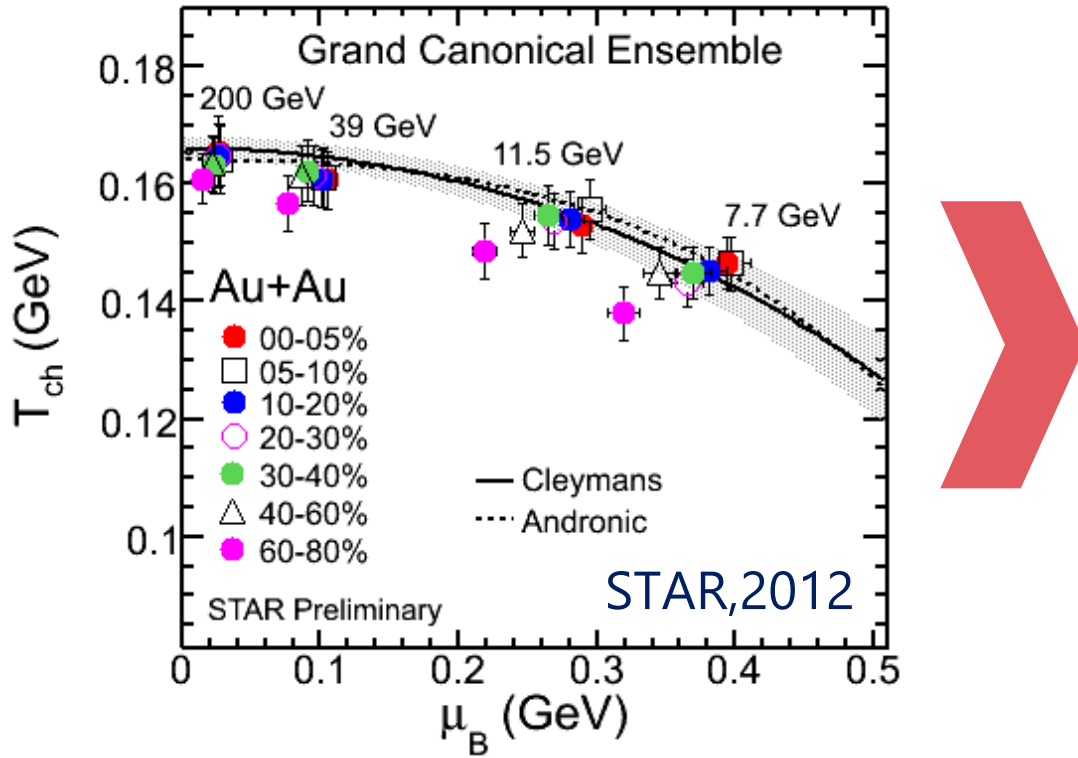
Key Questions

- What is **the optimal collision energy** to explore the baryon-rich matter?
- **How high density** is accessible?

Our Answer

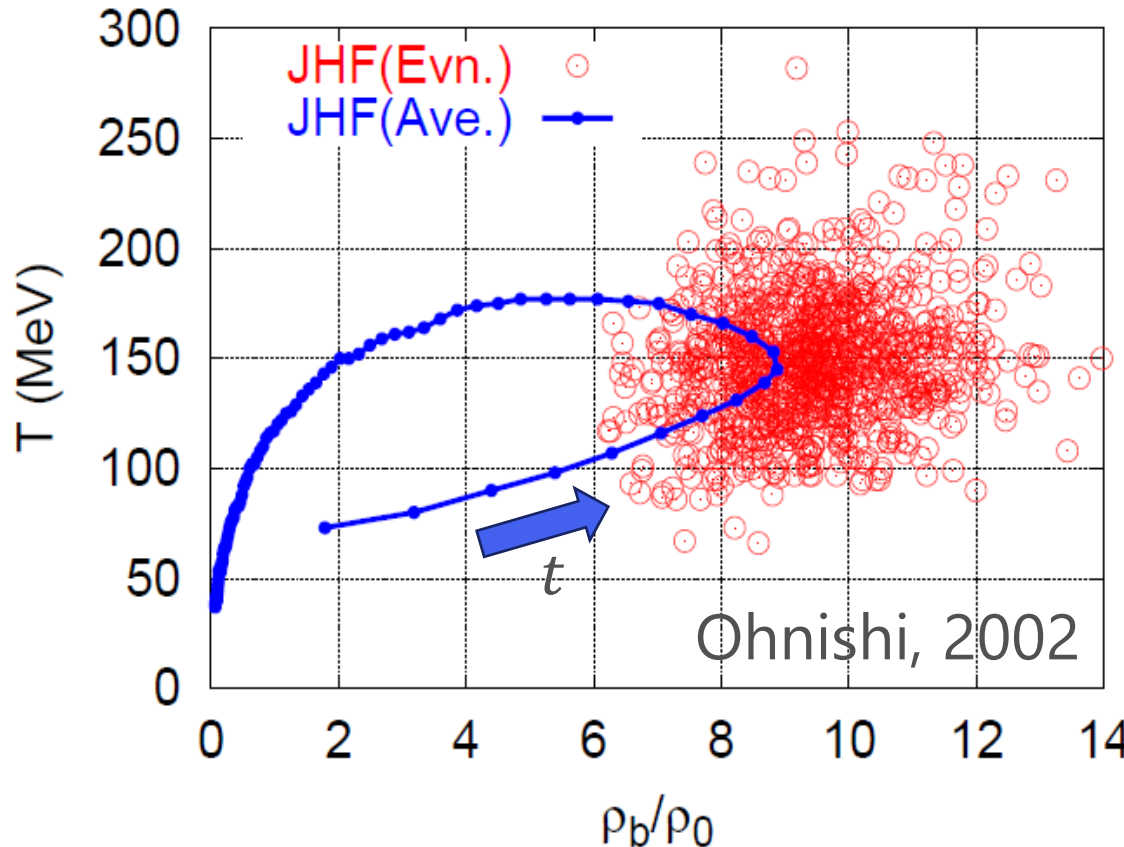
- $\sqrt{s_{NN}} = 3 \text{ GeV}$ is enough to study $\rho = 3\rho_0$.
- $\rho/\rho_0 = 4\sim 5$ may be accessible with $\sqrt{s_{NN}} = 3\sim 6 \text{ GeV}$.

Chemical Freezeout



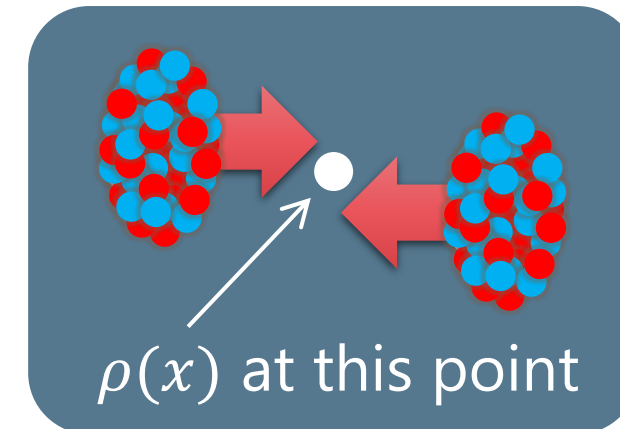
- Highest baryon density **at chemical freezeout** at $\sqrt{s_{NN}} \simeq 6 - 10 \text{ GeV}$?
- Not the highest density in the early stage.
- Density in earlier stage? ➡ Analysis in dynamical models

Baryon Density at Collision Point



Simulation by JAM

$$E/A = 20\text{GeV}, \sqrt{s_{NN}} \simeq 6\text{GeV}$$



- Maximum baryon density exceeds $\rho/\rho_0 \simeq 8$!
- Large event-by-event fluctuations
- How large is the high-density region? How long is the lifetime?

Volume of Dense Region

Taya, Jinno, MK, Nara, 2409.07685

Volume where the local baryon density is larger than a threshold value ρ_{th}

$$V_3(\rho_{\text{th}}, t) = \int_{\rho(x) > \rho_{\text{th}}} d^3x \gamma$$

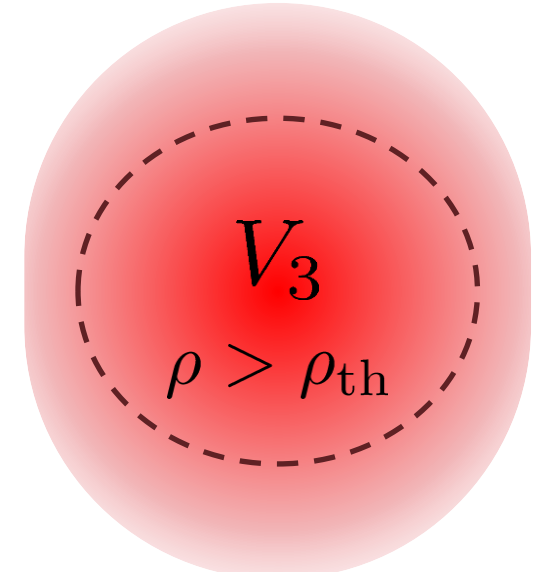
Baryon current $J^\mu(x)$

Baryon density $\rho(x) = \sqrt{J^\mu(x) J_\mu(x)}$

Lorentz factor $\gamma = (1 - (\mathbf{J}/J_0)^2)^{-1/2}$

Note:

- Event-by-event basis / no event average
- Directly calculable in a dynamical model
- We do not care about local thermalization.
 - V_3 is the upper limit of thermalized volume.
 - Even non-thermal, dense region is interesting!



Simulation Setup in JAM

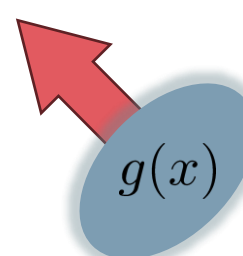
- Au+Au collision for $2.4 \leq \sqrt{s_{NN}} \leq 20$ GeV
- Impact parameter $b \leq 3$ fm : top 5% centrality
- Momentum-dependent mean field (MF2) Nara, Ohnishi, 2022
 - Setup reproducing $\sqrt{s_{NN}}$ dep. of $d\nu_1/d\eta$ and ν_2

Smeared baryon current

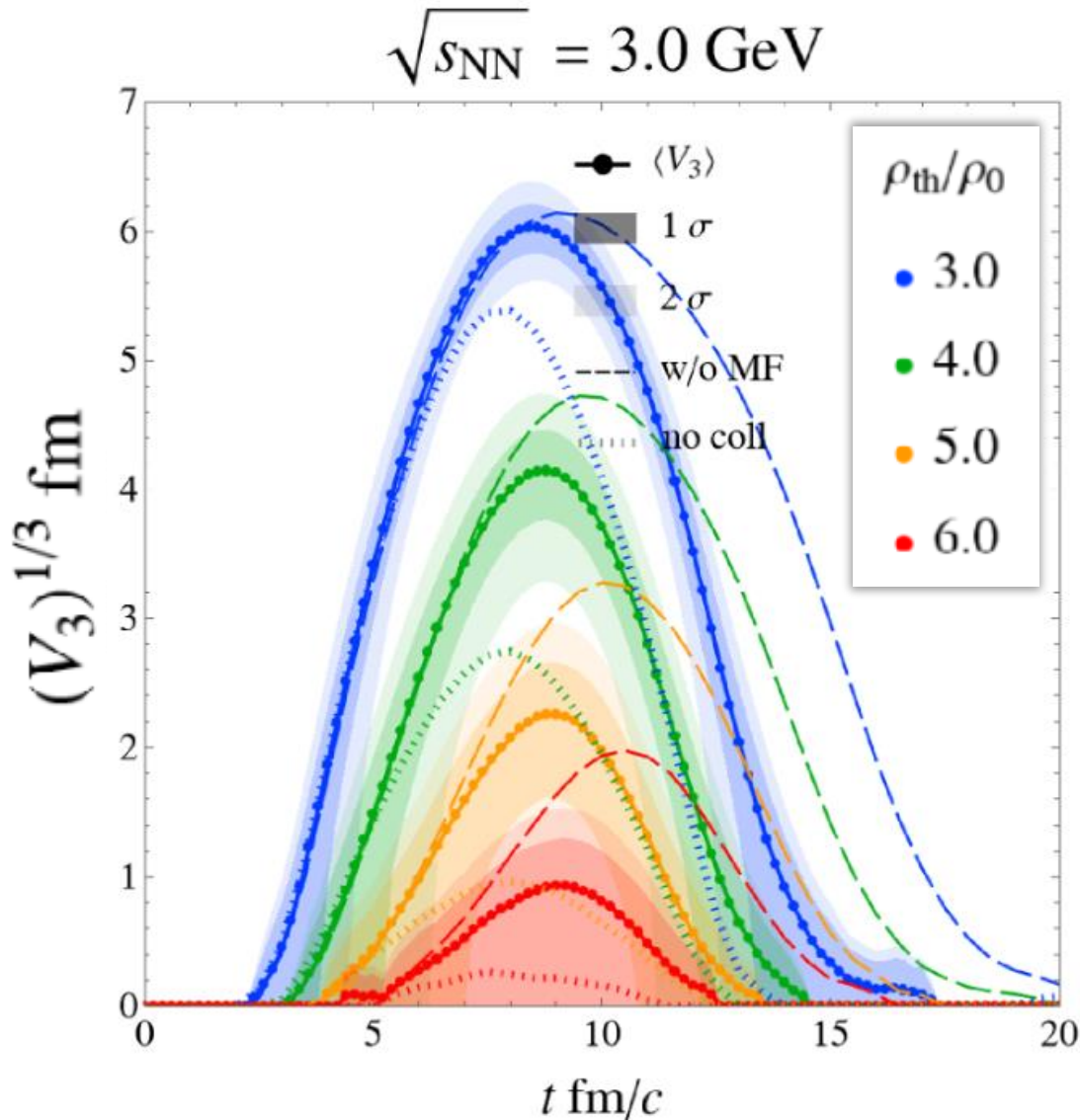
discrete particle distribution → continuous current by smearing

$$J^\mu(x) = \sum_{i \in \text{baryons}} B_i g(x; X_i, P_i) \frac{P_i^\mu}{P_i^0}$$

$$g(x; X, P) := \frac{\gamma}{(\sqrt{2\pi}r)^3} e^{-\frac{|\mathbf{x}-\mathbf{X}|^2 + (\gamma \mathbf{V} \cdot (\mathbf{x}-\mathbf{X}))^2}{2r^2}} \quad r = 1 \text{ fm}$$

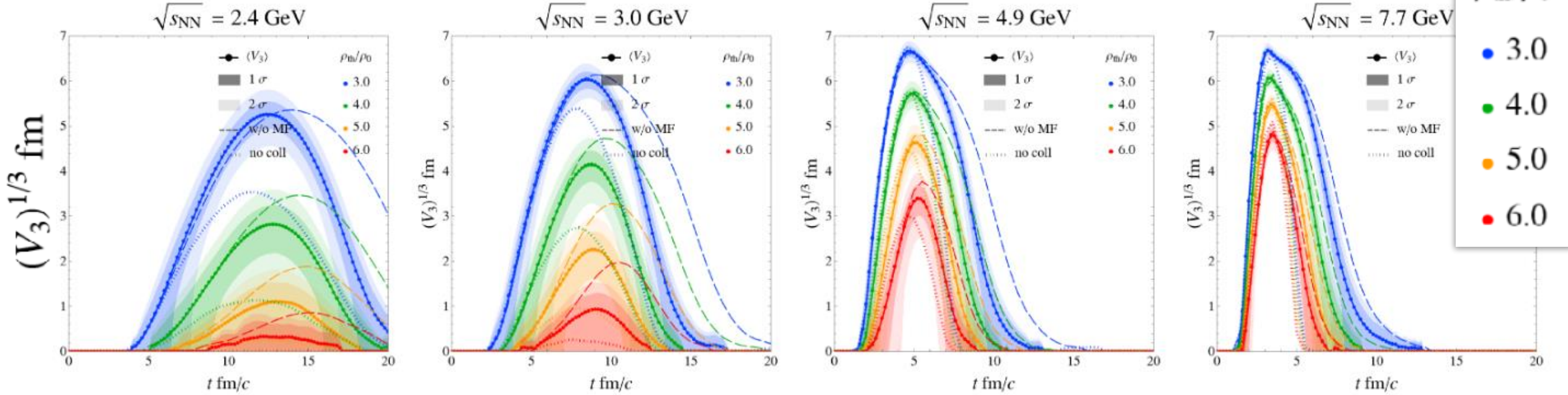


V_3 in JAM



- Formation of dense region:
 - $V_3(3\rho_0, t) = (6 \text{ fm})^3$
 - $V_3(4\rho_0, t) = (4 \text{ fm})^3$
- Large e-v-e fluctuations
→ separable by event selection?
- Repulsive MF → weaker compression
- Compression owing to interaction

V_3 for various $\sqrt{s_{NN}}$



As $\sqrt{s_{NN}}$ becomes larger,

- $\max V_3(\rho_{\text{th}}, t)$ becomes larger.
- The lifetime of dense region becomes shorter.
- E-v-e fluctuations are more suppressed.

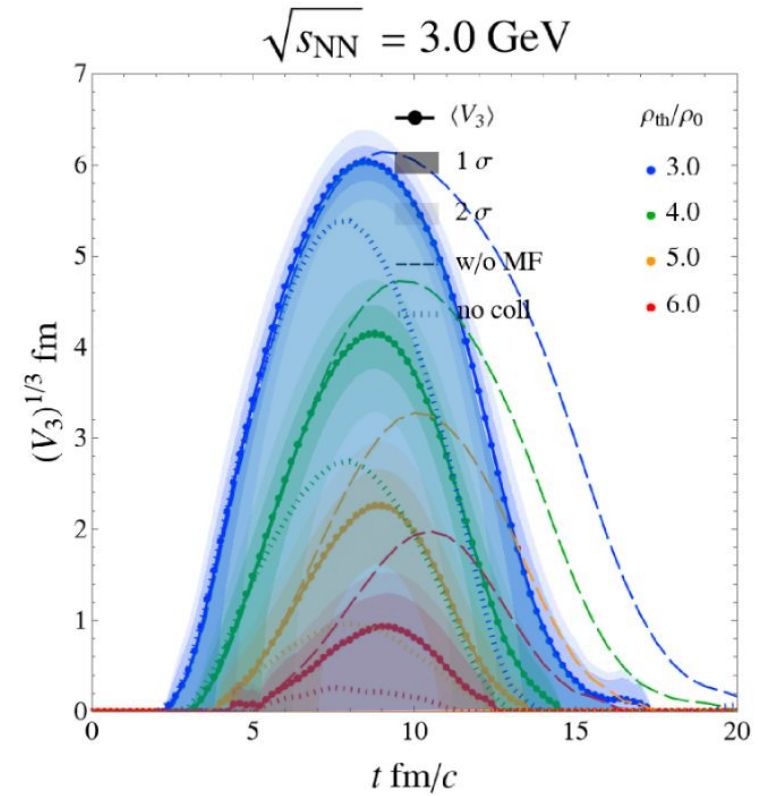
Four-Volume / Lifetime

Four Volume

$$V_4(\rho_{\text{th}}) = \int_{-\infty}^{\infty} dt \int_{\rho(x) > \rho_{\text{th}}} d^3x$$

Lifetime

$$\tau(\rho_{\text{th}}) = \frac{V_4(\rho_{\text{th}})}{\max V_3(\rho_{\text{th}}, t)}$$

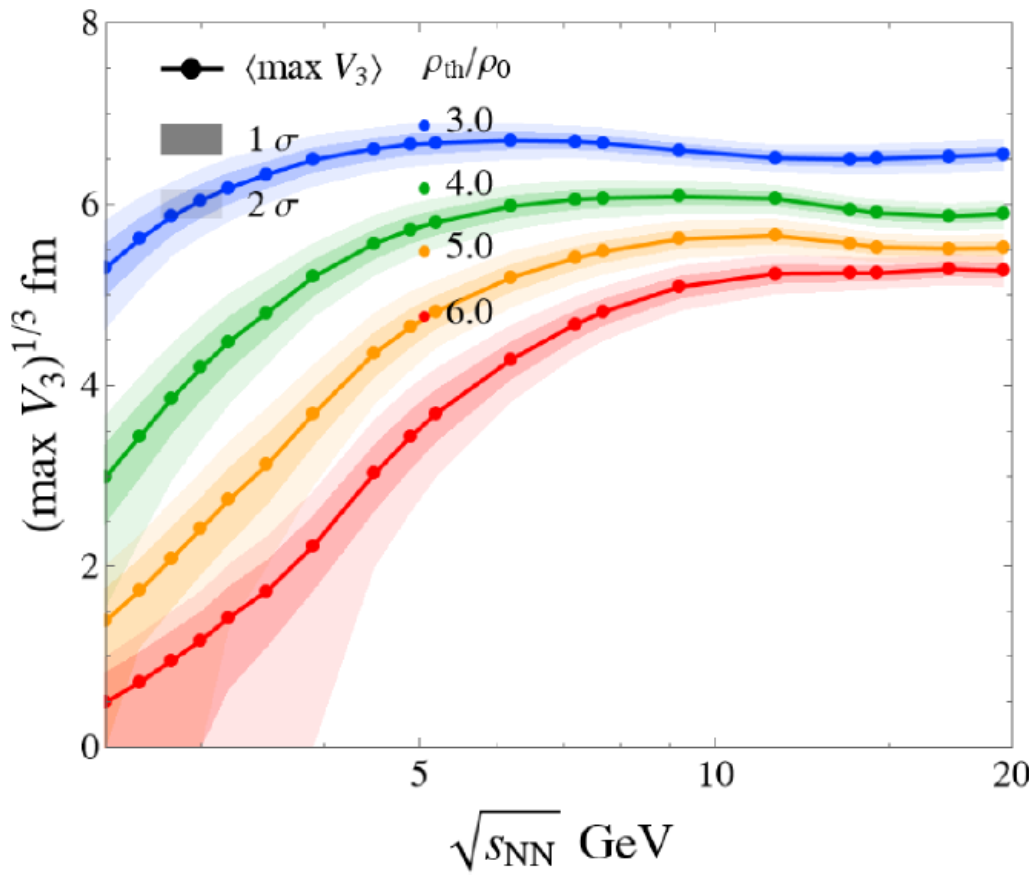


Note

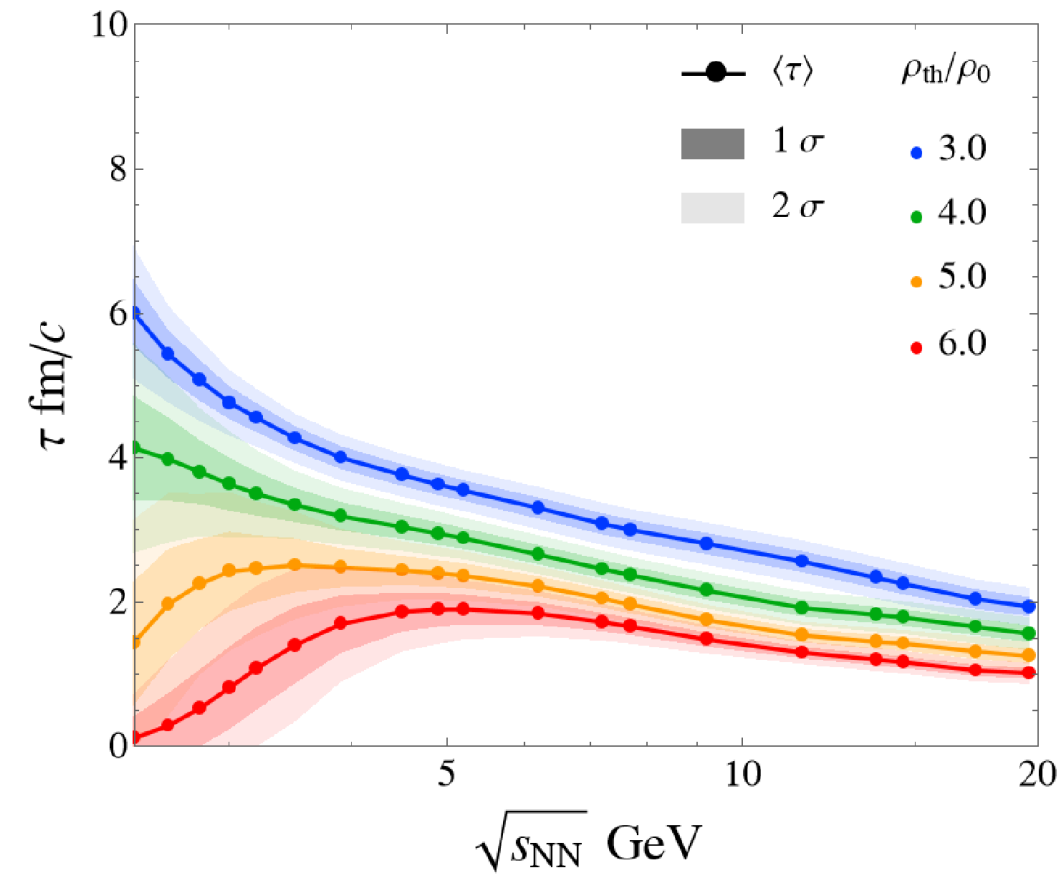
V_4 may be relevant for the dilepton production rate.

$\sqrt{s_{NN}}$ Dependence

$\max V_3$



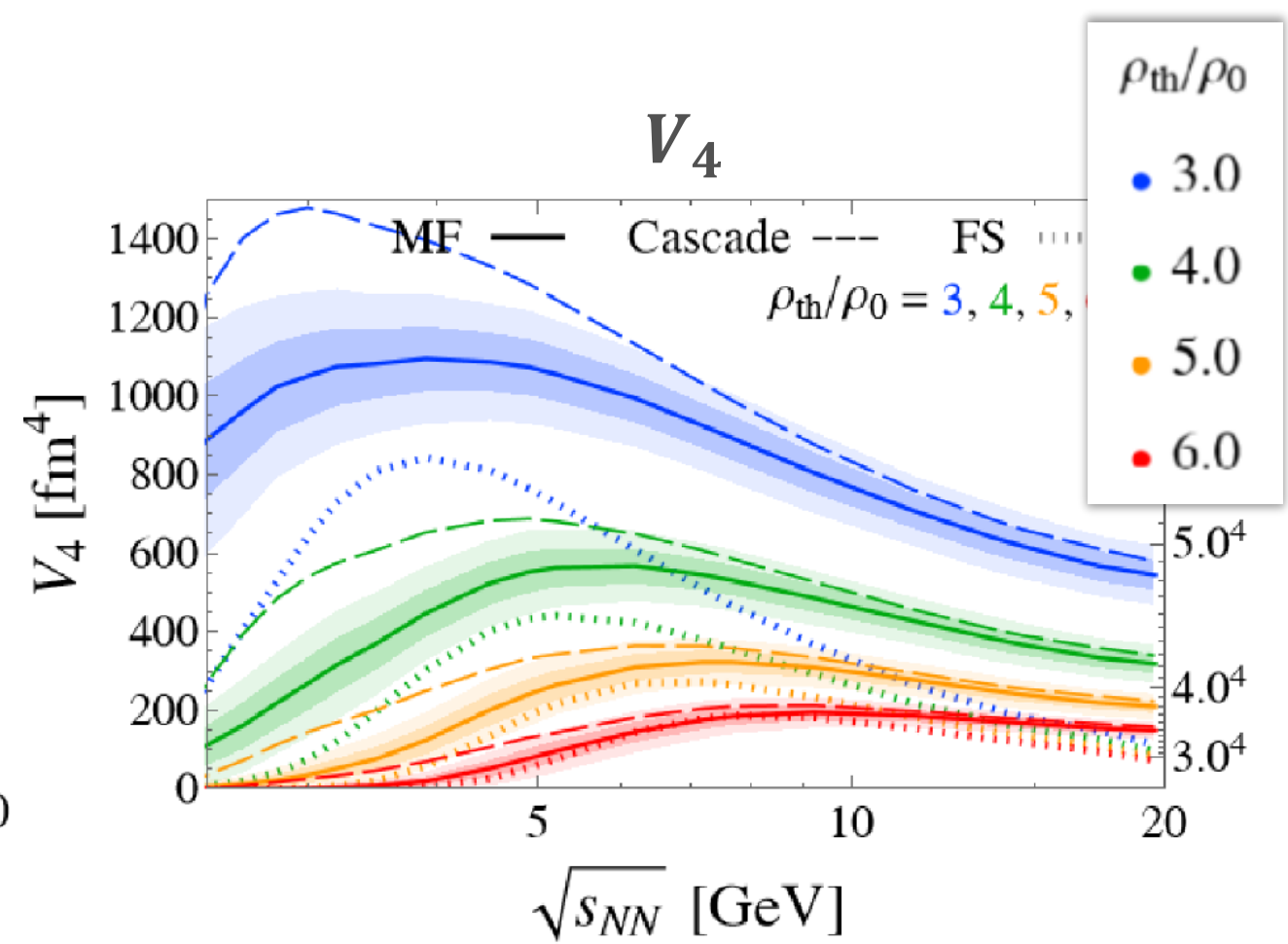
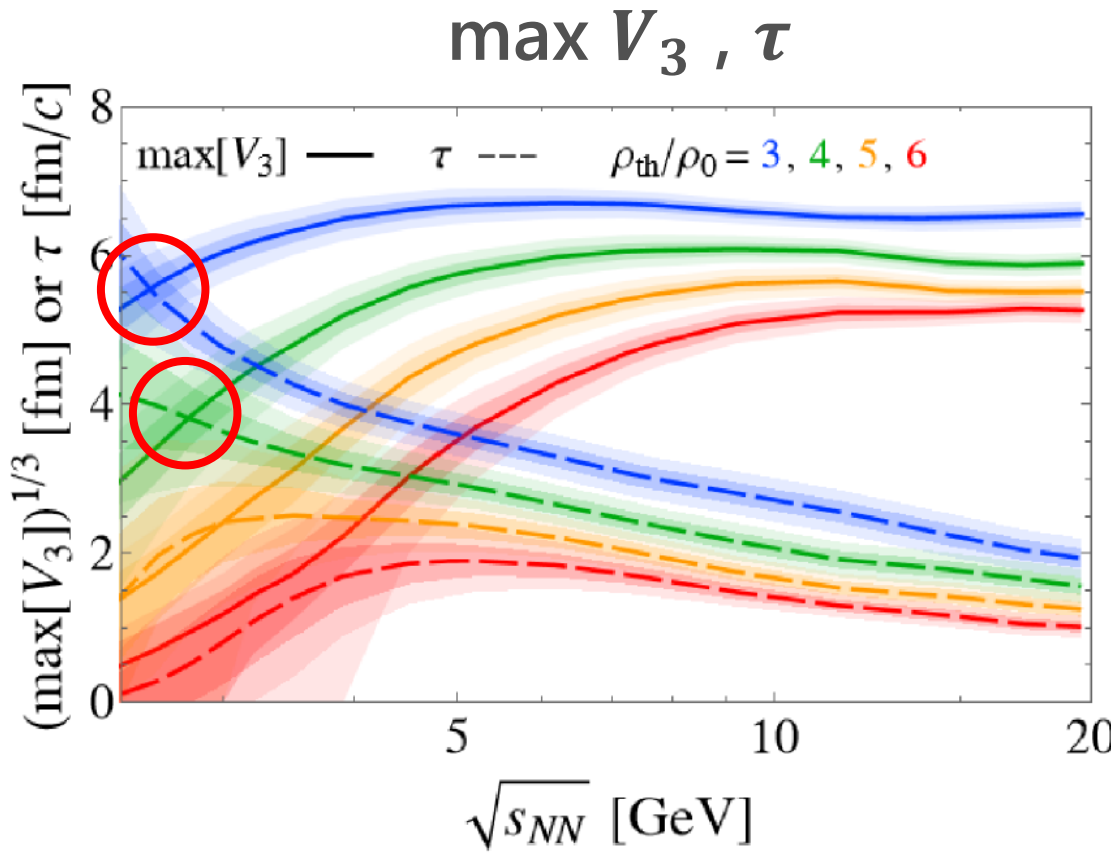
Lifetime



ρ_{th}/ρ_0

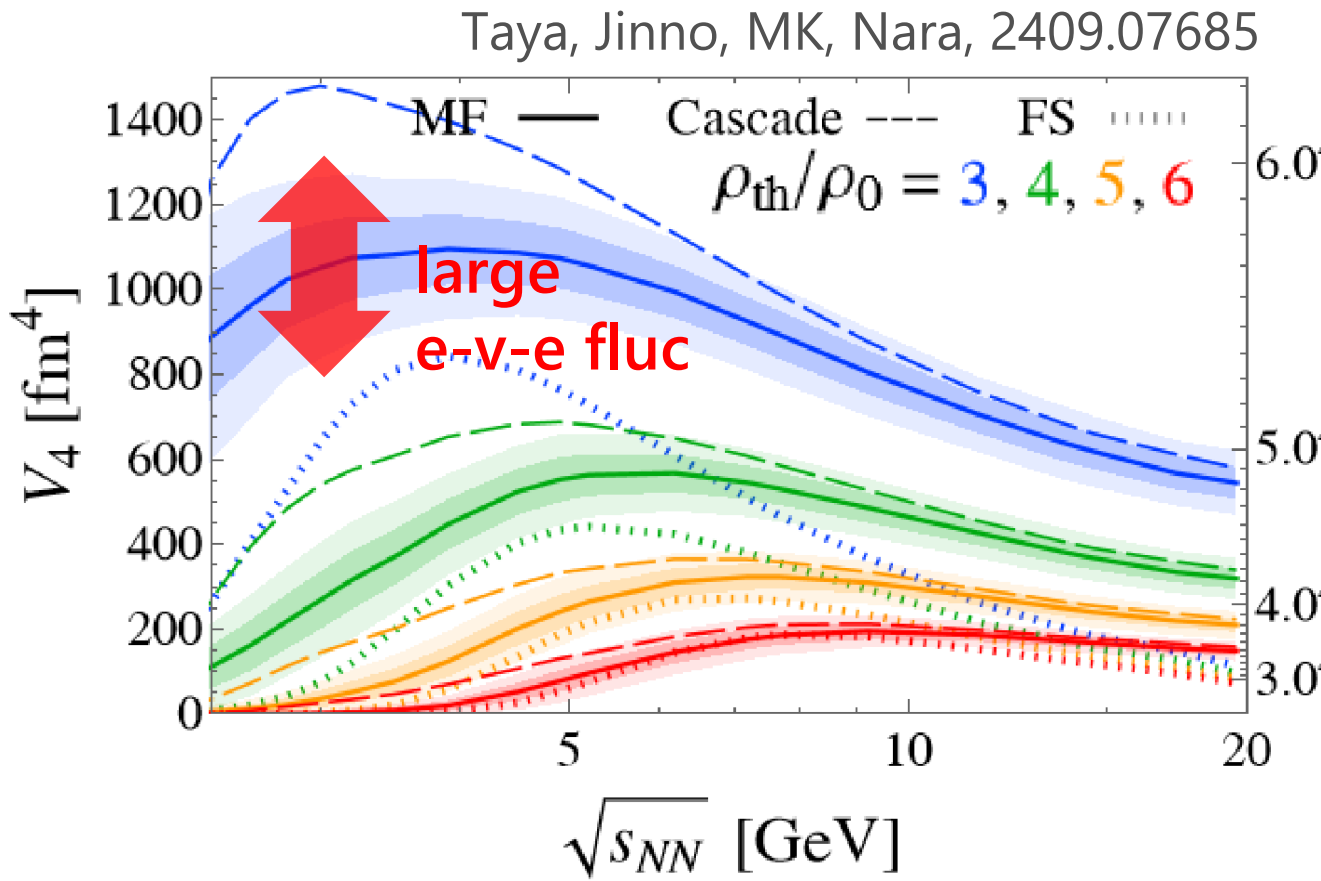
- 3.0
- 4.0
- 5.0
- 6.0

$\sqrt{s_{NN}}$ Dependence

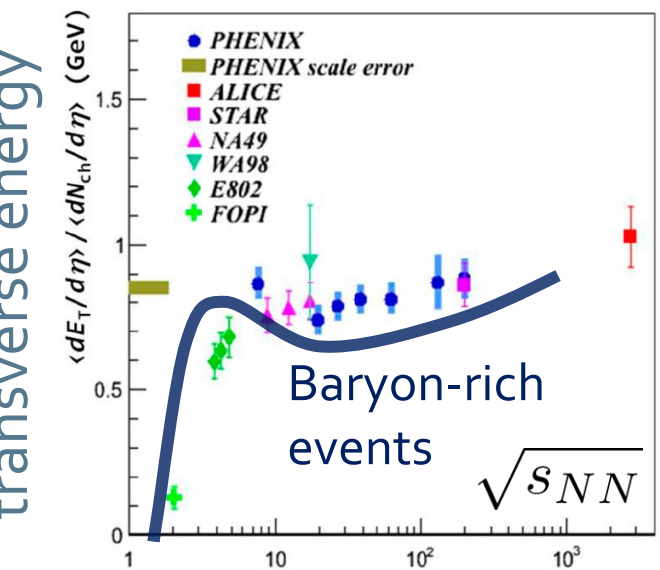
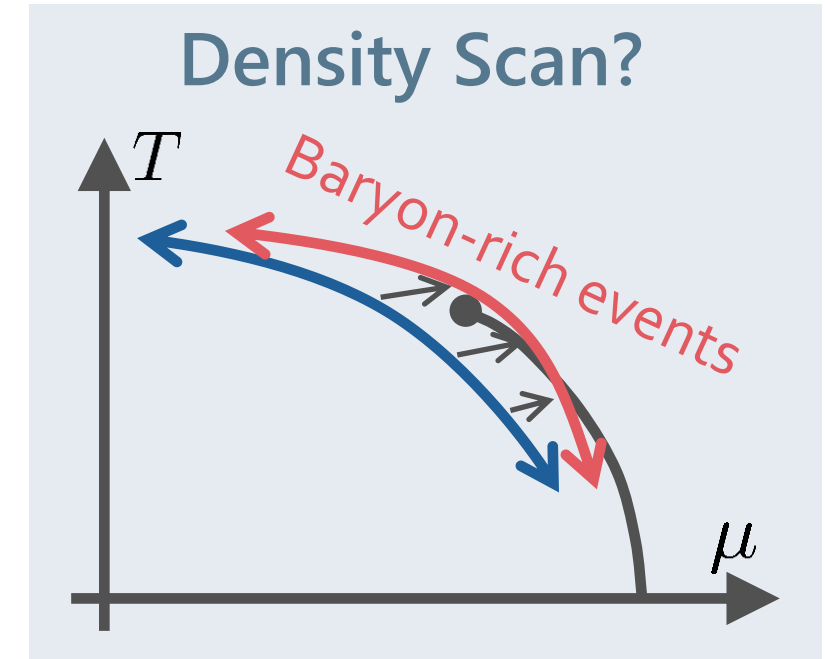


- ◻ $\sqrt{s_{NN}} \approx 3$ GeV would be the best energy to create $\rho = 3 \sim 4 \rho_0$ with large V_3 and τ .
- ◻ Lower $\sqrt{s_{NN}}$ is suitable to create colder matter.

Event Selection



- Event selections via highest baryon/energy density will allow us a detailed study of QCD phase diagram.



Summary

- $\sqrt{s_{NN}} = 3 \text{ GeV}$ is enough to study $\rho = 3\rho_0$.
- $\rho/\rho_0 = 4\sim 5$ may be accessible with $\sqrt{s_{NN}} = 3\sim 6 \text{ GeV}$.

Future

- Check model independence
 - Analyses in various models
- Experiments at the sweet spot $\sqrt{s_{NN}} = 2.5\sim 6 \text{ GeV}$
 - Future exps. at FAIR, NICA, HIAF, & J-PARC-HI

Contents

1. Optimal collision energy for studying dense matter in heavy-ion collisions

Taya, Jinno, MK, Nara, 2409.07685

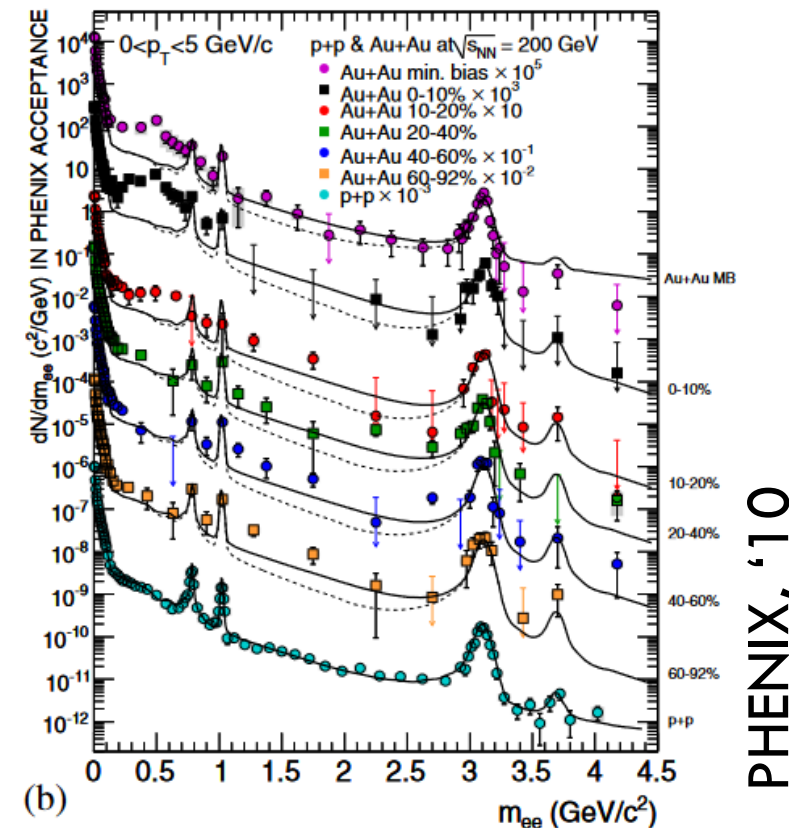
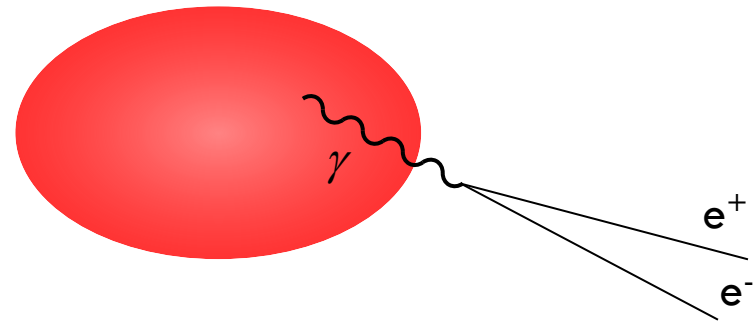
2. Dilepton production for a signal of phase transitions in dense matter

Nishimura, MK, Kunihiro, Ann. Phys. 469 (2024) 169768; PTEP 2023, 053D01; PTEP 2022, 093D02

3. Novel critical points in SU(3) Yang-Mills theory with boundary conditions

MK+, PRD99 (2019) 094507; Suenaga, MK, PRD107 (2023) 074502; Fujii, Iwanaka, Suenaga, MK, PRD110 (2024) 094016

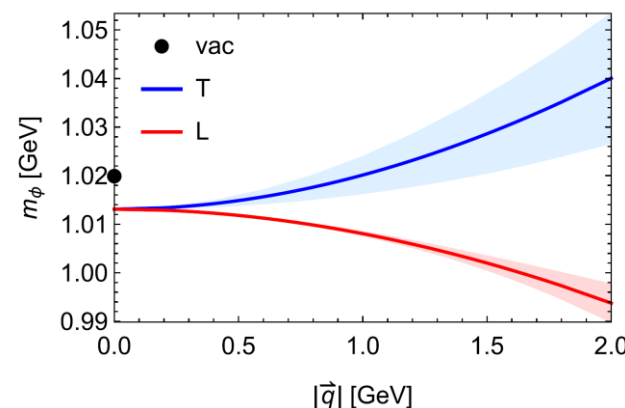
Dilepton Production Rate



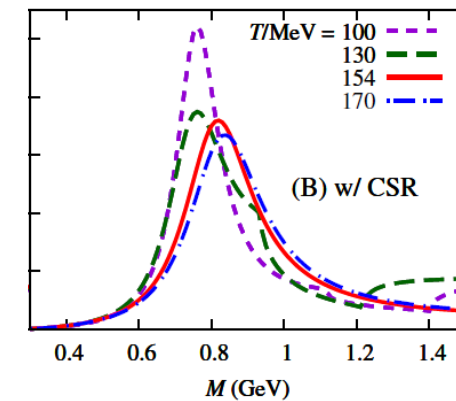
- Generated by the decay of virtual photons
- Carry information of primordial medium

Physics accessible with DPR

- Medium temperature
- Dispersion relations
- Chiral mixing by chiral restoration
- Signal of phase transitions



Kim, Gubler, 2020



Sakai+, 2024

Soft Modes of Second-order Phase Transitions

□ Soft modes

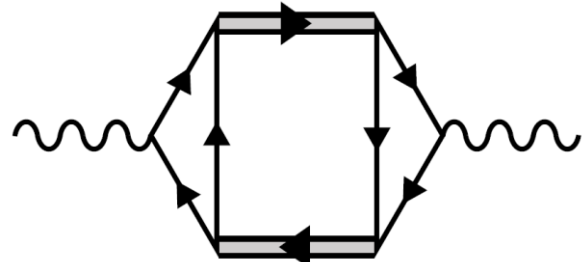
- Divergence of the order-parameter fluctuations at a 2nd-order transition.
- Collective fluctuations become massless there.
- QCD-CP : density-density fluctuations
- CSC : diquark-pair field



$$\begin{aligned} \text{QCD-CP: } & \text{Diagram of two loops connected by a horizontal line, followed by a plus sign and three dots.} \\ \text{CSC: } & \text{Diagram of two loops connected by a horizontal line, followed by a plus sign and three dots.} \end{aligned}$$

□ Coupling of soft modes with dynamical observables

- Ex.: dilepton production rate

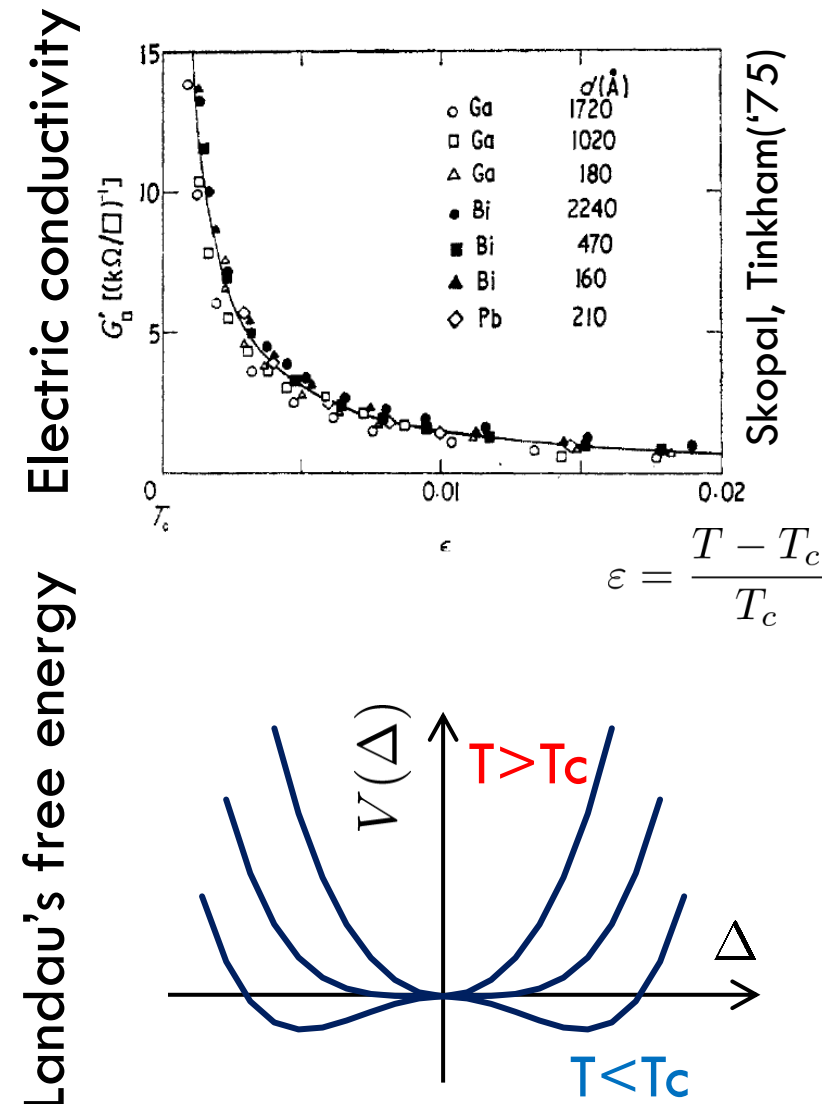


Precursor in Metallic Superconductors

□ Anomalous behavior of observables near but above T_c of SC

- electric conductivity
- magnetic susceptibility
- pseudogap

- Enhanced pair fluctuations is one of the origins of precursory phenomena.
- More significant phenomena in strongly-coupled systems.

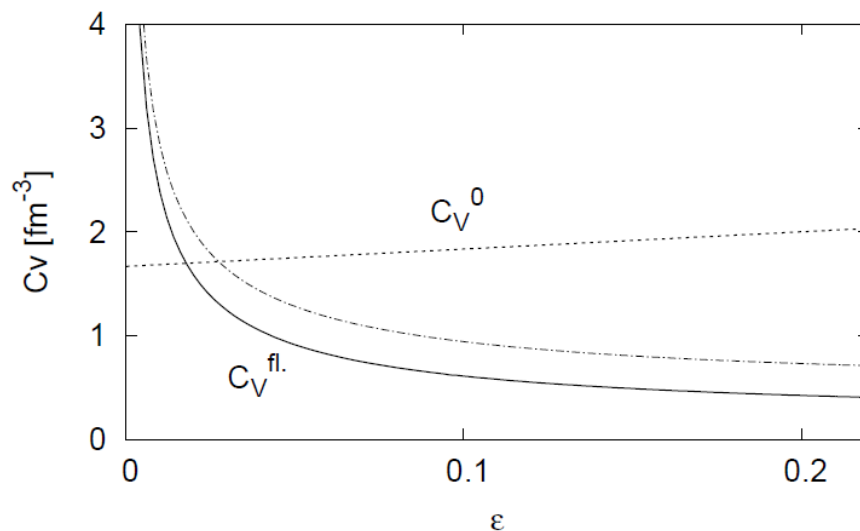


Precursor of Color Superconductivity

MK, Koide, Kunihiro, Nemoto, '03, '05

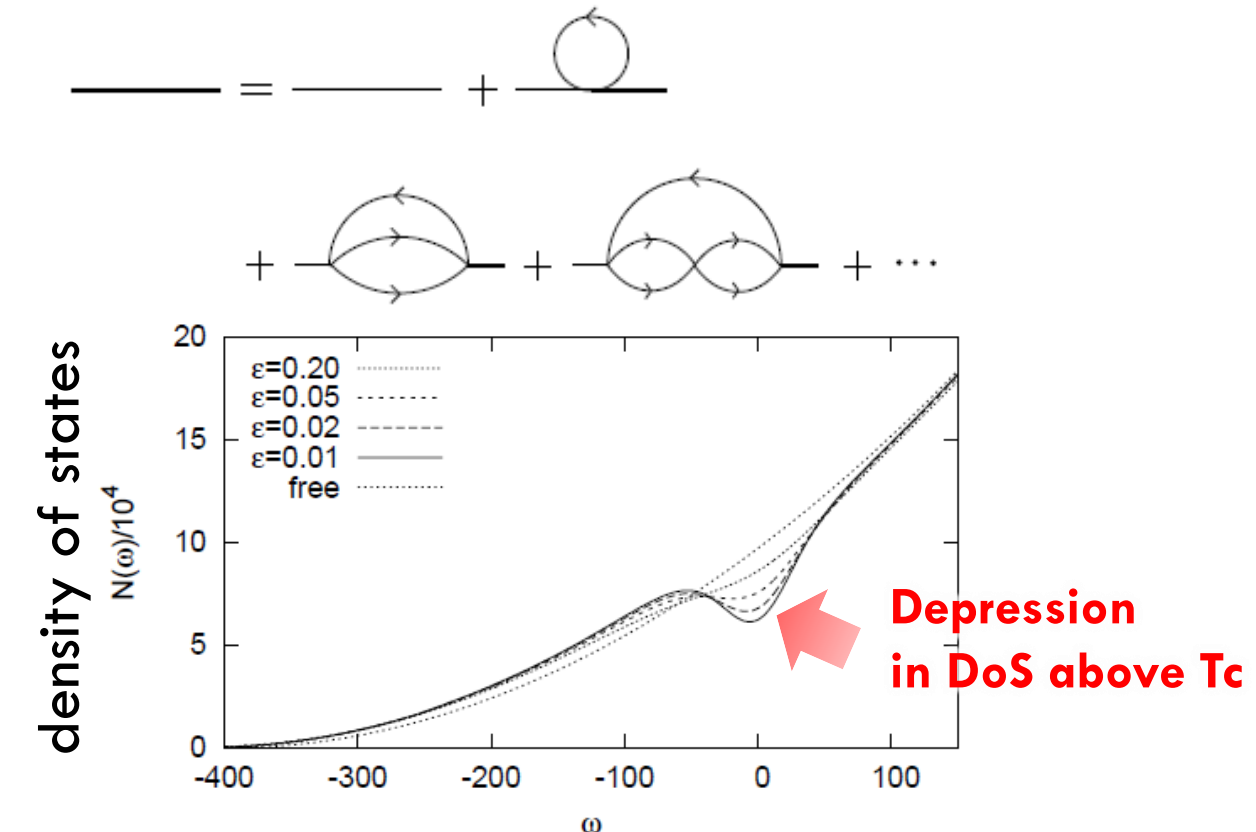
□ Thermodynamic Potential

$$\Omega = \text{Diagram of a loop with arrows} \rightarrow \text{Specific heat}$$
$$c = -T \frac{\partial^2 \Omega}{\partial T^2}$$



$$\varepsilon = \frac{T - T_c}{T_c}$$

□ Pseudogap



Model

NJL model (2-flavor)

$$\mathcal{L} = \bar{\psi} i\partial^\mu \psi + \mathcal{L}_S + \mathcal{L}_C$$

$$\mathcal{L}_S = G_S ((\bar{\psi}\psi)^2 + (\bar{\psi}i\gamma_5\tau\psi)^2)$$

$$\mathcal{L}_C = G_C ((\bar{\psi}i\gamma_5\tau_A\lambda_A\psi^C)(\text{h.c.})$$

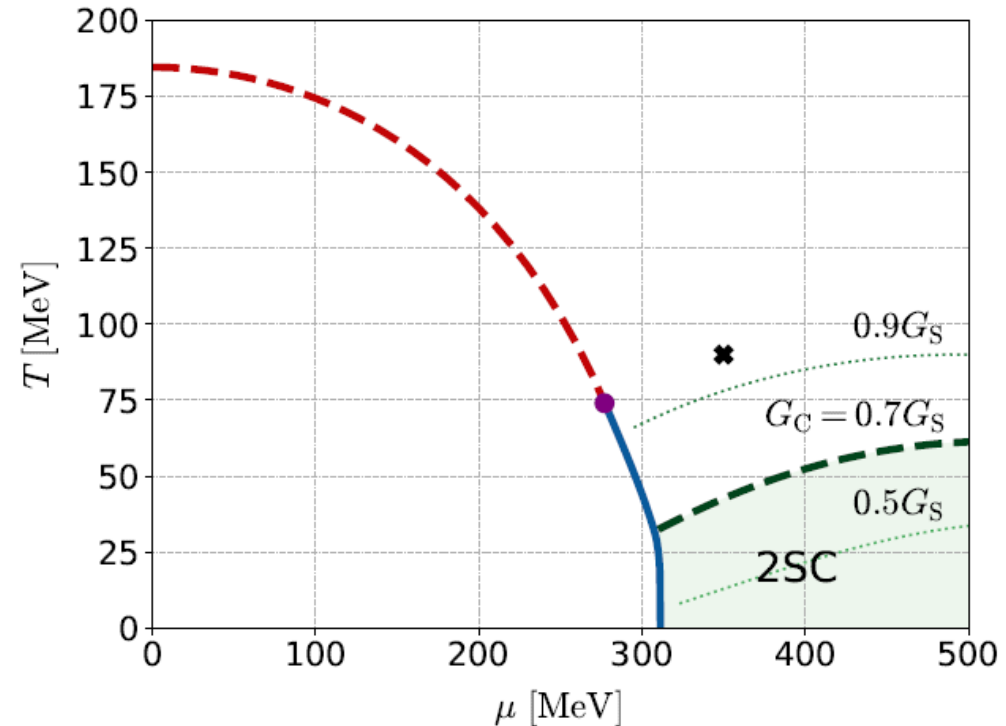
diquark interaction

Parameters

$$G_S = 5.01 \text{ GeV}^{-2}, \quad \Lambda = 650 \text{ MeV}, \quad m_q = 0$$



Phase Diagram in MFA



- Order of phase transition
 - 2nd in the MFA
 - can be 1st due to gauge fluctuation

Matsuura+(’04), Giannakis+(’04)
Noronha+(’06), Fejos, Yamamoto(’19)

Di-quark Fluctuations

□ Diquark Propagator

$$D^R(x) = \langle [\Delta^\dagger(x), \Delta(0)] \rangle \theta(t) = \Rightarrow$$

□ Random Phase Approximation

$$\Rightarrow = \text{---} + \text{---} + \dots$$

$$= \frac{Q^R(\mathbf{k}, \omega)}{1 + G_C Q^R(\mathbf{k}, \omega)}$$

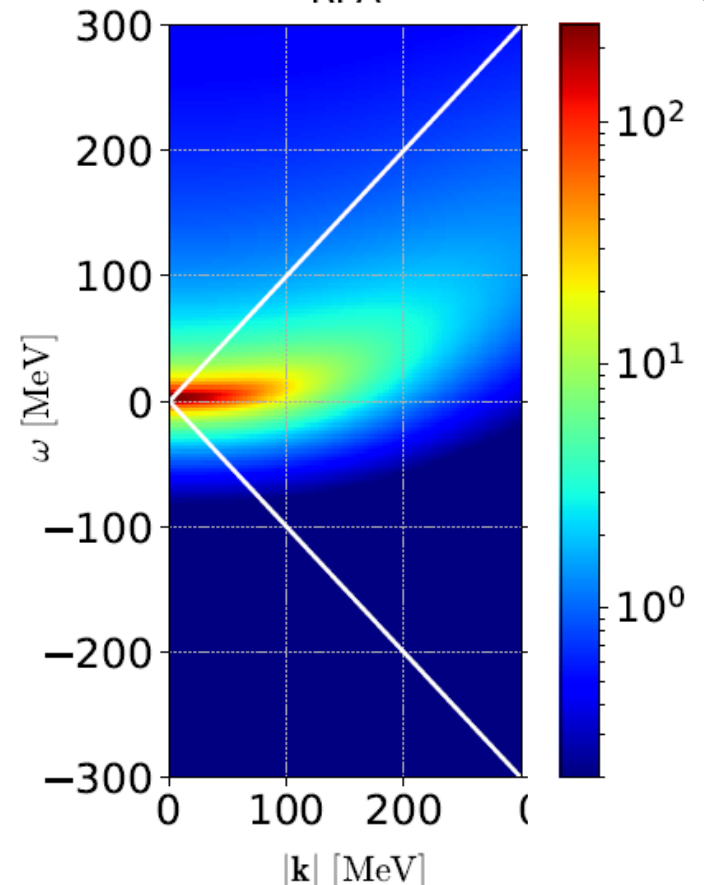
$$Q^R(\mathbf{k}, \omega) = \text{---}$$

- Diquark field becomes massless at $T=T_c$
- Soft mode of CSC transition
- Strength in the space-like region

Dynamical Structure Factor

$$S(\mathbf{k}, \omega) = -\frac{1}{\pi} \frac{1}{1 - e^{-\beta\omega}} \text{Im}D^R(\mathbf{k}, \omega)$$

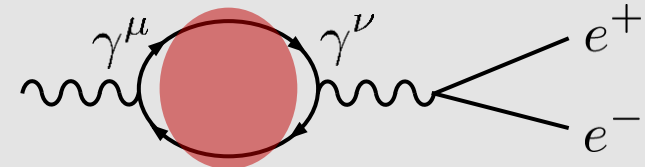
RPA $T = 1.05T_c$



Photon Self-Energy: Precursor of CSC

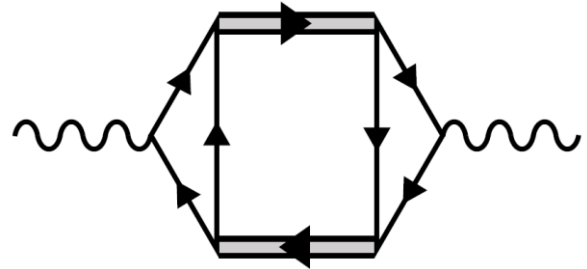
□ Dilepton Production Rate

$$\frac{d^4\Gamma}{dk^4} = \frac{\alpha}{12\pi^4} \frac{1}{k^2} \frac{1}{e^{\beta\omega-1}} \text{Im}\Pi_\mu^{R\mu}(k)$$

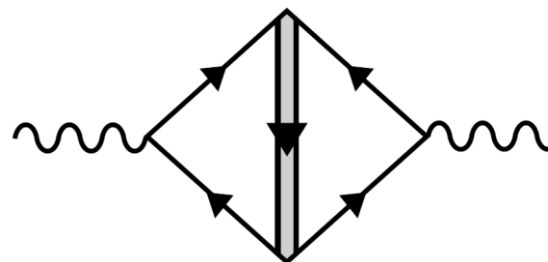


□ Effect of Di-quarks on $\Pi^{\mu\nu}(k)$

Aslamasov-Larkin term



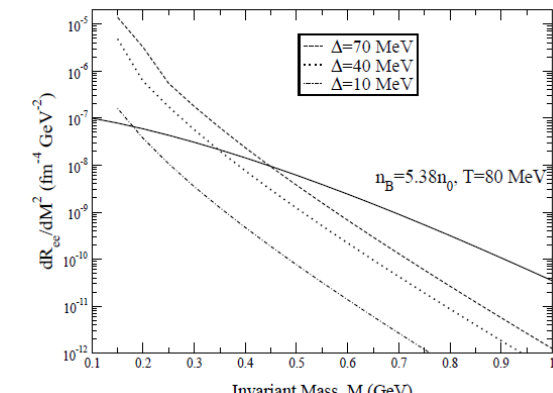
Maki-Thompson term



Well-known diagrams in metallic SC
for describing paraconductivity

□ DPR from CFL phase

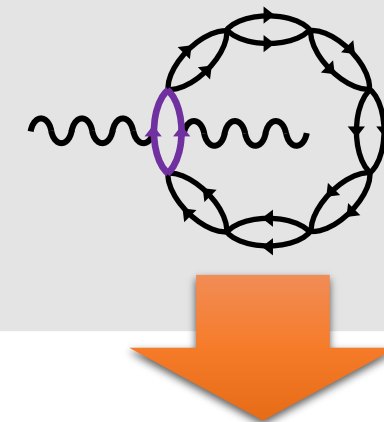
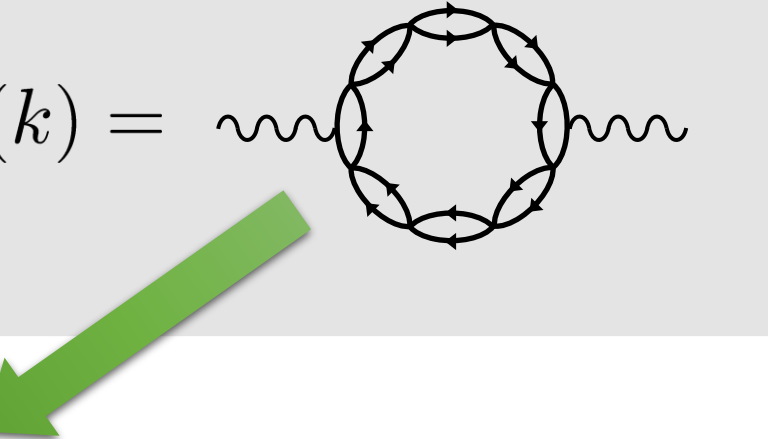
Jaikumar, Rapp, Zahed ('02)



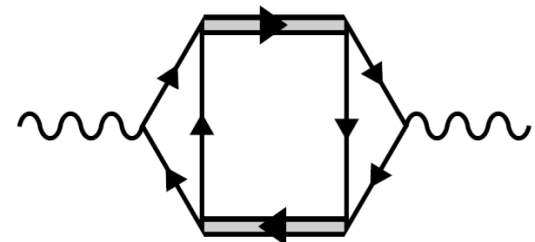
Gauge-Invariant Construction of $\Pi_{\mu\nu}(k)$

Insert two photon vertices in thermodynamic potential

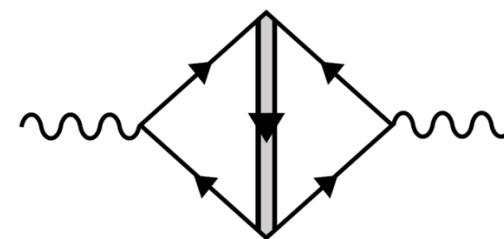
$$\Pi^{\mu\nu}(k) =$$



Aslamasov-Larkin (AL)



Maki-Thompson (MT)



Density of States (DoS)



- WT identity $k_\mu \Pi^{\mu\nu}(k) = 0$ is satisfied with AL, MT and DoS terms.

(Modified) Time-Dependent Ginzburg-Landau Approximation

TDGL approximation for T-matrix

$$\Xi^R(\mathbf{k}, \omega) = \frac{G_C}{1 + G_C Q^R(\mathbf{k}, \omega)} \simeq \frac{1}{c\omega + \Xi^R(\mathbf{k}, 0)^{-1}} \quad c = \frac{\partial(\Xi^R)^{-1}}{\partial\omega} \Big|_{\omega=0}$$

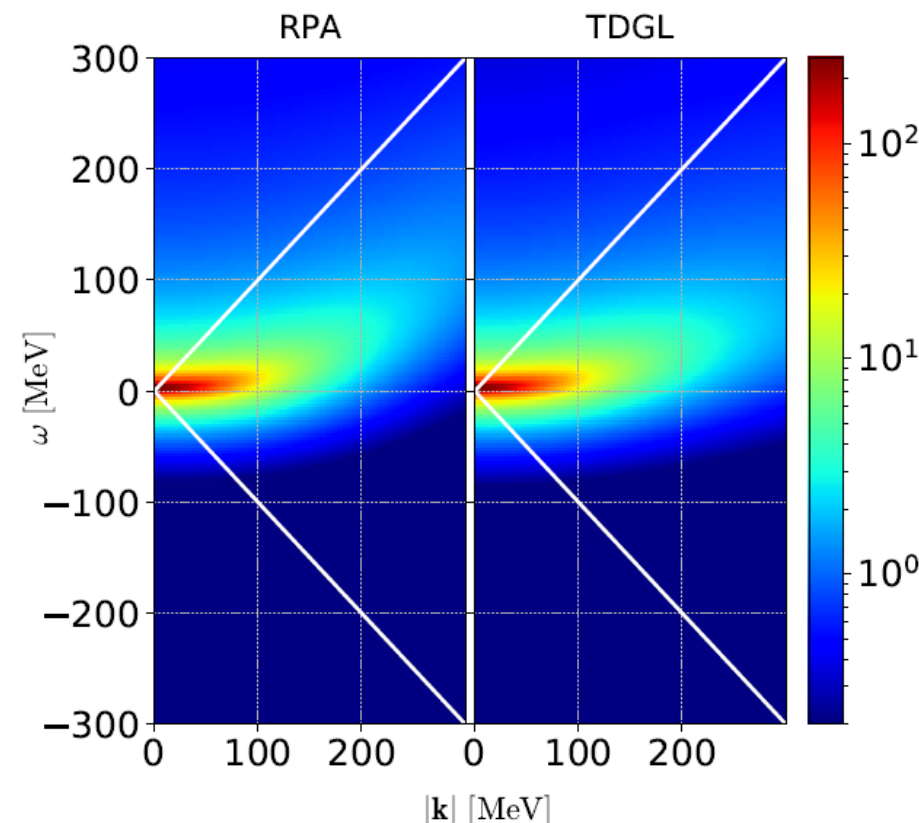
$$\begin{aligned}\Xi^R(\mathbf{k}, \omega) \\ = \frac{G_C}{Q^R(\mathbf{k}, \omega)} D^R(\mathbf{k}, \omega)\end{aligned}$$

Note:

- ◻ Valid in low energy region
- ◻ $[\Xi^R(0,0)]^{-1} = 0$ at $T = T_c$
- ◻ We do not expand w.r.t. \mathbf{k}

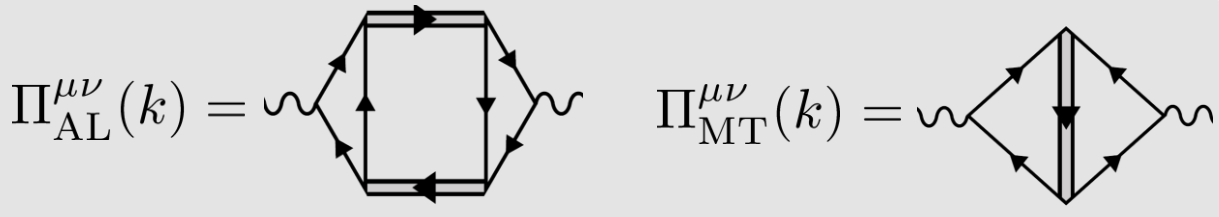
$$\Xi^R(\mathbf{k}, \omega) \simeq \frac{1}{c\omega + \Xi^R(\mathbf{k}, 0)^{-1}} \simeq \frac{1}{c\omega + a + b\mathbf{k}^2}$$

↔ TDGL equation: $ic\frac{\partial}{\partial t}\Delta + a\Delta - b\nabla^2\Delta = 0$



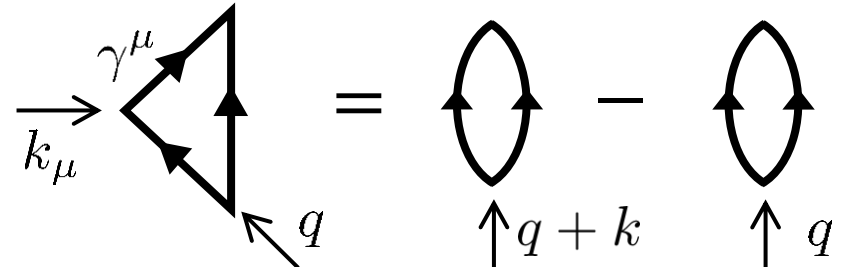
Vertices

Vertices must be determined to be consistent with the TDGL approx.



□ WT identity for AL vertex

$$k_\mu \Gamma^\mu(q, q+k) = \Xi^{-1}(q+k) - \Xi^{-1}(q)$$

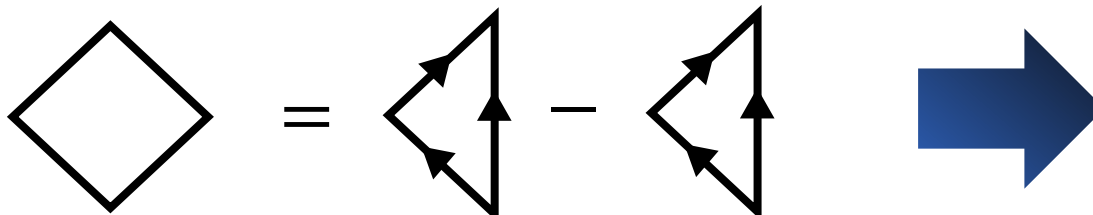


At the lowest order in k

$$\left\{ \begin{array}{l} \Gamma^0 = e_\Delta c \\ \Gamma^i = e_\Delta \frac{\partial^2 \Xi(q)^{-1}}{\partial q^2} (2q^i + k^i) \end{array} \right.$$

e_Δ : electric charge of diquarks

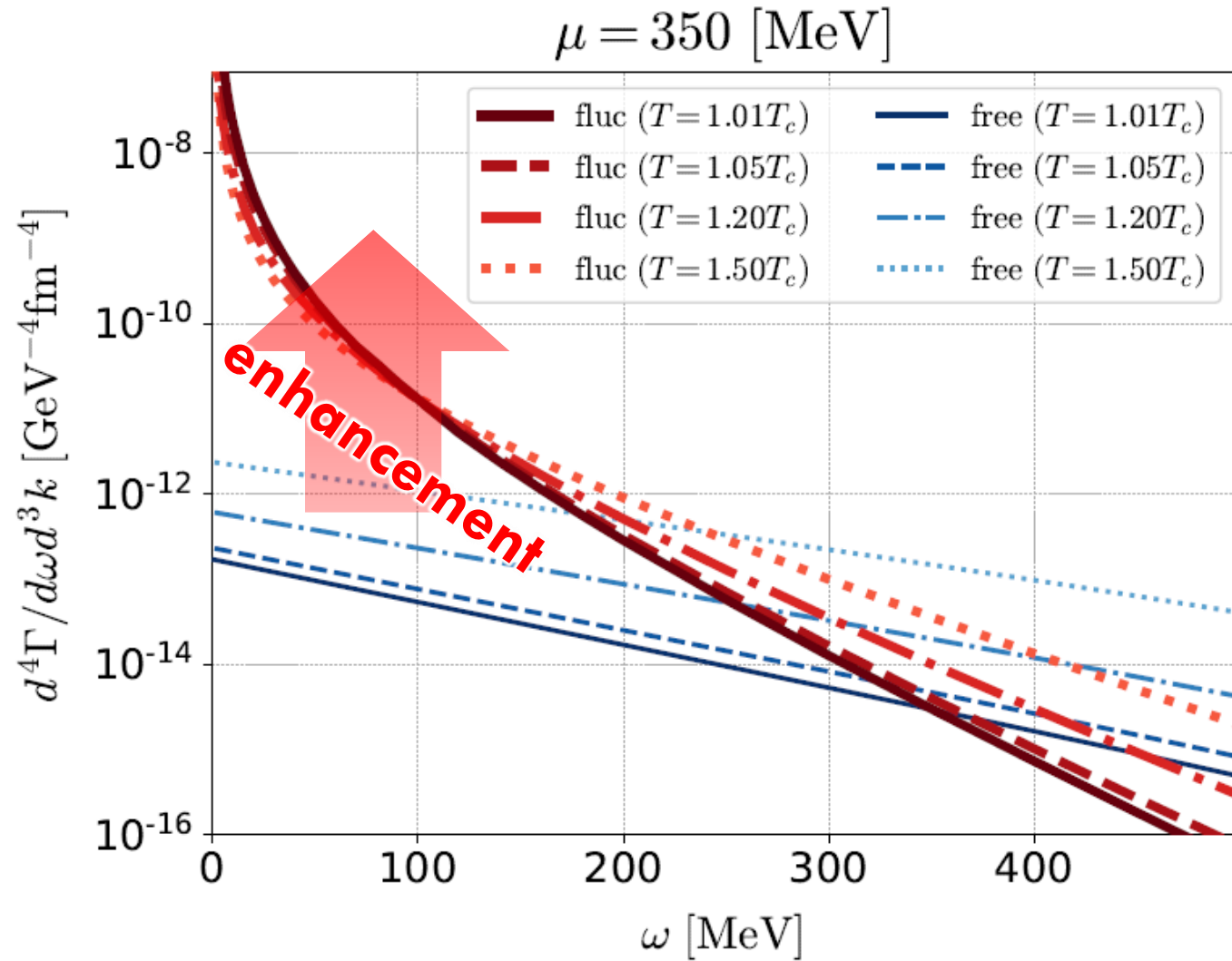
□ MT+DoS



Similar formula for
MT+DoS vertex

Production Rate at $k = 0$

Nishimura, MK, Kunihiro ('22)



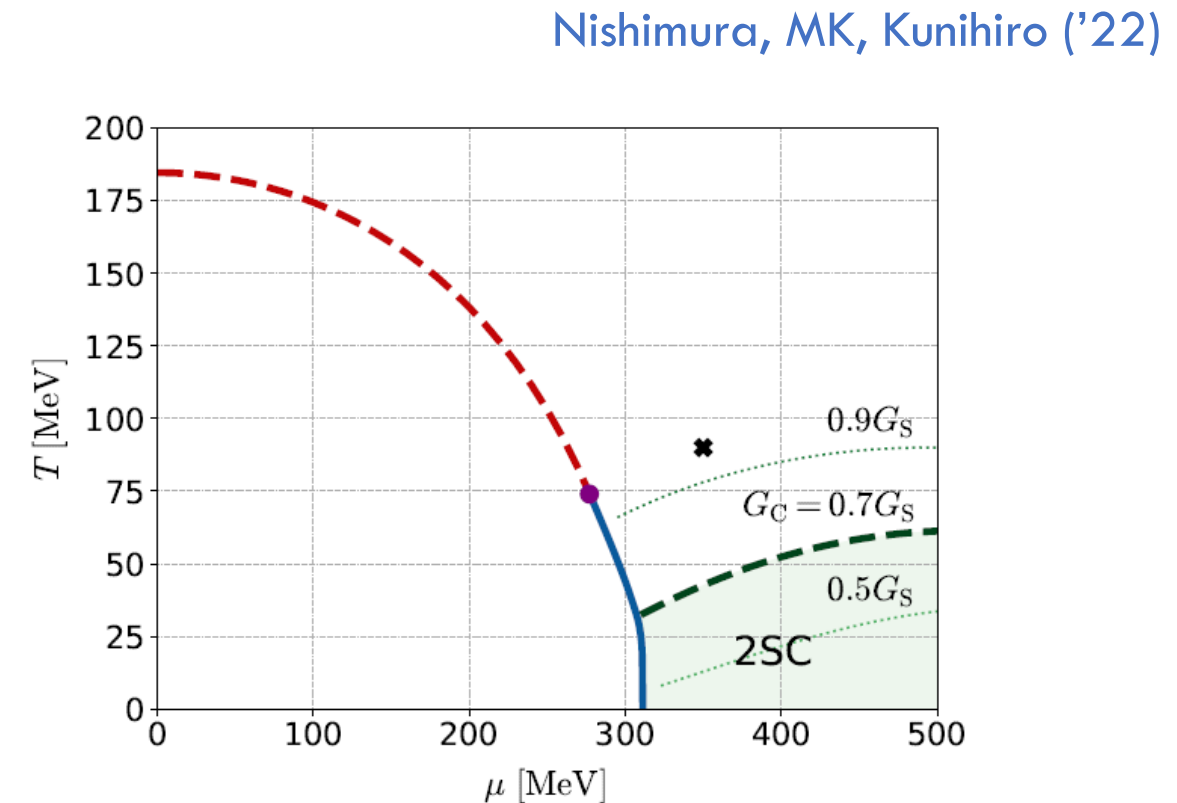
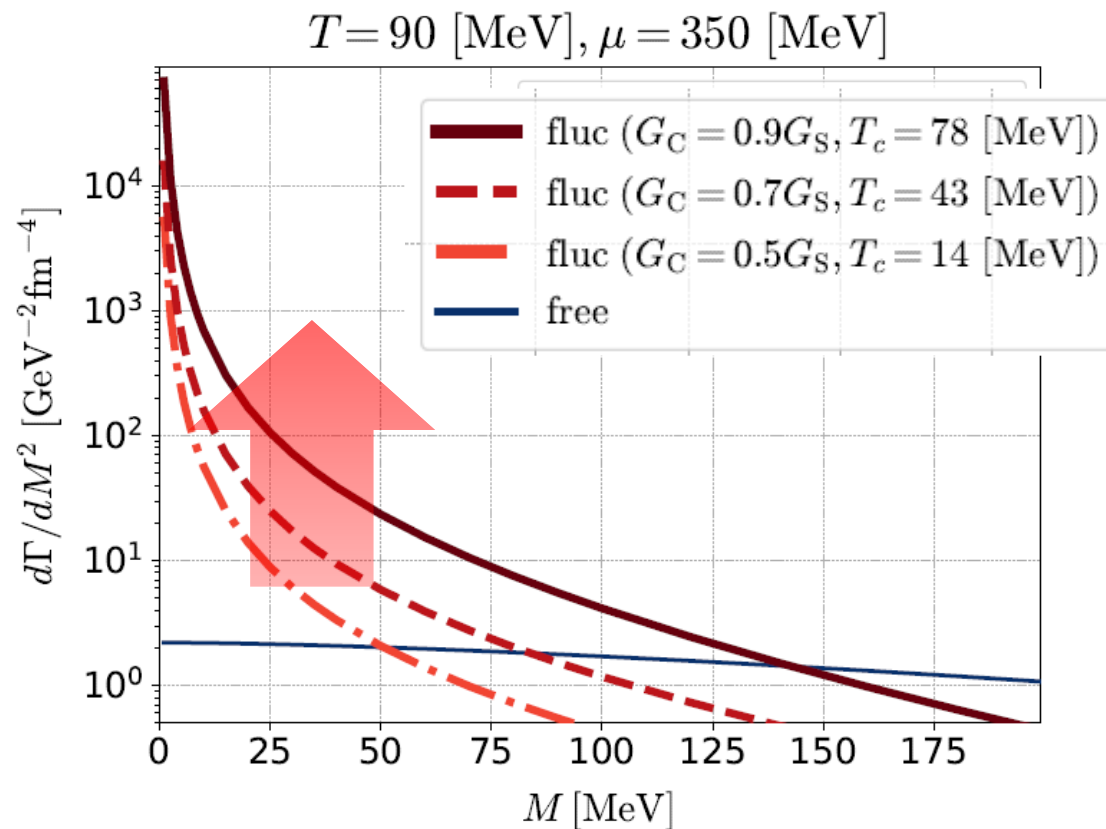
Red: fluctuation contribution

Blue: free quarks

$$G_C = 0.7G_S, T_c \simeq 45 \text{ MeV}$$

- Di-quark fluctuations give rise to large enhancement in the low energy region $\omega < 200 \text{ MeV}$ and $T < 1.5T_c$.
- Anomalous enhancement is not sensitive to T .

Invariant-Mass Spectrum



- Strong enhancement at low invariant mass.
- Observable in the HIC?

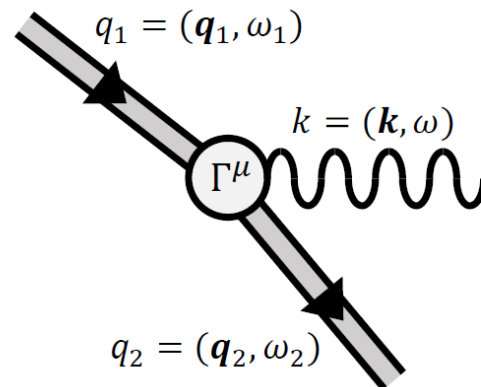
Production Mechanism of Virtual Photons

□ Production mechanism

- scattering of diquarks
- diquarks: **space-like region**

$$\omega = \omega_1 - \omega_2$$

$$k = q_1 - q_2$$

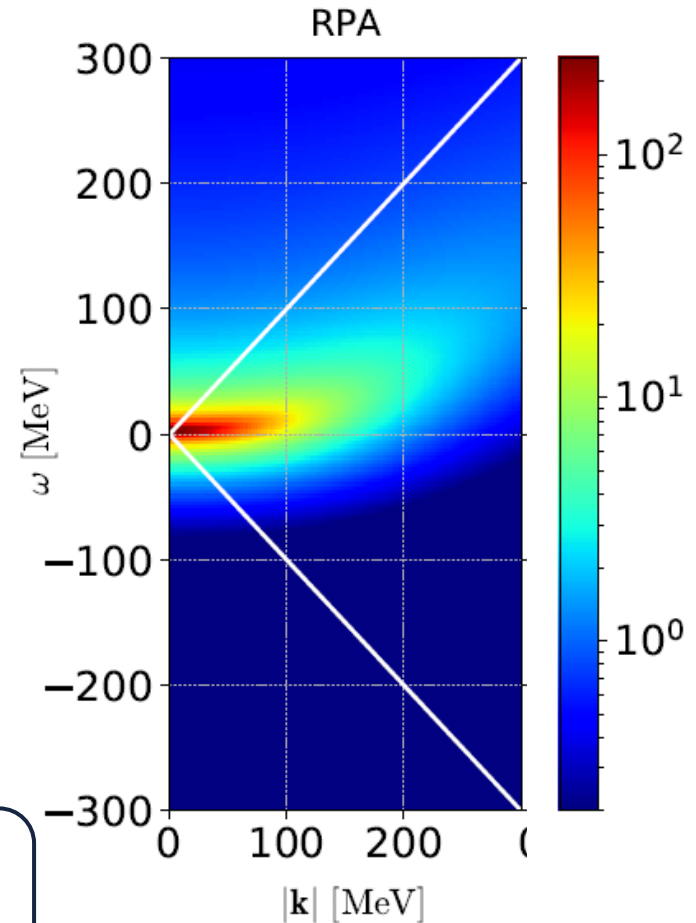
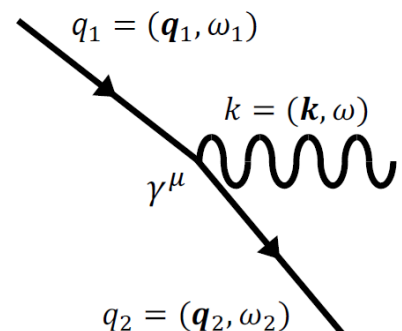


→ Production in the **time-like region** is possible.



- C.f.) Scattering of free quarks produces virtual photons only in the **space-like region**.

$$|q_1 - q_2| \geq \omega_1 - \omega_2$$



Dileptons from QCD Critical Point

NJL model (2-flavor)

$$\mathcal{L} = \bar{\psi}(i\cancel{\partial} - m)\psi + G_S((\bar{\psi}\psi)^2 + (\bar{\psi}i\gamma_5\tau\psi)^2)$$

Parameters

$$G_S = 5.5 \text{ GeV}^{-2}, \Lambda = 631 \text{ MeV}, m_q = 5.5 \text{ MeV}$$

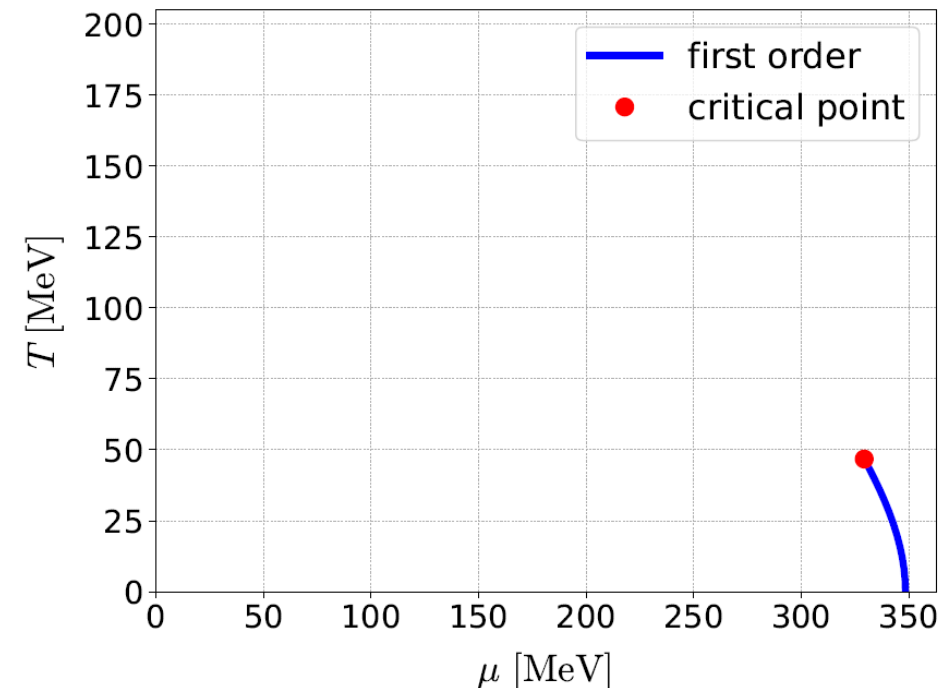
Soft Mode of QCD-CP

= fluctuation of scalar ($\bar{q}q$) channel

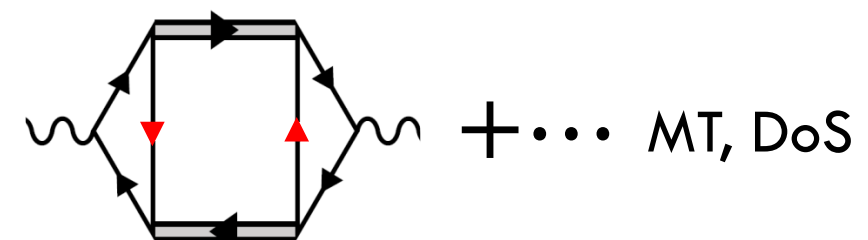
$$D^R(x) = \langle [\bar{\psi}\psi(x), \bar{\psi}\psi(0)] \rangle \theta(t) = \Rightarrow$$

Random Phase Approximation

$$\Rightarrow = \text{loop diagram} + \text{loop diagram} + \dots$$

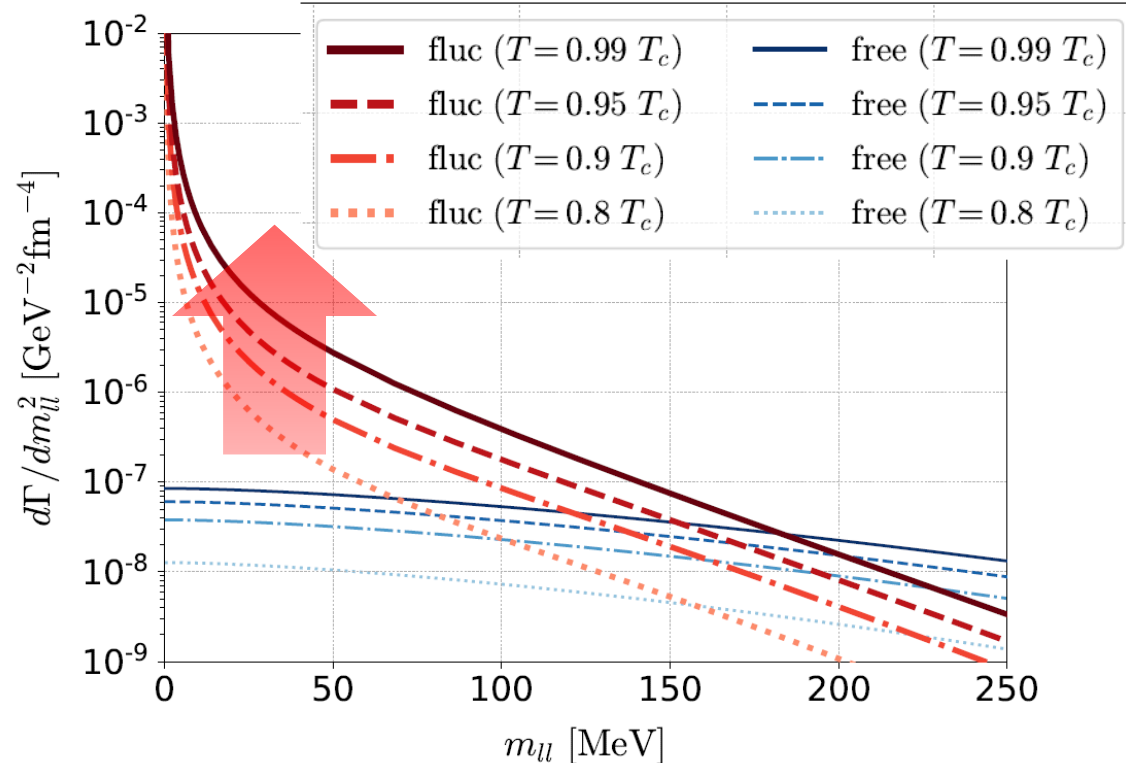


Modification of dilepton production through

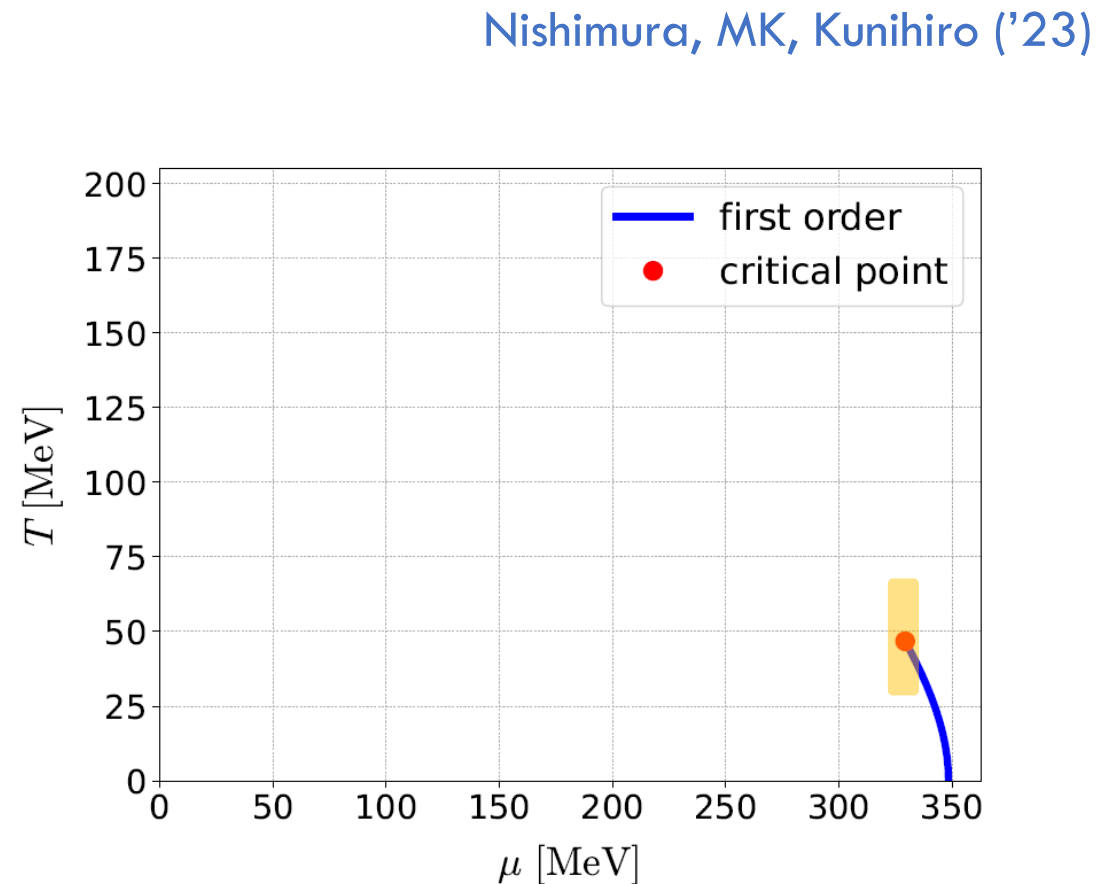


Dilepton production rate near QCD-CP

Invariant mass spectrum



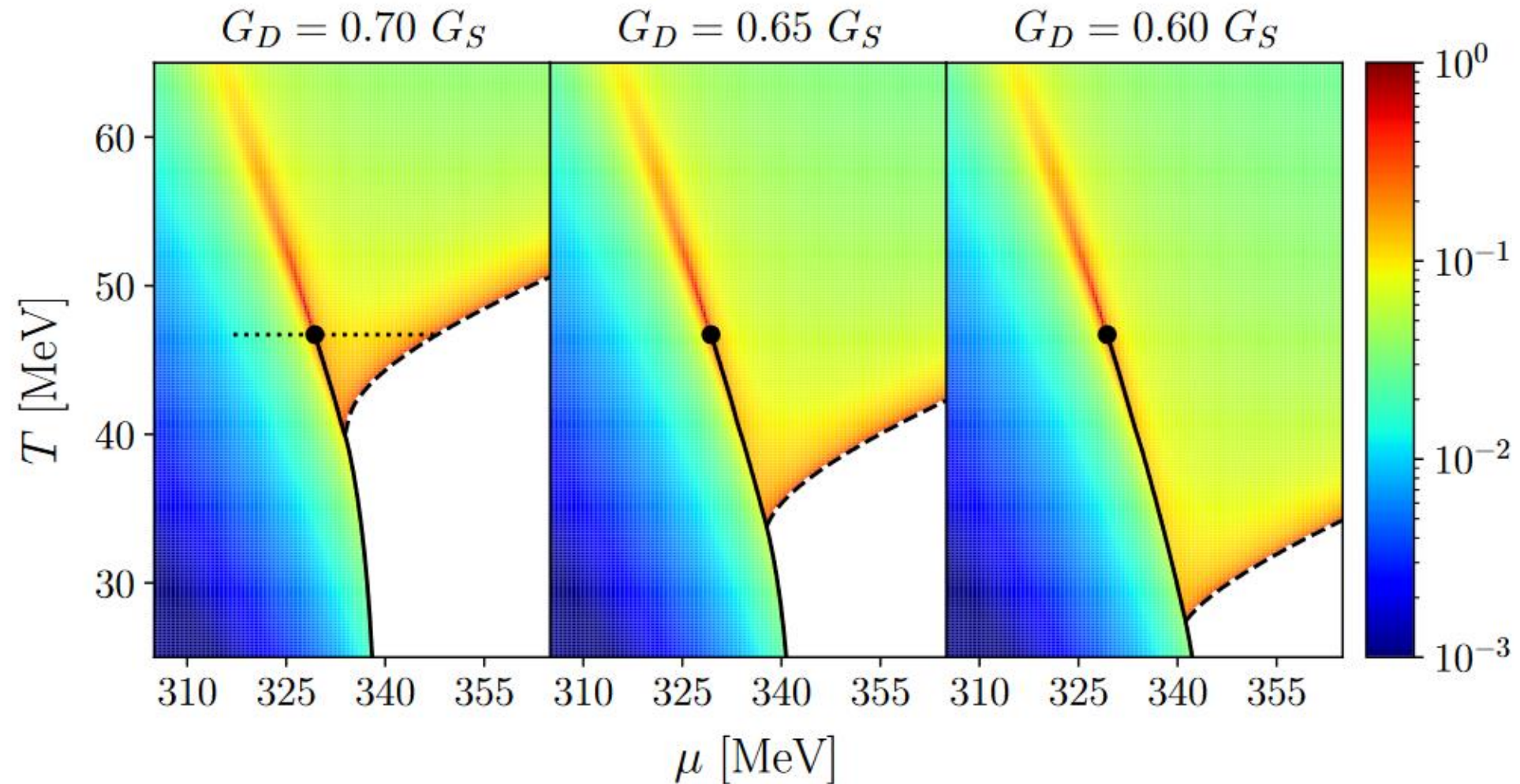
for fixed chem. pot.: $\mu = \mu_c$



- ❑ Enhancement at low M_{ll} region near QCD-CP
- ❑ Distinguishment from diquark soft mode may be difficult.

Nishimura, MK, Kunihiro ('23)

Electric Conductivity on QCD Phase Diagram

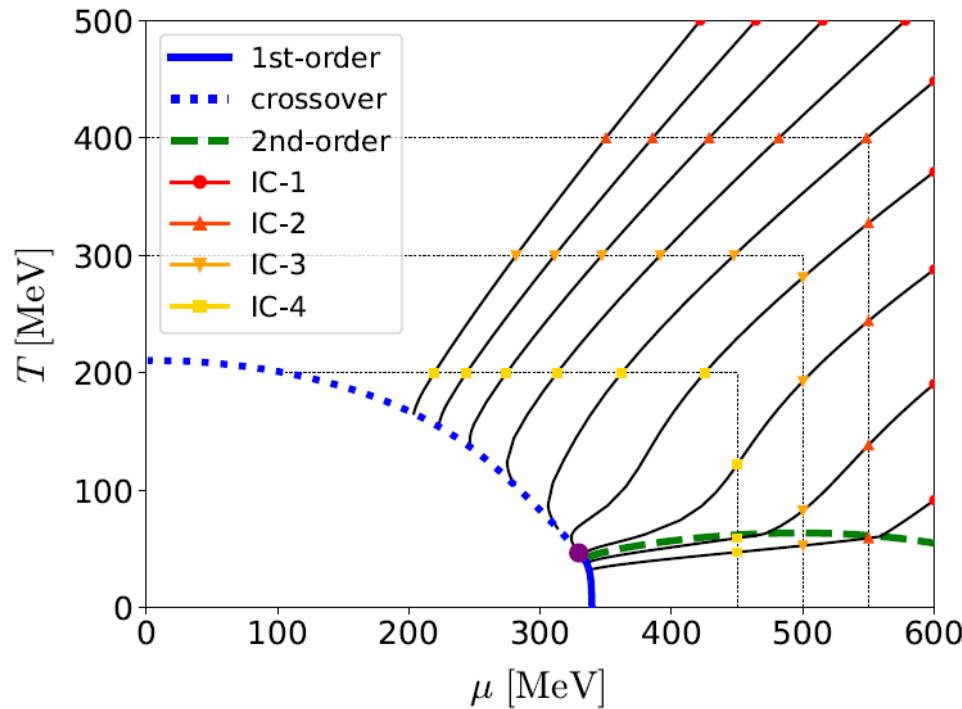


- ◻ DPR in the low-energy limit = electric conductivity
- ◻ Two “hot spots” on the T - μ plane

Dilepton Yields: Beam-Energy Scan

Dilepton yields
 \simeq integrated rate along isentropic lines

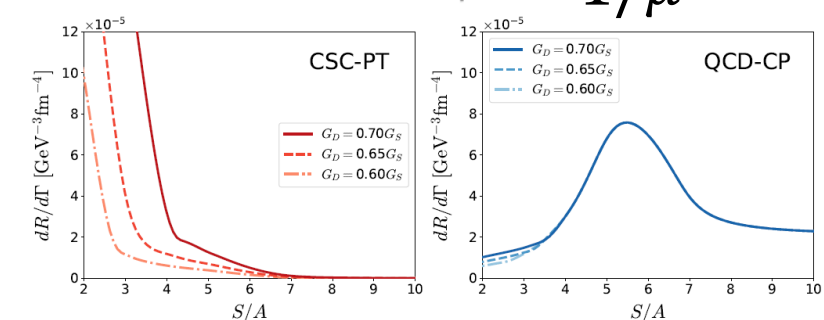
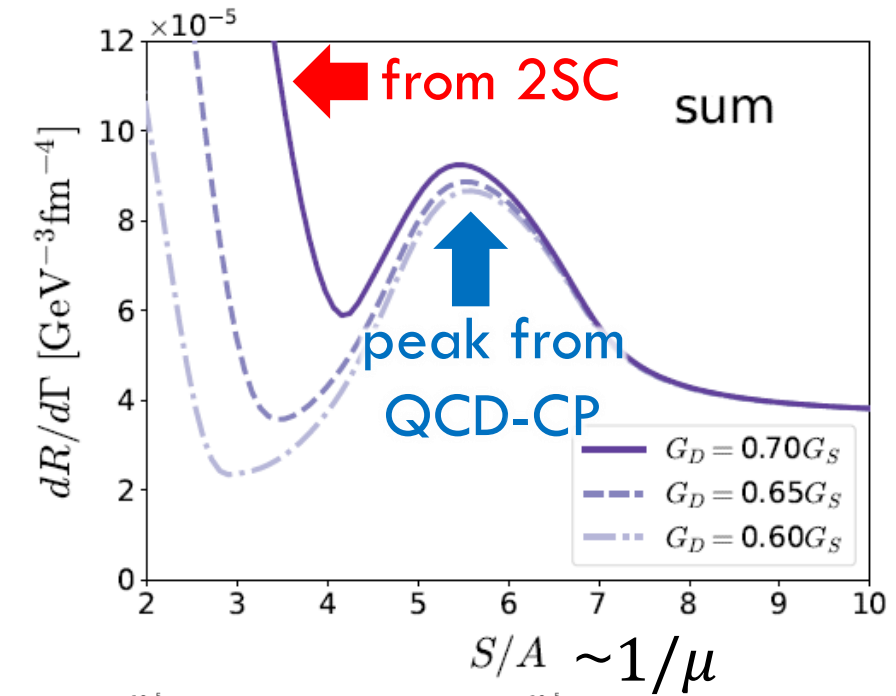
Isentropic lines in NJL model



Effect of 1st-tr on evolution: Savchuk+ 2209.05267

Nishimura, Nara, Steinheimer, Eur.Phys.J.A 60, 2024

Dilepton Yields $50 < M < 100$ MeV



Summary

- Divergence of fluctuations at 2nd-order phase transition
 - Soft modes near the CSC phase transitions & QCD-CP
 - Modification of medium property near the phase transitions

- Anomalous enhancement of the dilepton production in the ultrasoft invariant-mass region.
 - Experimental signature to measure CSC and QCD-CP?

Future

- Competition with Dalitz decay
- DPR from CSC phases

Contents

1. Optimal collision energy for studying dense matter in heavy-ion collisions

Taya, Jinno, MK, Nara, 2409.07685

2. Dilepton production for a signal of phase transitions in dense matter

Nishimura, MK, Kunihiro, Ann. Phys. 469 (2024) 169768; PTEP 2023, 053D01; PTEP 2022, 093D02

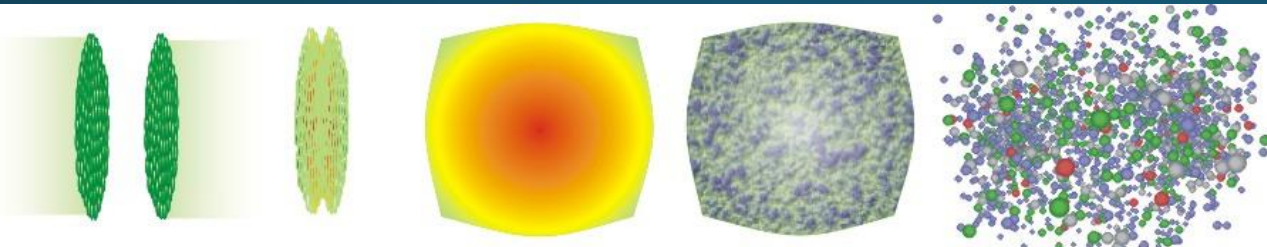
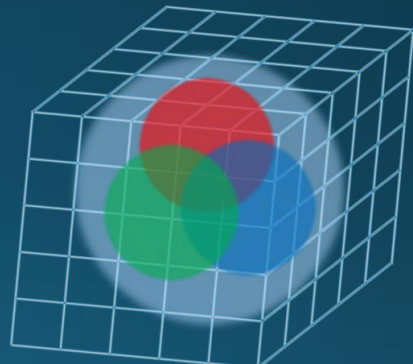
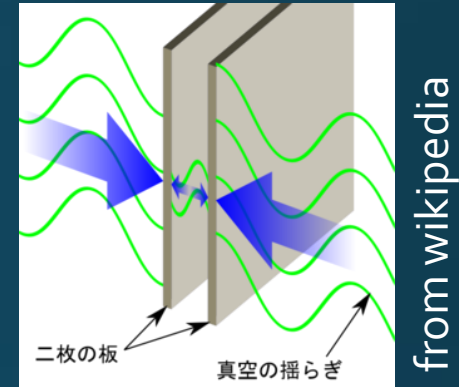
3. Novel critical points in SU(3) Yang-Mills theory with boundary conditions

MK+, PRD99 (2019) 094507; Suenaga, MK, PRD107 (2023) 074502; Fujii, Iwanaka, Suenaga, MK, PRD110 (2024) 094016

Boundary Conditions in QFT

Many motivations

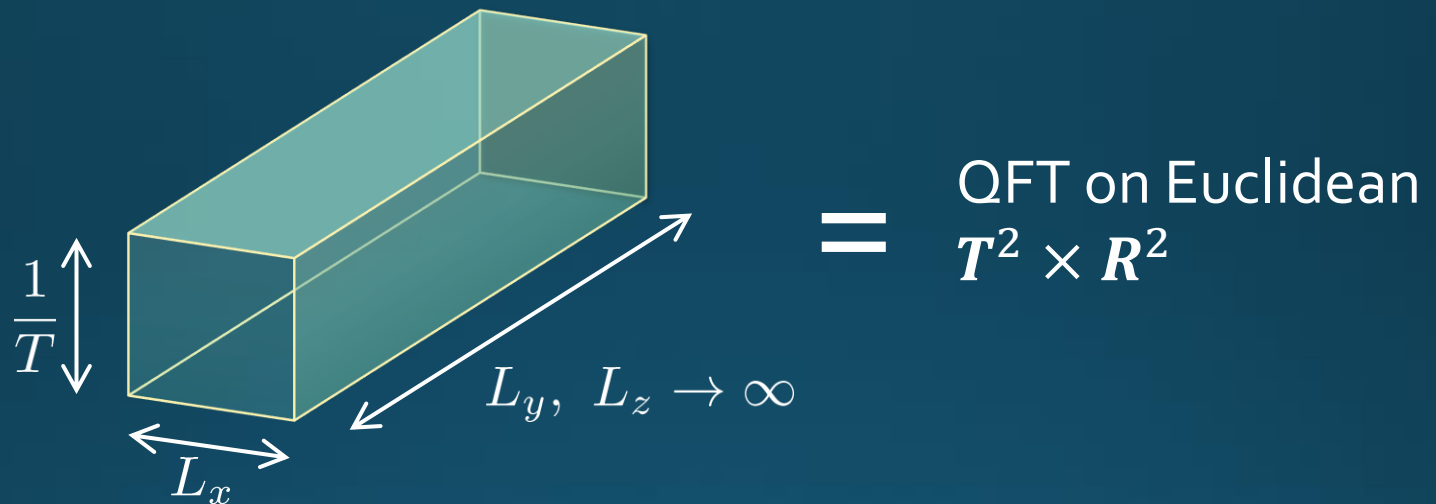
- Casimir effect
- Relativistic heavy-ion collisions
- Numerical simulations (ex. lattice QCD)
- Matsubara formalism for thermal systems



$$L_\tau = \frac{1}{T}$$

Purpose

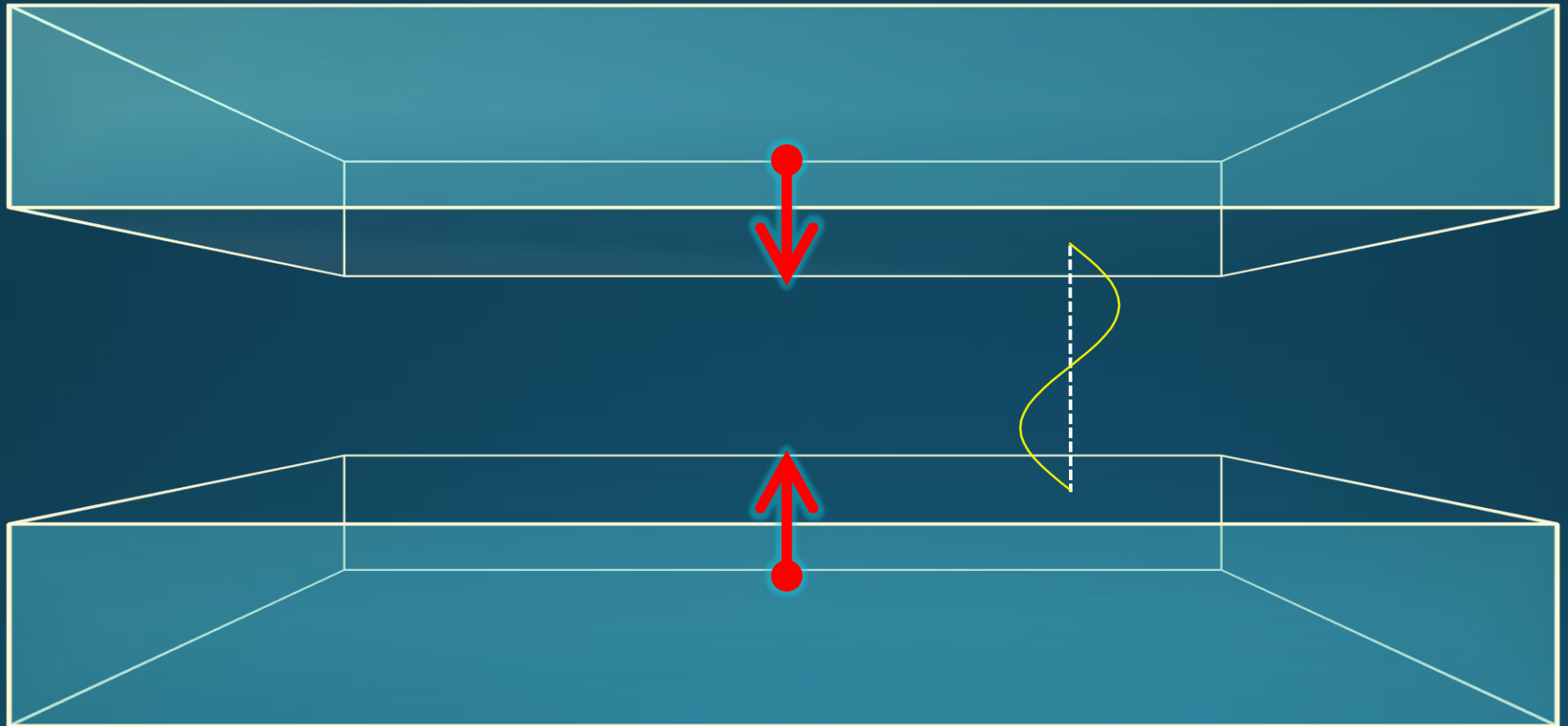
Thermal SU(3) YM with PBC along x direction



How does thermodynamics behave w.r.t. T and L_x ?

- Thermal Casimir effect in a non-perturbative system
- QCD phase diagram as a function of L_x
- Anisotropic pressure
- 2 Polyakov loops will play important roles

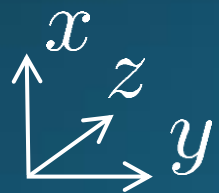
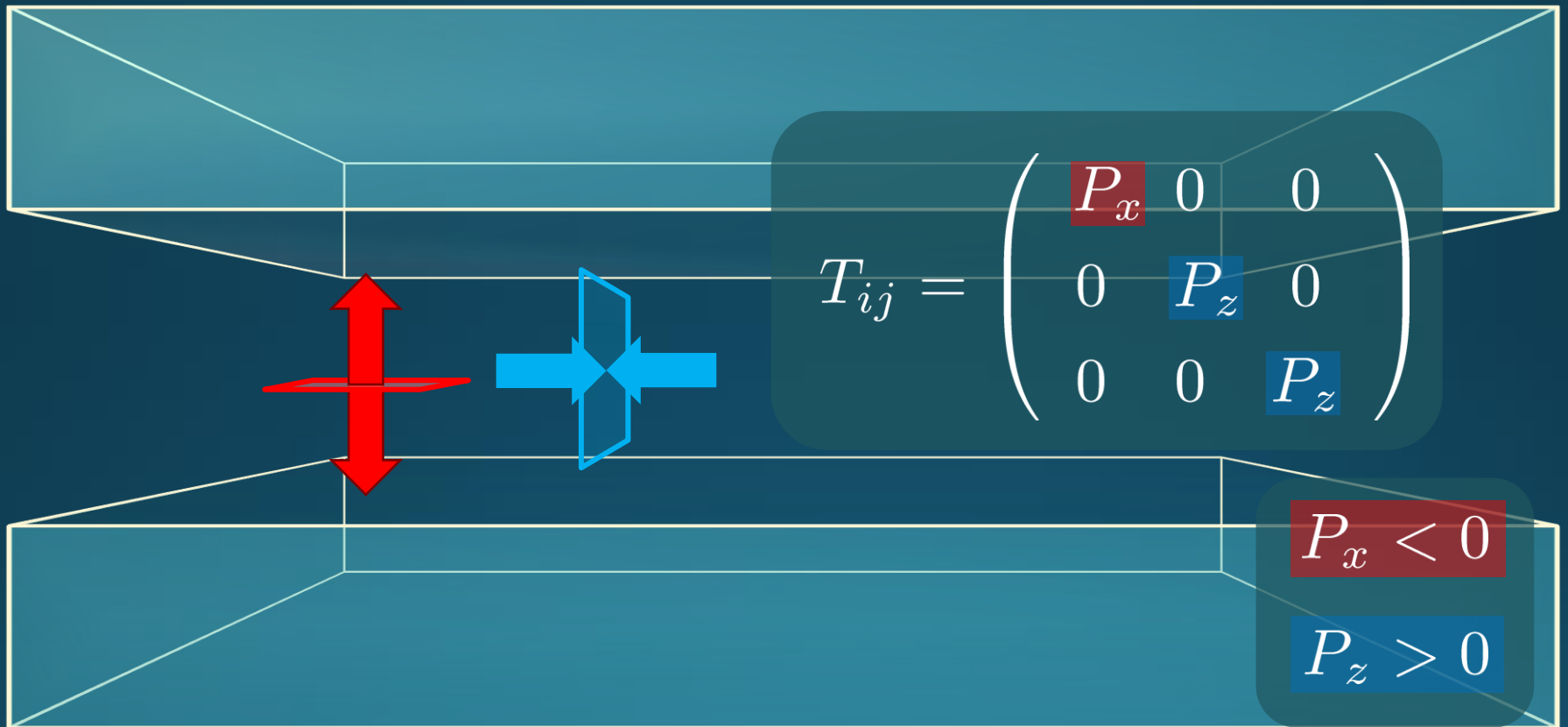
Casimir Effect



attractive force between two conductive plates

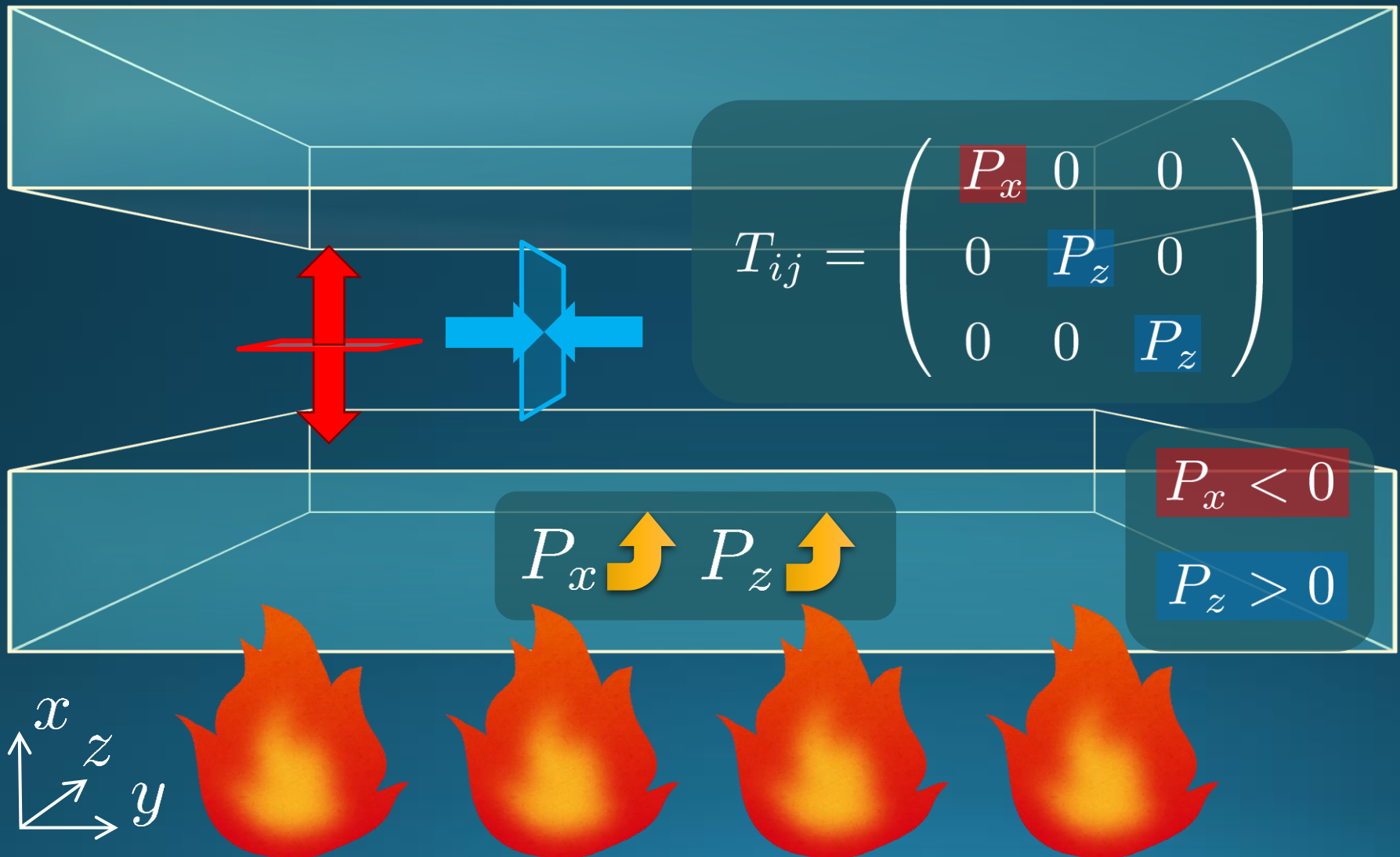
Casimir Effect

Brown, Maclay
1969



Casimir Effect

Brown, Maclay
1969



Contents

1. Lattice study

MK+, Phys. Rev. D**99** (2019) 094507

2. Model analyses

Suenaga, MK, Phys. Rev. D**107** (2023) 074502

D. Fujii, A. Iwanaka, D. Suenaga, MK, arXiv:2404.07899

Thermodynamics on the Lattice

Various Methods

- Integral, differential, moving frame, non-equilibrium, ...
- rely on thermodynamic relations valid in $V \rightarrow \infty$

$$P = \frac{T}{V} \ln Z \quad sT = \varepsilon + P \quad \longrightarrow \text{Not applicable to anisotropic systems}$$

- We employ **Gradient Flow (SFtX) Method**

$$\varepsilon = \langle T_{00} \rangle \quad P = \langle T_{11} \rangle$$

Components of EMT are directly accessible!

Yang-Mills Gradient Flow

$$\frac{\partial}{\partial t} A_\mu(t, x) = - \frac{\partial S_{\text{YM}}}{\partial A_\mu}$$

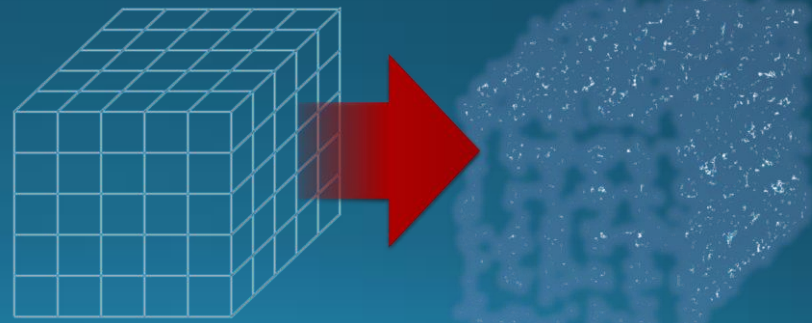
t: "flow time"
dim:[length²]

$$A_\mu(0, x) = A_\mu(x)$$

leading

$$\partial_t A_\mu = D_\nu G_{\mu\nu} = \boxed{\partial_\nu \partial_\nu A_\mu} + \dots$$

- diffusion equation in 4-dim space
- diffusion distance $d \sim \sqrt{8t}$
- "continuous" cooling/smearing
- No UV divergence at $t > 0$



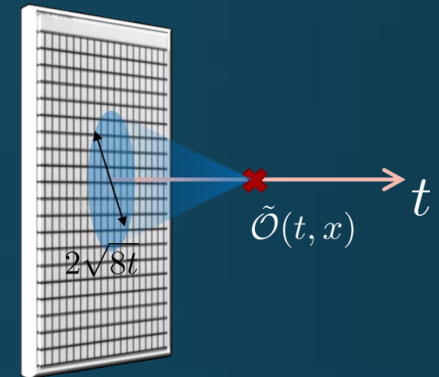
Constructing EMT

Suzuki, 2013

$$U_{\mu\nu}(t, x) = \alpha_U(t) \left[T_{\mu\nu}^R(x) - \frac{1}{4} \delta_{\mu\nu} T_{\rho\rho}^R(x) \right] + \mathcal{O}(t)$$

$$E(t, x) = \langle E(t, x) \rangle + \alpha_E(t) T_{\rho\rho}^R(x) + \mathcal{O}(t)$$

vacuum substr.



Remormalized EMT

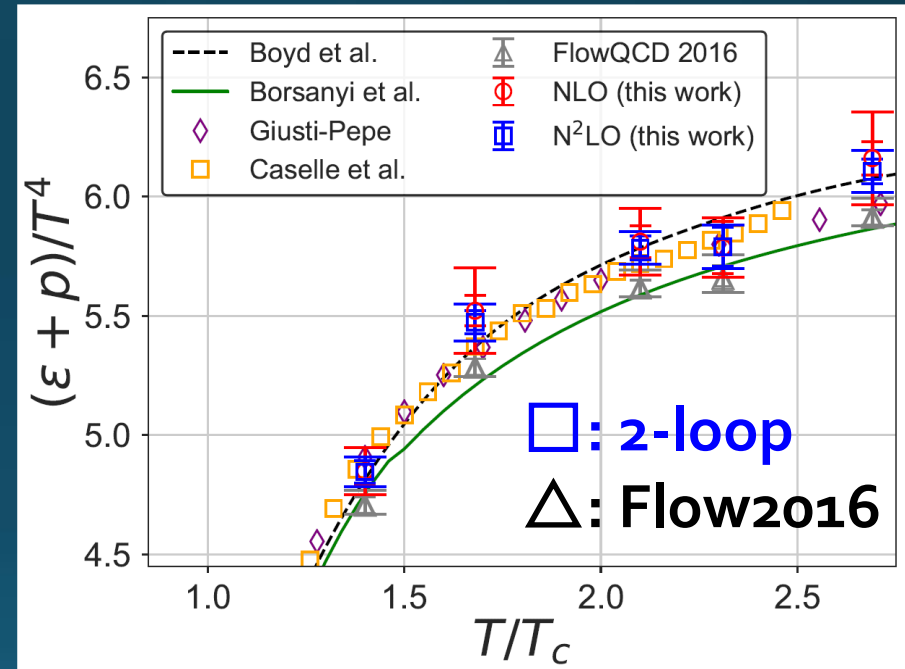
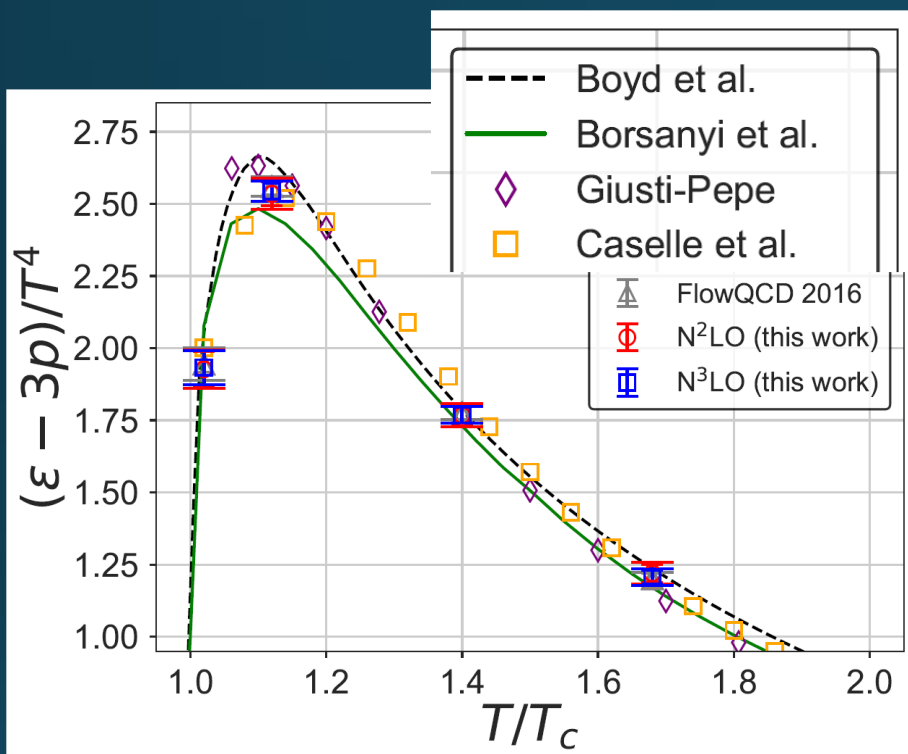
$$T_{\mu\nu}^R(x) = \lim_{t \rightarrow 0} [c_1(t) U_{\mu\nu}(t, x) + \delta_{\mu\nu} c_2(t) E(t, x)_{\text{subt.}}]$$

Perturbative coefficient:

Suzuki (2013); Makino, Suzuki (2014); Harlander+ (2018); Iritani, MK, Suzuki, Takaura (2019)

Thermodynamics

Iritani, MK, Suzuki, Takaura, 2019



Systematic error: μ_0 or μ_d , Λ , $t \rightarrow 0$ function, fit range

- Good agreement within **1% level**
- Our method can deal with the anisotropic pressure

Numerical Setup

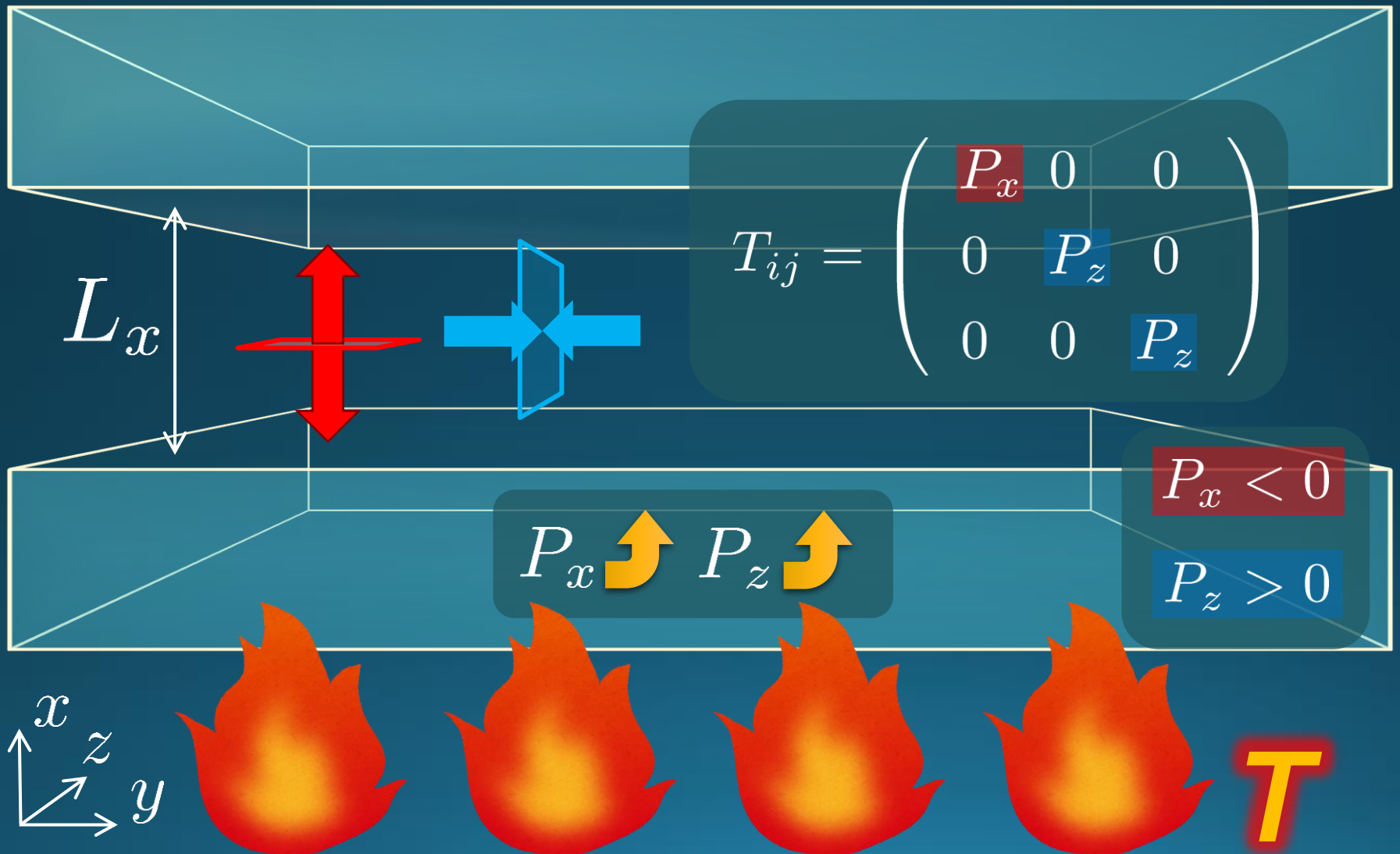
- SU(3)YM theory
- Wilson gauge action
- $N_t = 16, 12$
- $N_z/N_t = 6$
- 2000~4000 confs.
- Even N_x
- No Continuum extrap.
- Same System volume
 - $12 \times 72^2 \times 12 \sim 16 \times 96^2 \times 16$
 - $18 \times 72^2 \times 12 \sim 24 \times 96^2 \times 16$

T/T_c	β	N_z	N_τ	N_x	N_{vac}
1.12	6.418	72	12	12, 14, 16, 18	64
	6.631	96	16	16, 18, 20, 22, 24	96
1.40	6.582	72	12	12, 14, 16, 18	64
	6.800	96	16	16, 18, 20, 22, 24	128
1.68	6.719	72	12	12, 14, 16, 18, 24	64
	6.719	96	12	14, 18	64
	6.941	96	16	16, 18, 20, 22, 24	96
2.10	6.891	72	12	12, 14, 16, 18, 24	72
	7.117	96	16	16, 18, 20, 22, 24	128
2.69	7.086	72	12	12, 14, 16, 18	-
$\simeq 8.1$	8.0	72	12	12, 14, 16, 18	-
$\simeq 25$	9.0	72	12	12, 14, 16, 18	-

Simulations on
OCTOPUS/Reedbush

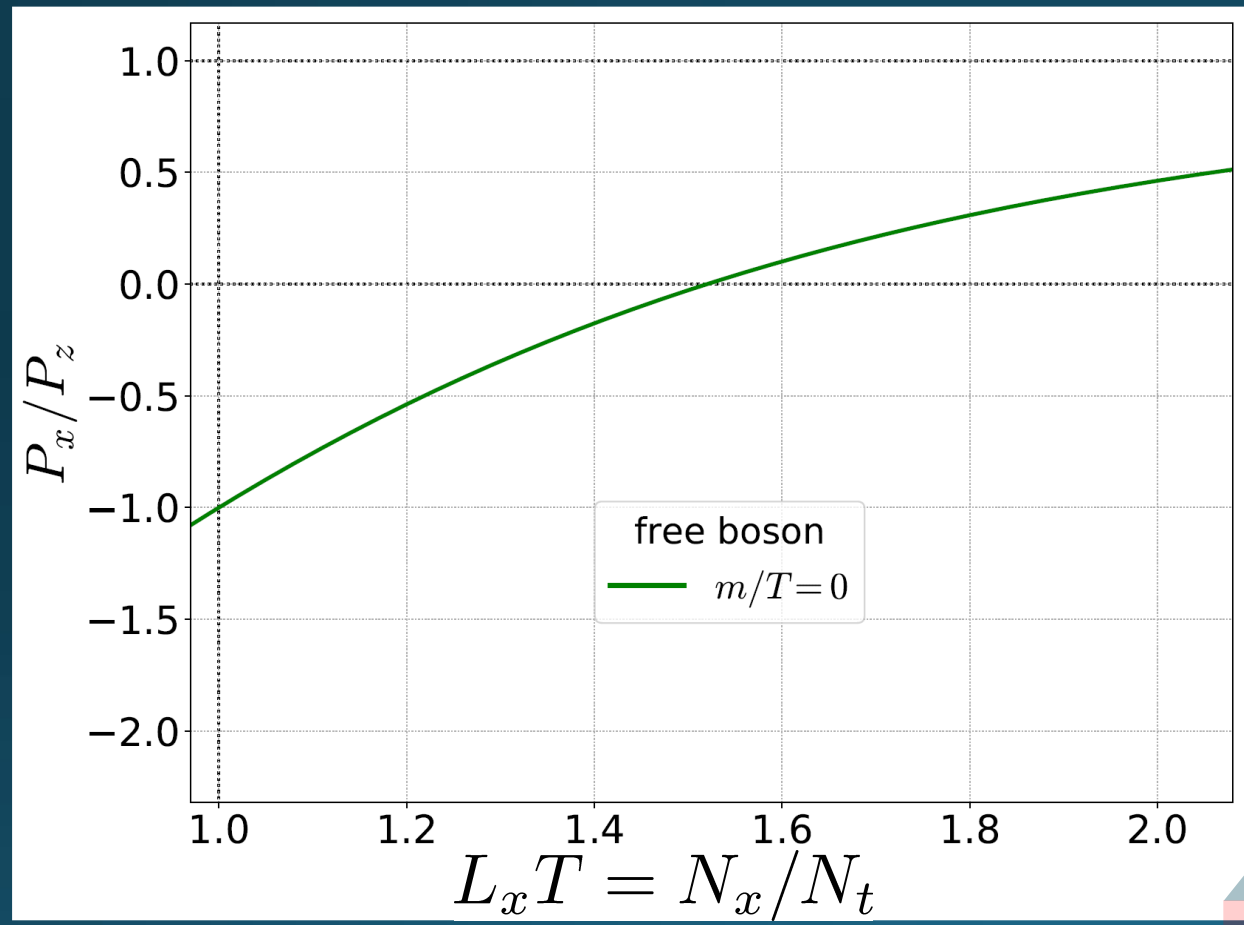
Casimir Effect

Brown, Maclay
1969



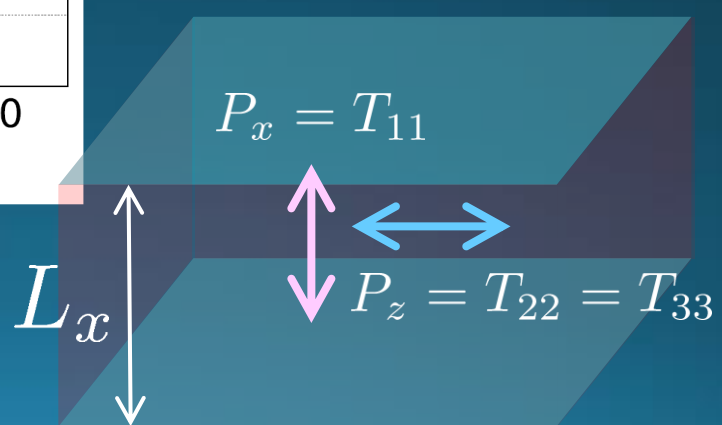
Pressure Anisotropy @ $T \neq 0$

MK, Mogliacci, Kolbe,
Horowitz ('21)



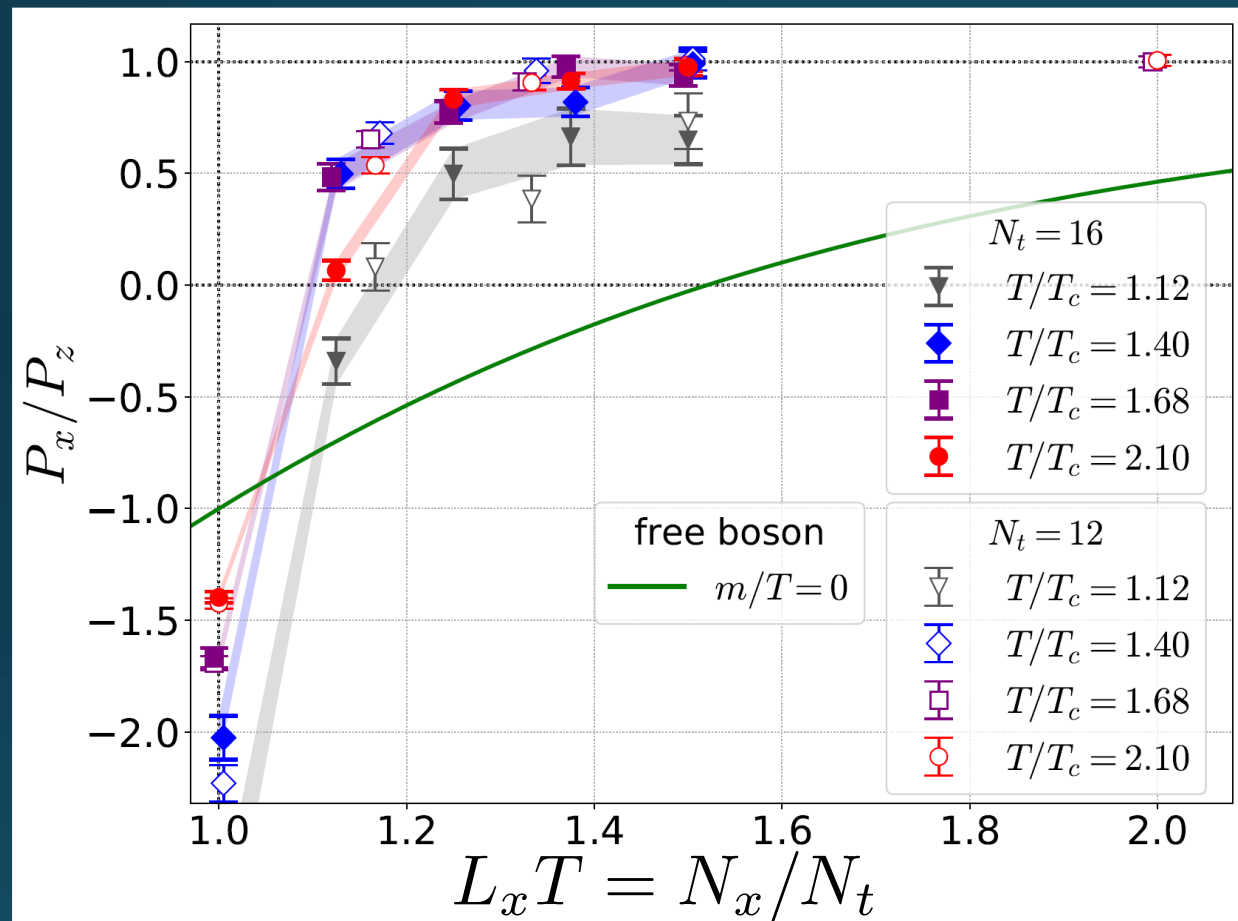
Free scalar field

- ◻ $L_2=L_3=\infty$
- ◻ Periodic BC



Pressure Anisotropy @ $T \neq 0$

MK, Mogliacci, Kolbe,
Horowitz ('21)



Free scalar field

- ◻ $L_2=L_3=\infty$
- ◻ Periodic BC

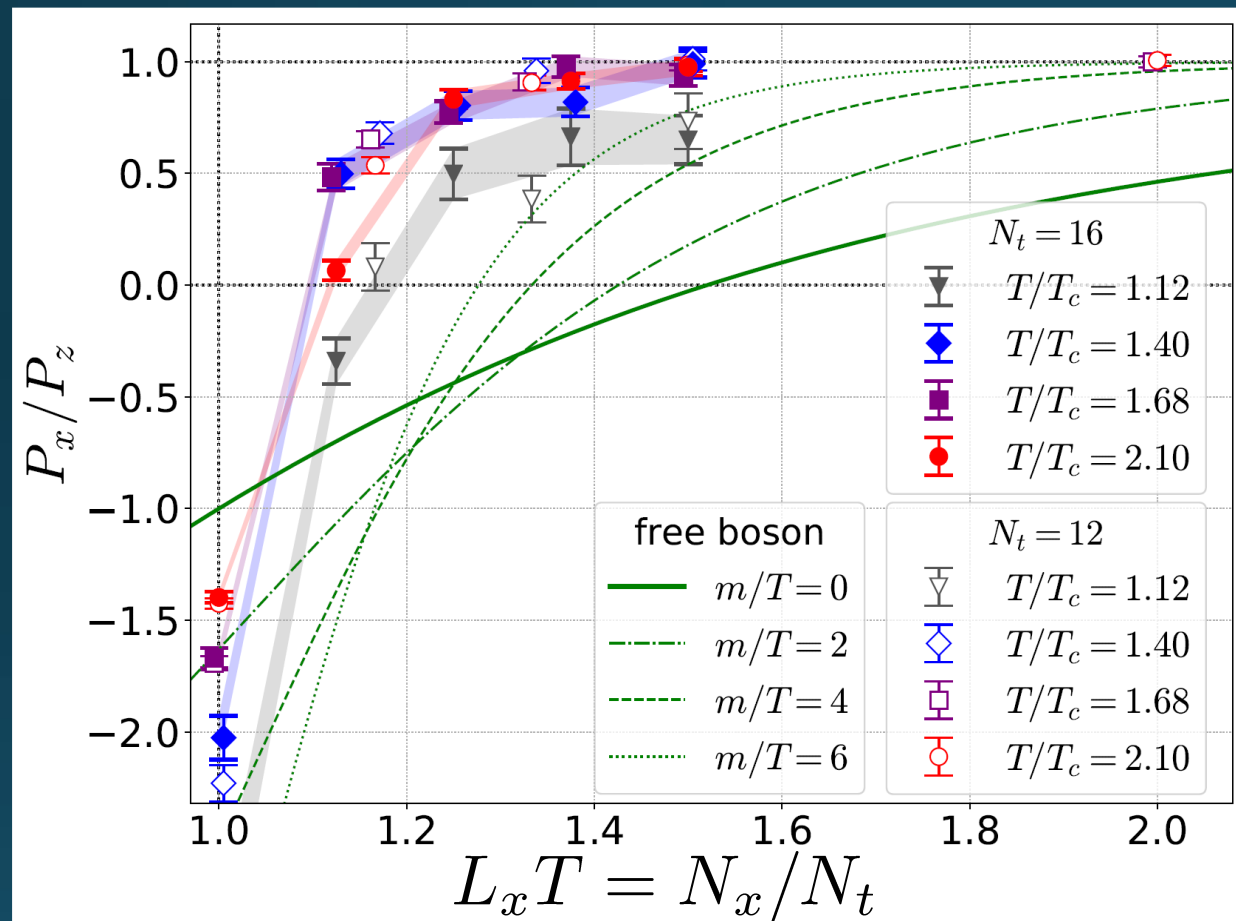
Lattice result

- ◻ Periodic BC
- ◻ Only $t \rightarrow 0$ limit
- ◻ Error: stat.+sys.

Medium near T_c is remarkably insensitive to finite size!

Pressure Anisotropy @ $T \neq 0$

MK, Mogliacci, Kolbe,
Horowitz ('21)



Free scalar field

- $L_2=L_3=\infty$
- Periodic BC

Lattice result

- Periodic BC
- Only $t \rightarrow 0$ limit
- Error: stat.+sys.

Medium near T_c is remarkably insensitive to finite size!

Higher T

High- T limit: massless free gluons

How does the anisotropy approach this limit?

Difficulties

- Vacuum subtraction requires large-volume simulations.
- Lattice spacing not available → $c_1(t)$, $c_2(t)$ are not determined.

Higher T

High- T limit: massless free gluons

How does the anisotropy approach this limit?

Difficulties

- Vacuum subtraction requires large-volume simulations.
- Lattice spacing not available $\rightarrow c_1(t), c_2(t)$ are not determined.

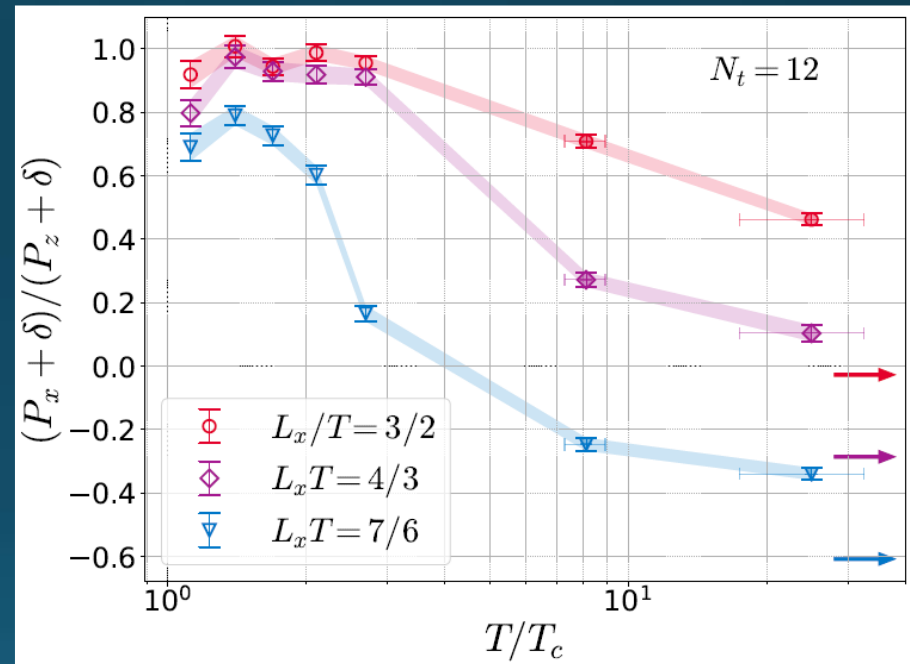
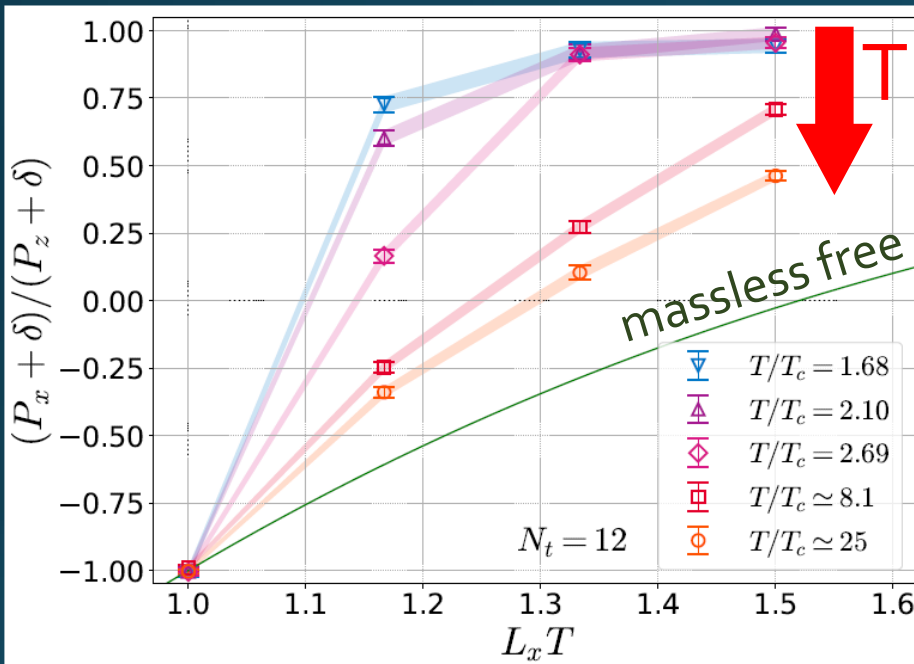


We study

$$R = \frac{P_x + \delta}{P_z + \delta} \quad \delta = -\frac{1}{4} \sum_{\mu} T_{\mu\mu}^E$$

No vacuum subtr.
nor Suzuki coeffs.
necessary!

$$\frac{P_x + \delta}{P_z + \delta}$$



$$T/T_c \approx 8.1 (\beta = 8.0), T/T_c \approx 25 (\beta = 9.0)$$

- Ratio approaches the asymptotic value for large T .
- But, large deviation exists even at $T/T_c \approx 25$.
- 1st-order phase transition??

Contents

1. Lattice study

MK+, Phys. Rev. D99 (2019) 094507

2. Model analyses

Suenaga, MK, Phys. Rev. D107 (2023) 074502

D. Fujii, A. Iwanaka, D. Suenaga, MK, arXiv:2404.07899

Polyakov-loop Effective Models

Meisinger+, PRD (2003)

General Idea

Constant Polyakov loop P as dynamical variable

$$P = \text{Tr} \left[\mathcal{P} \exp \left(i \int_0^{L_\tau} A_\tau d\tau \right) \right]$$

- $P = 0$: confinement
- $P \neq 0$: deconfinement

Free Energy

$$F(T; P) = F_{\text{pert.}}(T; P) + F_{\text{pot.}}(T; P)$$

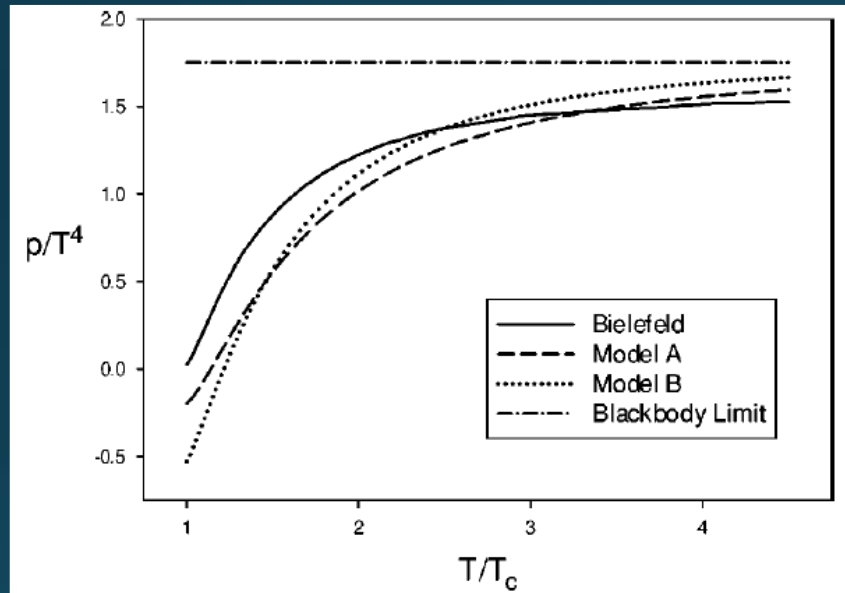
massless free gluons
with constant $A_0(x)$

Phenomenological
potential term

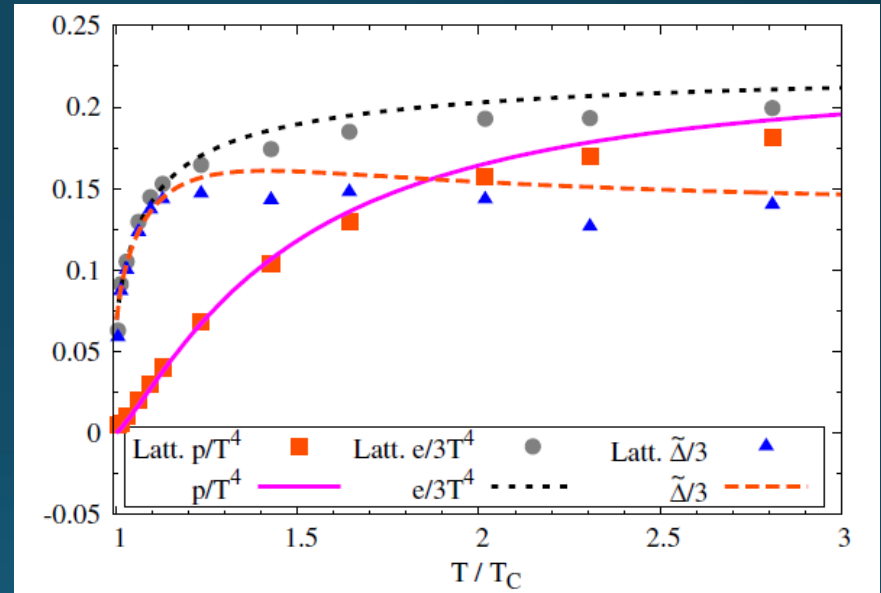
→ $\langle P \rangle$ is determined to minimize $F(T; P)$.

Thermodynamics

Meisinger+, PRD ('03)



Dumitru+, PRD ('12)



Qualitative behavior of lattice thermodynamics near and above T_c is well reproduced.

Extension to $T^2 \times R^2$

Suenaga, MK ('23); Fujii+ ('24)

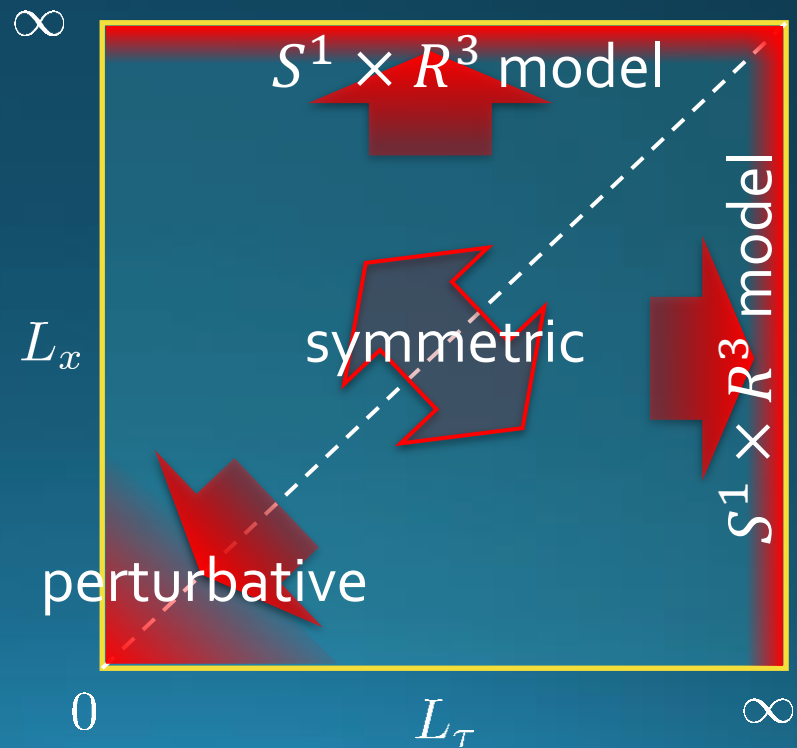
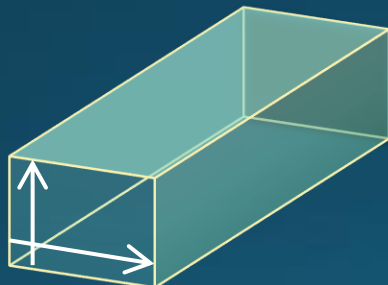
2 Polyakov loops along τ and x directions

$$P_\tau = \text{Tr} \left[\mathcal{P} \exp \left(i \int_0^{L_\tau} A_\tau d\tau \right) \right]$$

$$P_x = \text{Tr} \left[\mathcal{P} \exp \left(i \int_0^{L_\tau} A_x d\tau \right) \right]$$

Free Energy

- Function of 2 Polyakov loops.
- Constructed under constraints in various limits and symmetries



Polyakov-loop Potential Term

Fujii+ (2024)

$$F_{\text{pot}} = F_{\text{sep}} + F_{\text{cross}}$$

$$F_{\text{sep}}(P_\tau, P_x; L_\tau, L_x) = F_{\text{pot}}^{S^1 \times R^3}(P_\tau, L_\tau) + F_{\text{pot}}^{S^1 \times R^3}(P_x, L_x)$$

Potential on $S^1 \times R^3$
from Dmitru+'12

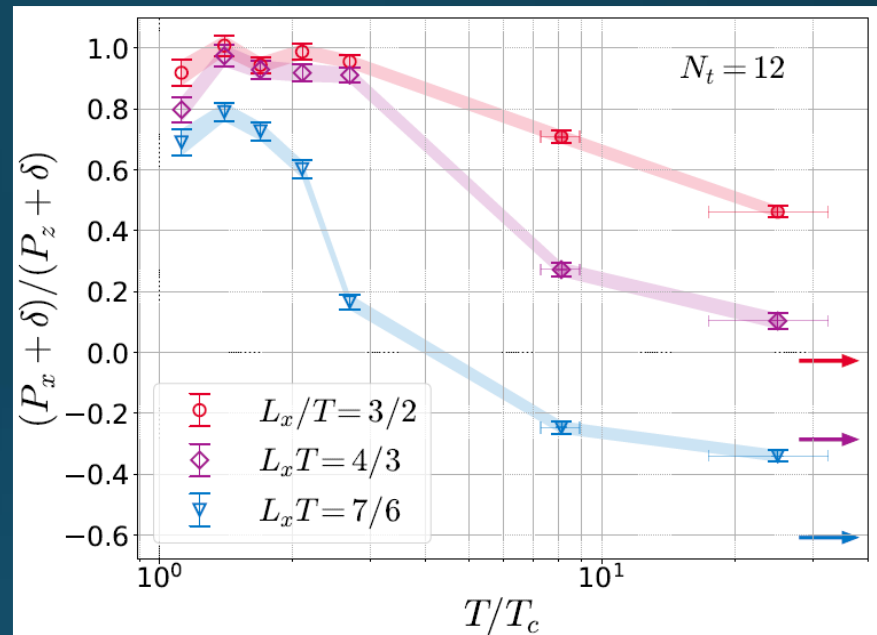
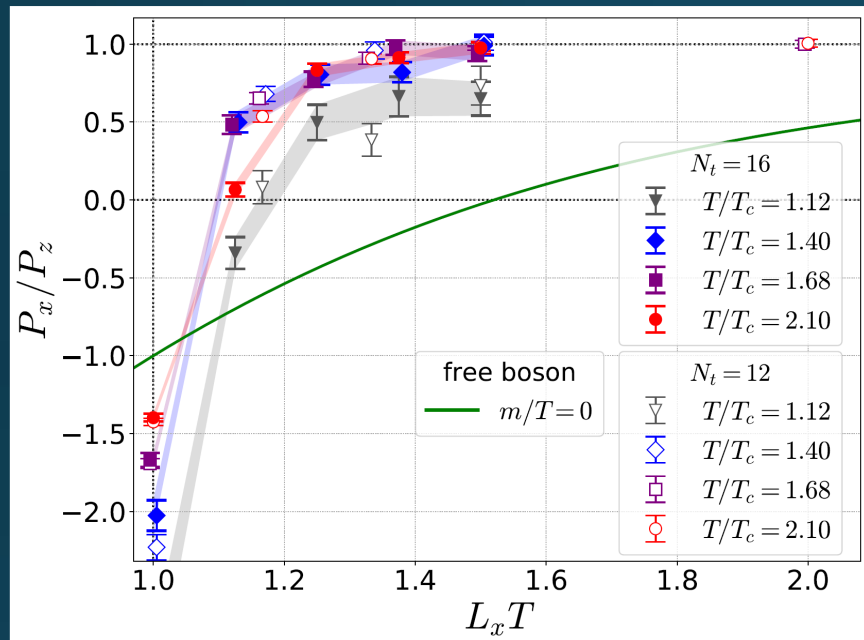
$$\begin{aligned} F_{\text{cross}} = g(L_\tau, L_x) & \left[c_4 \text{Tr}[P_\tau^\dagger P_\tau] \text{Tr}[P_x^\dagger P_x] \right. \\ & + c_5 (\text{Tr}[P_\tau^\dagger P_\tau] \text{Tr}[P_x^3] + \text{Tr}[P_\tau^3] \text{Tr}[P_x^\dagger P_x]) \\ & \left. + c_6 \text{Tr}[P_\tau^3] \text{Tr}[P_x^3] \right] \end{aligned}$$

$$g(L_\tau, L_x) = T_c^4 \left((T_c L_\tau)^2 + (T_c L_x)^2 \right)^{-n}$$

c_4, c_5, c_6, n : parameters in the model

Result

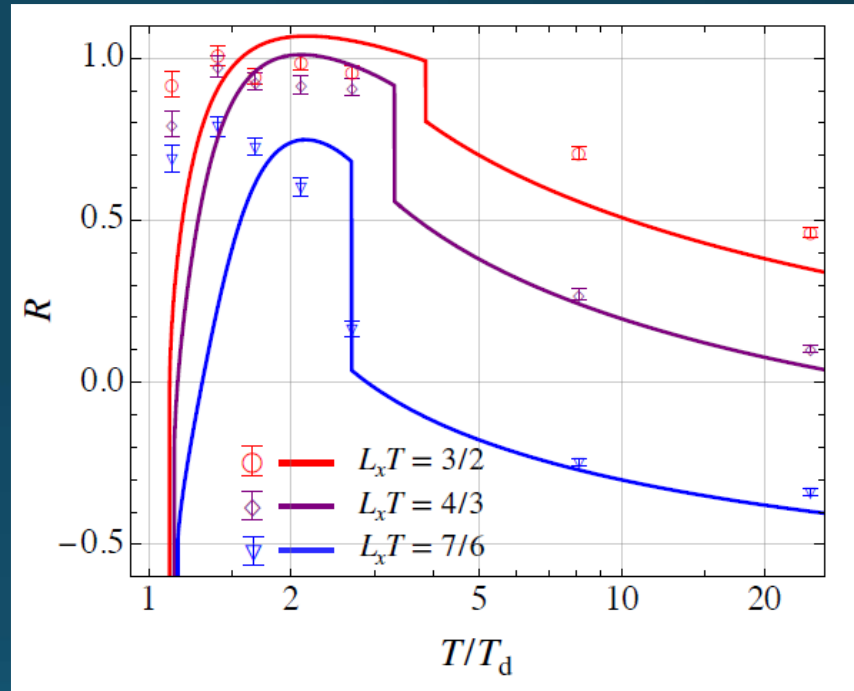
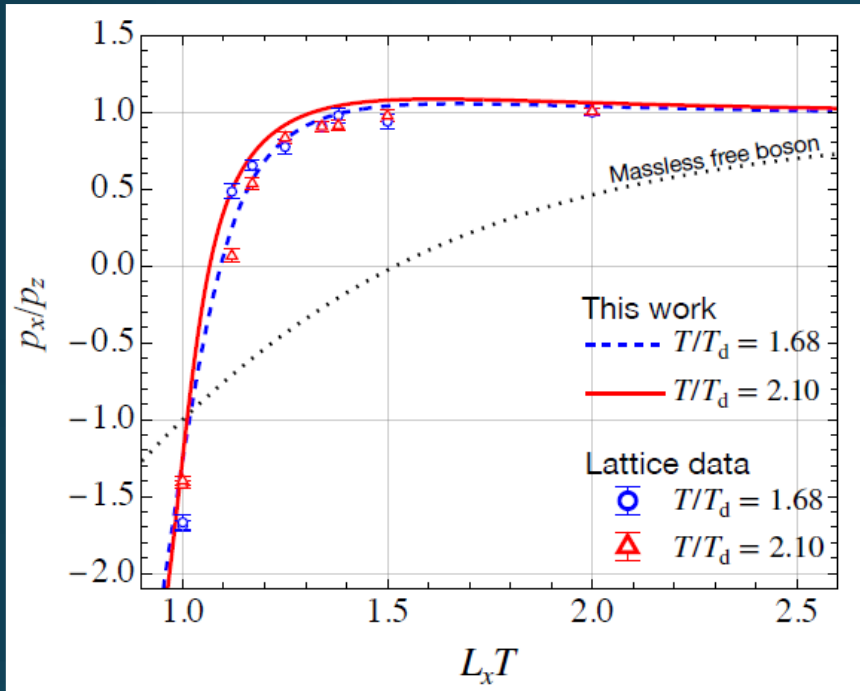
$$R = \frac{P_x + \delta}{P_z + \delta}$$



- Lattice results for $T/T_c > 1.5$ are well reproduced.
- No parameters to fit the results for $T/T_c = 1.4, 1.12$.
- Appearance of discontinuity = 1st-order PT

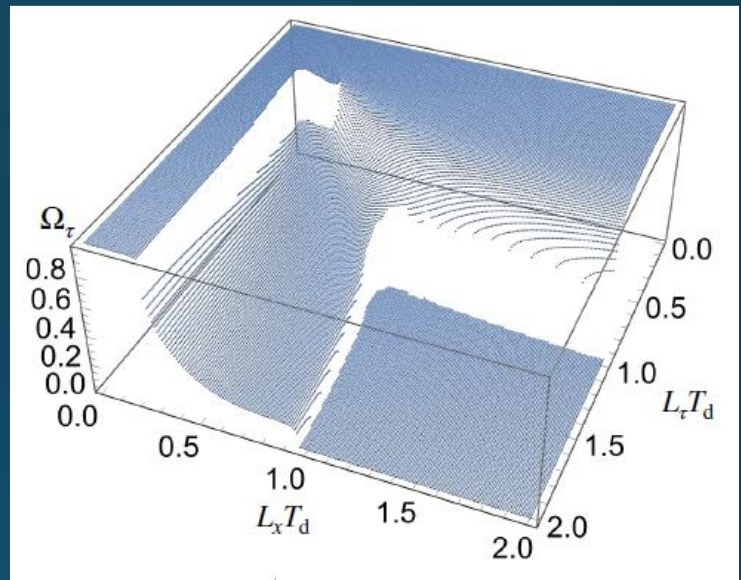
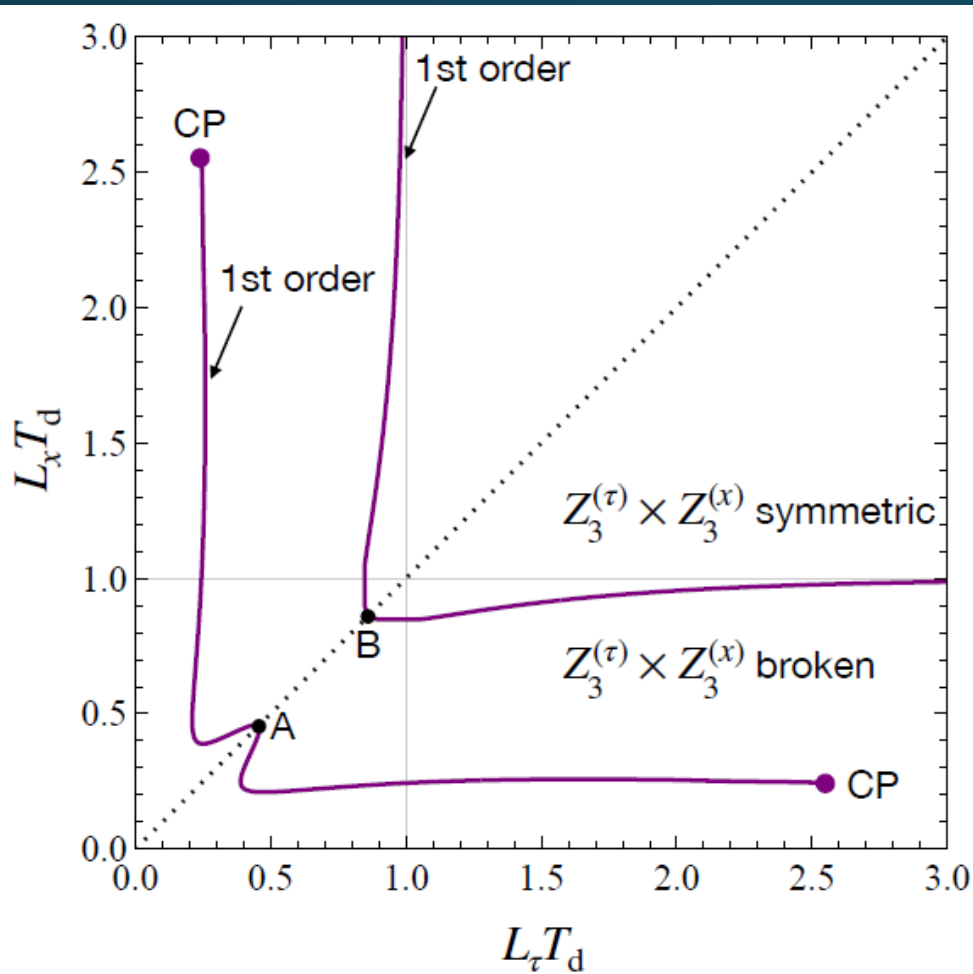
Result

$$R = \frac{P_x + \delta}{P_z + \delta}$$



- ❑ Lattice results for $T/T_c > 1.5$ are well reproduced.
- ❑ No parameters to fit the results for $T/T_c = 1.4, 1.12$.
- ❑ Appearance of discontinuity = 1st-order PT

Phase Diagram



2 first-order transitions!
B: connected to deconf. tr.
on $S^1 \times R^3$
A: new phase transition

Novel 1st-tr & CP induced by interplay between 2 Polyakov loops

Summary

Lattice thermodynamics in $SU(3)$ YM on $T^2 \times R^2$ has peculiar behaviors:

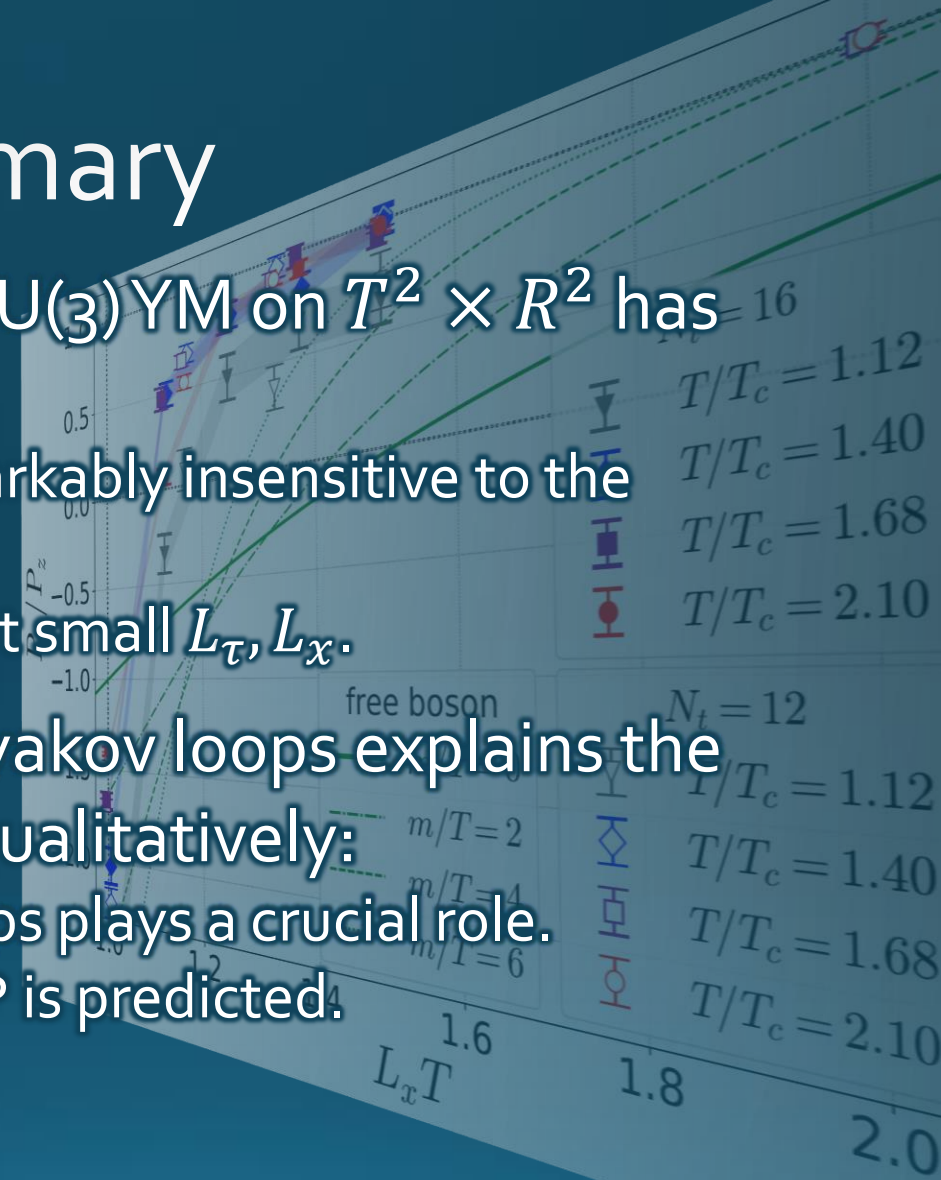
- Medium at $1.4 < T/T_c < 2.1$ is remarkably insensitive to the boundary.
- Slow approach to the SB limit at small L_τ, L_x .

Model analysis with two Polyakov loops explains the lattice results for $T \geq 1.5T_c$ qualitatively:

- Interplay b/w two Polyakov loops plays a crucial role.
- Appearance of new 1st-PT & CP is predicted.

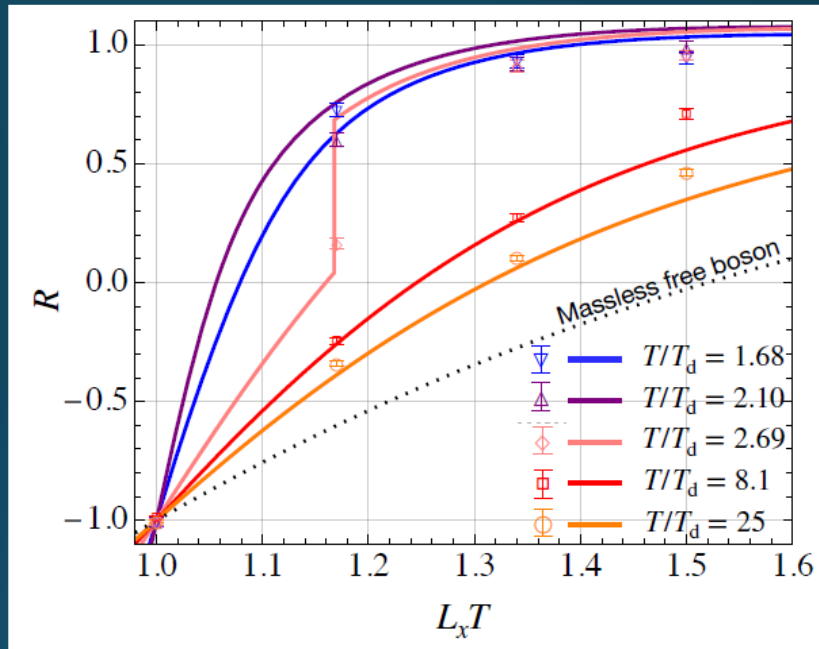
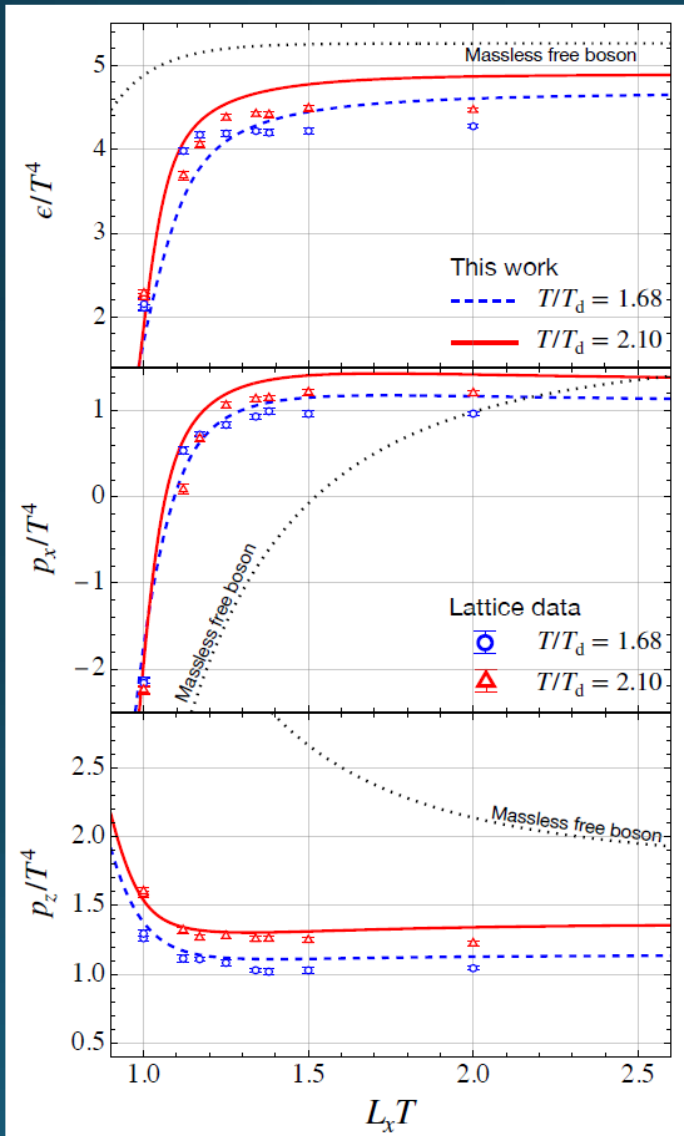
Future

- More lattice results to confirm the existence of the 1st PT
- Anti-periodic / Dirichlet BCs, BC for two directions, below T_c , ...



backup

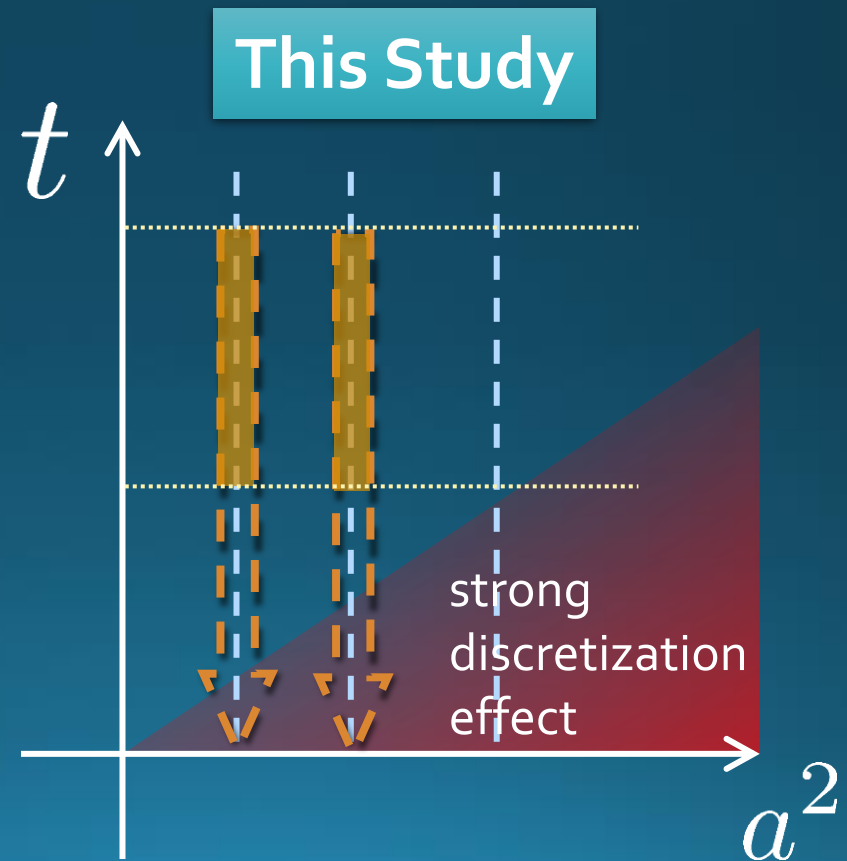
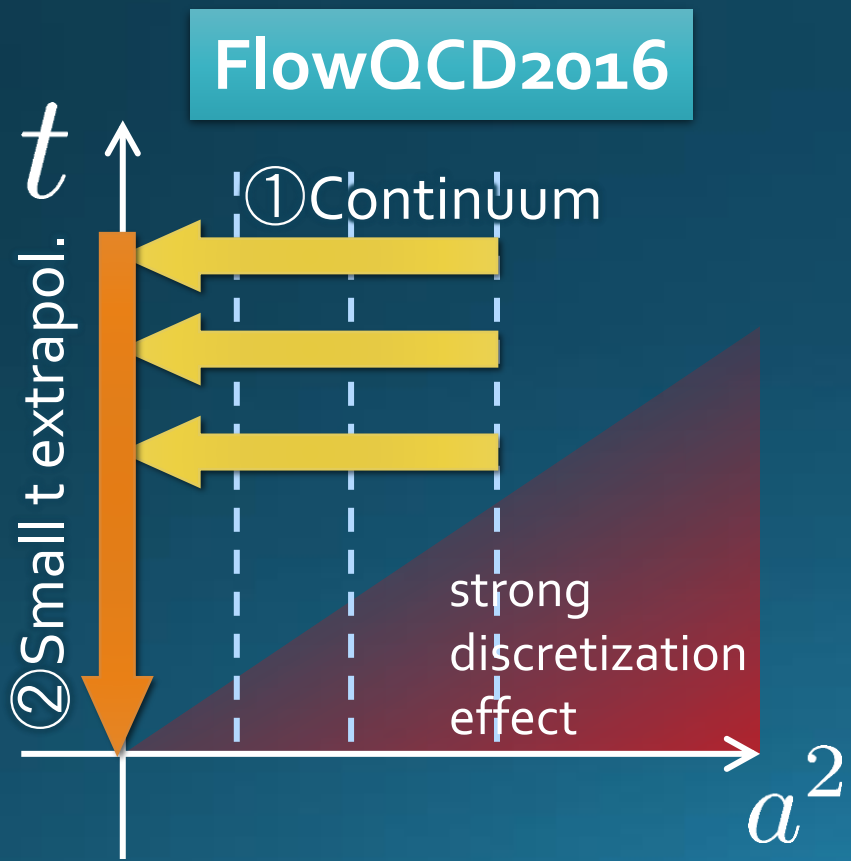
Numerical Results



Extrapolations $t \rightarrow 0, a \rightarrow 0$

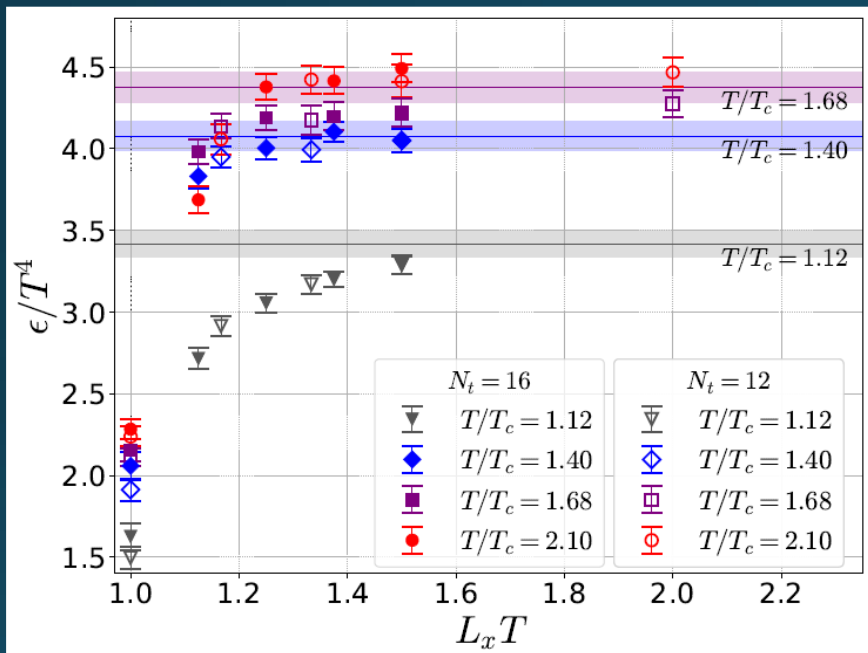
$$\langle T_{\mu\nu}(t) \rangle_{\text{latt}} = \langle T_{\mu\nu}(t) \rangle_{\text{phys}} + C_{\mu\nu} t + D_{\mu\nu}(t) \frac{a^2}{t}$$

$O(t)$ terms in SFT_E lattice discretization

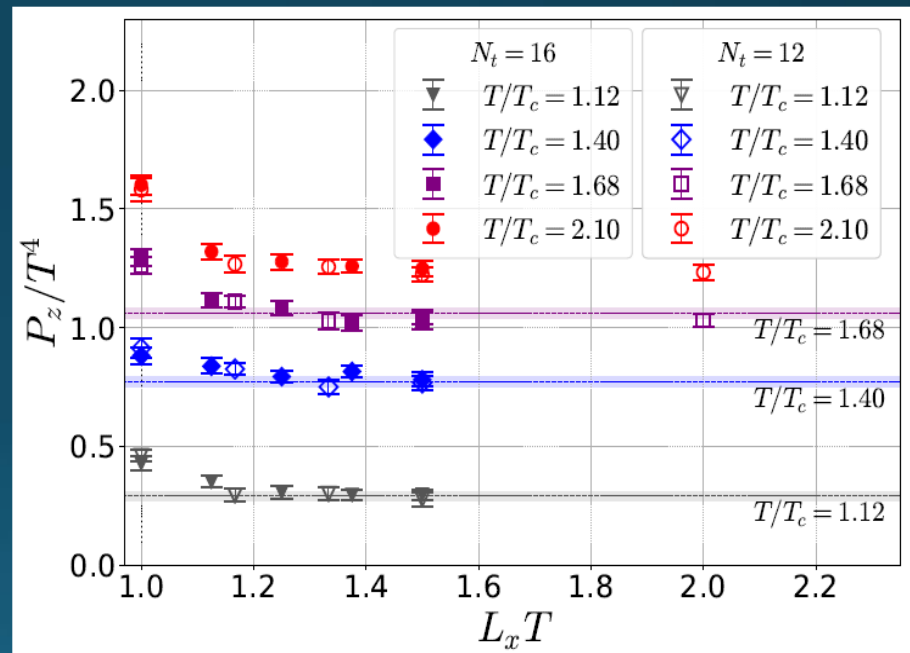


energy densty / transverse P

Energy Density

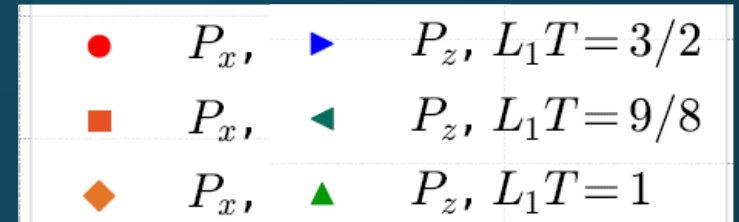
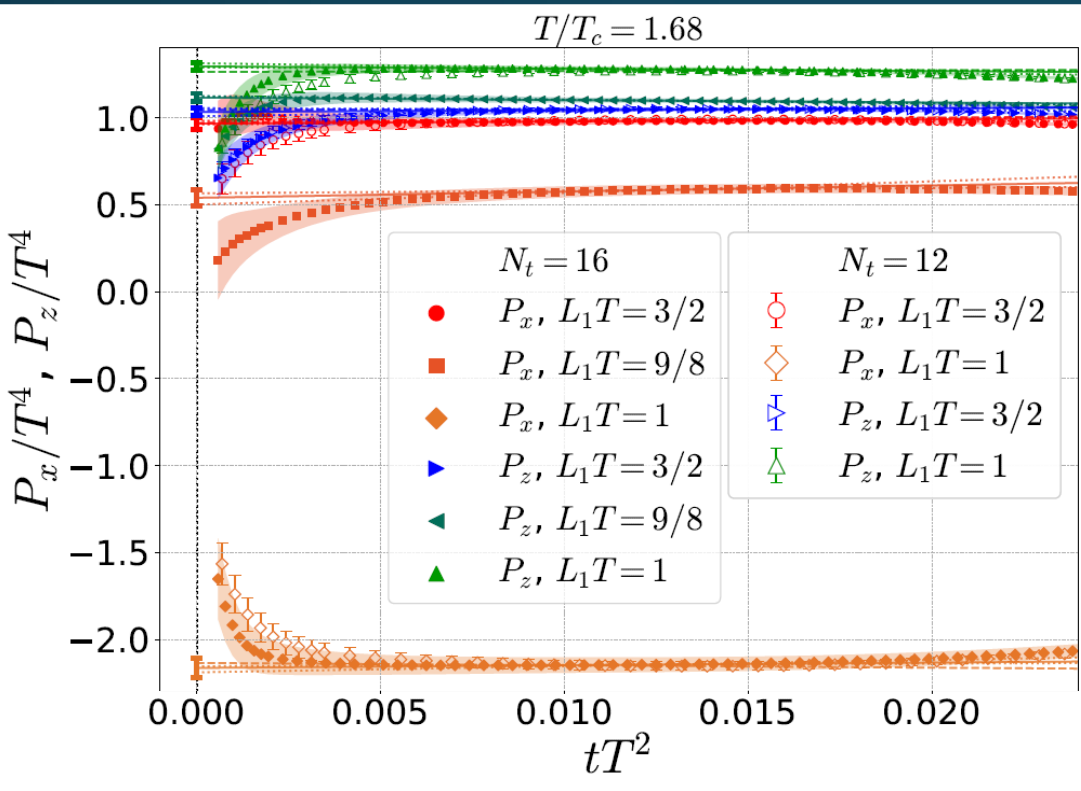


Transverse Pressure P_z



Small-t Extrapolation

$$T/T_c = 1.68$$



Filled: $N_t=16$ / Open: $N_t=12$

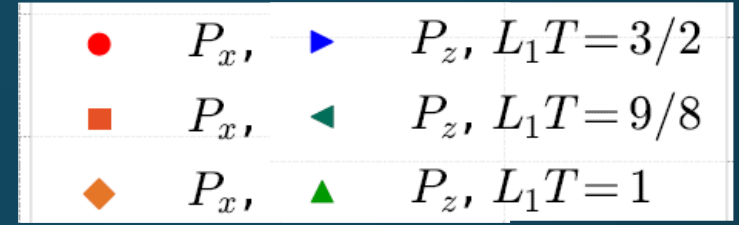
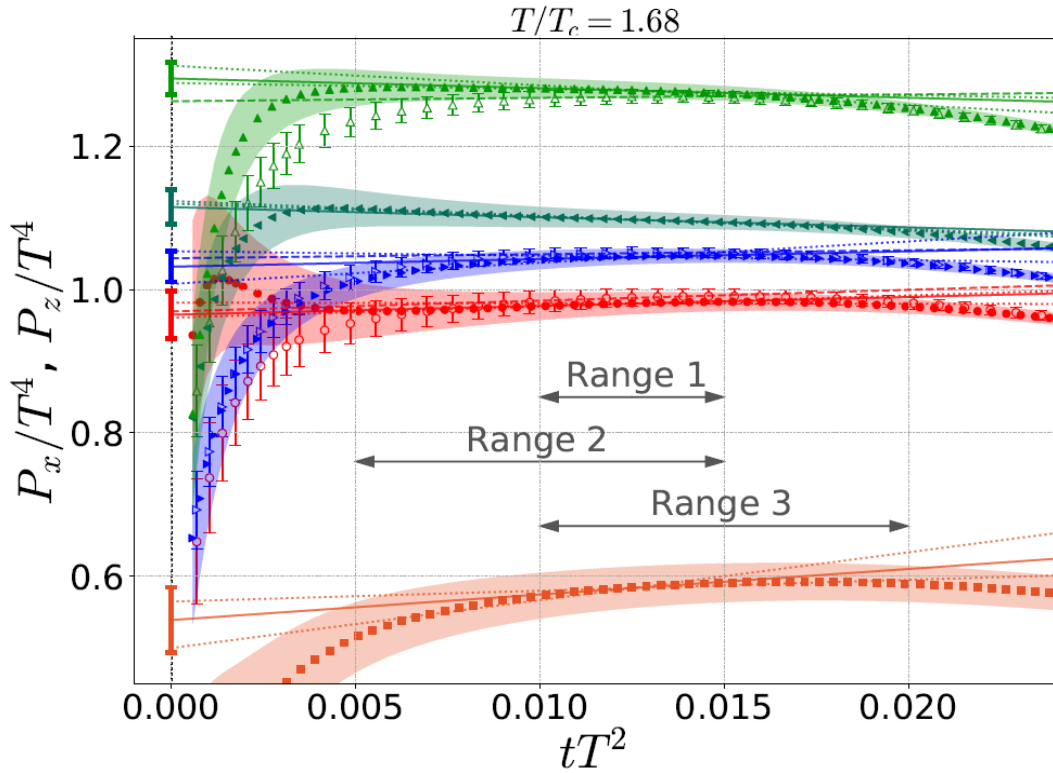
Small-t extrapolation

- Solid: $N_t=16$, Range-1
- Dotted: $N_t=16$, Range-2,3
- Dashed: $N_t=12$, Range-1

- Stable small-t extrapolation
- No N_t dependence within statistics for $L_x T=1, 1.5$

Small-t Extrapolation

$$T/T_c = 1.68$$



Filled: $N_t = 16$ / Open: $N_t = 12$

Small-t extrapolation

- Solid: $N_t = 16$, Range-1
- Dotted: $N_t = 16$, Range-2,3
- Dashed: $N_t = 12$, Range-1

- Stable small-t extrapolation
- No N_t dependence within statistics for $L_x T = 1, 1.5$